

1  
2  
3  
4  
5  
6  
7  
8  
9  
10  
11  
12  
13  
14  
15  
16  
17  
18  
19  
20  
21  
22  
23

**Numerical study of the heat transfer in wound woven wire matrix of a  
Stirling regenerator**

S.C. Costa<sup>a\*</sup>, Harritz Barrutia<sup>b</sup>, Jon Ander Esnaola<sup>b</sup>, Mustafa Tutar<sup>b,c</sup>

<sup>a</sup> CS Centro Stirling S. Coop, Avda. Alaba 3, 20550, Aretxabaleta, Spain

<sup>b</sup> Mechanical and Manufacturing Department, Engineering Faculty of Mondragon  
University, Loramendi 4, 20500, Mondragon, Spain

<sup>c</sup> IKERBASQUE, Basque Foundation for Science, 48011, Bilbao, Spain

\*Corresponding author. Tel.: +34 943 037 948 ; Fax: +34 943 792 393

E-mail address: [ccosta@centrostirling.com](mailto:ccosta@centrostirling.com) (S.C.Costa)

1 **Abstract**

2

3 Nusselt number correlation equations are numerically derived by characterizing the  
4 heat transfer phenomena through porous medium of both stacked and wound woven  
5 wire matrices of a Stirling engine regenerator over a specified range of Reynolds  
6 number, diameter and porosity. A finite volume method (FVM) based numerical  
7 approach is proposed and validated against well known experimentally obtained  
8 empirical correlations for a random stacking woven wire matrix, the most widely used  
9 due to fabrication issues, for Reynolds number up to 400. The results show that the  
10 numerically derived correlation equation corresponds well with the experimentally  
11 obtained correlations with less than 6 percent deviation with the exception of low  
12 Reynolds numbers. Once the numerical approach is validated, the study is further  
13 extended to characterize the heat transfer in a wound woven wire matrix model for a  
14 diameter range from 0,08 to 0,11 mm and a porosity range from 0,60 to 0,68 within the  
15 same Reynolds number range. Thus, the new correlation equations are numerically  
16 derived for different flow configurations of the Stirling engine Regenerator. It is  
17 believed that the developed correlations can be applied with confidence as a cost  
18 effective solution to characterize and hence to optimize stacked and wound woven wire  
19 Stirling regenerator in the above specified ranges.

20

21 *Keyword: Stirling engine; heat transfer; Nusselt number; porosity; CFD.*

22

1 **Nomenclature**

2	$A:$	Heat transfer area	$[\text{m}^2]$
3	$A_{wr}:$	Regenerator matrix wetted area	$[\text{m}^2]$
4	$c_1, c_2, c_3:$	Nusselt correlation constants	$[-]$
5	$c_p:$	Heat capacity at constant pressure	$[\text{J/kg K}]$
6	$c_v:$	Heat capacity at constant volume	$[\text{J/kg K}]$
7	$d_h:$	Regenerator matrix hydraulic diameter	$[\text{m}]$
8	$d_w:$	Wire diameter	$[\text{m}]$
9	$E:$	Total energy	$[\text{J}]$
10	$h:$	Heat transfer coefficient	$[\text{W/m}^2 \text{ K}]$
11	$h:$	Sensible enthalpy	$[\text{J/kg}]$
12	$\vec{J}_j:$	Diffusion flux of species	$[\text{kg/m}^2 \text{ s}]$
13	$k:$	Thermal conductivity	$[\text{W/m K}]$
14	$k_{eff}:$	Effective conductivity	$[\text{W/m K}]$
15	$k_g:$	Working gas thermal conductivity	$[\text{W/m K}]$
16	$k_t:$	Turbulent thermal conductivity	$[\text{W/m K}]$
17	$\dot{m}:$	Mass flow rate	$[\text{kg/s}]$
18	$Nu:$	Nusselt number	$[-]$
19	$p:$	Pressure	$[\text{Pa}]$
20	$Pe:$	Peclet number	$[-]$
21	$Q:$	Heat transfer	$[\text{W}]$
22	$q:$	Heat flux	$[\text{W/m}^2]$
23	$R:$	Gas-law constant	$[\text{J/kg K}]$
24	$Re:$	Reynolds number	$[-]$
25	$S_h:$	Volumetric rate of heat generation	$[\text{W/m}^3]$
26	$s:$	Cell size	$[\text{m}]$
27	$s:$	Pitch of the mesh	$[-]$
28	$T:$	Temperature	$[\text{K}]$
29	$T_g:$	Working gas temperature	$[\text{K}]$
30	$T_r:$	Regenerator matrix temperature	$[\text{K}]$
31			

1	$t$ :	Time	[s]
2	$u$ :	Velocity magnitude in x direction	[m/s]
3	$u_{max}$ :	Matrix velocity	[m/s]
4	$V_t$ :	Total volume of regenerator matrix	[m <sup>3</sup> ]
5	$\vec{v}$ :	Overall velocity vector	[m/s]
6	$Y_j$ :	Mass fraction of species	[-]
7	$\mu$ :	Fluid dynamic viscosity	[kg/m s]
8	$\rho$ :	Fluid density	[kg/m <sup>3</sup> ]
9	$\Pi_v$ :	Regenerator matrix volumetric porosity	[-]
10	$\varphi$ :	Regenerator matrix specific heat transfer area	[1/m]
11	$\phi$ :	Regenerator matrix shape factor	[1/m]
12	$\tau$ :	Non-dimensional time	[-]
13	$\bar{\tau}$ :	Stress tensor	[Pa]
14			
15			

## 1. Introduction

Stirling engine technology has been identified as an excellent candidate for energy cogeneration applications due to its elevated total efficiency (higher than 90%), the possibility to operate with any kind of temperature heat source (solar, combustible material, field waste, biomass, nuclear, etc.) and low noise and contamination levels [1-3]. The regenerator is considered by many researchers as the key component to improve the efficiency of the next generation of Stirling engine systems [4-8]. In the Stirling-engine regenerators, the heat transfer and the pressure drop are the main phenomena associated to energy efficiency and have been studied by many researchers [6, 9-14, 16]. For this reason, the characterization of these two phenomena through experimental, theoretical and numerical studies is crucial to maximize the thermal efficiency and incoming outsource energy in Stirling engine.

Research efforts [4-5, 8-10, 15] have shown that high fluid-to-matrix heat transfer together with low pressure drop can be obtained by using a matrix with the characteristics of: smooth heat transfer surface, controlled flow acceleration rates, minimized flow separation and uniform passages flow distribution.

Currently, regenerators are usually made of stacked woven wire screen or random fibers. Thus, most of the research studies conducted for the thermal and fluid characterization in the Stirling regenerator have mainly focused on empirical characterization of these. The heat transfer between the matrix of the regenerator and the working gas has been studied from various points of view, many of them based on Hausen's (1929) reference work. Moreover, several experimental studies have been conducted in order to evaluate the heat transfer in different regenerator's matrices determining empirical correlation for Nusselt number  $Nu$ .

1 Tong and London [12] study the heat transfer and flow friction characteristics of woven  
2 wire screen and crossed rod in steady flow in a wide range of Reynolds number,  $Re$ . In  
3 the experiments each “screen element” is oriented  $45^\circ$  with its neighbor so as to  
4 simulate a “random stacking” in contrast to a “regular or aligned stacking” where all the  
5 wire elements, for instances, would be either parallel or right angles with each other.

6 Miyabe [9] in addition to his theoretical work derives generalized experimental  
7 equations of flow friction factor and heat transfer coefficient for packed wire screens  
8 with variety of geometries. Tanaka [6] investigates the flow and heat transfer  
9 characteristics of the regenerator materials in an oscillating flow for wire net and sponge  
10 metal. Gedeon and Wood [10] derive generic correlations for friction factor, Nusselt  
11 number, enhanced axial conduction ratio and overall heat flux ratio based on the test  
12 samples of a number of wire mesh (random stacking) and metal felt, with a range of  
13 porosities.

14 Thomas and Bolleber [17] compare different and often used correlations for heat  
15 transfer of Stirling engine regenerators. Each author formulates a different definition for  
16 Reynolds and Nusselt numbers as well as heat transfer area. All those authors use  
17 samples of wire screen or random fiber matrices for their investigations.

18 Generally, the Nusselt number is a function of Reynolds and Prandtl number (Peclet  
19 number) [10]. However, when dealing with the heat transfer in the regenerator of a  
20 Stirling machine, the Prandtl number is insignificant, since it can always be  
21 approximated as 0.7 for the gases used as working fluids in Stirling machines. The  
22 impact of  $Re$  is given by the following general correlation [17]:

23 
$$Nu = c_1 + c_2 Re^{c_3} \quad (1)$$

1 In Eq. (1) the coefficient are constants determined by the experimental data. Thomas  
2 and Bolleber [17] observe that the Nusselt number is not only a function of Reynolds  
3 number. The majority of experimental data reveal the additional impact of the porosity  
4 on Nusselt number. Thus the effect of the porosity must be attributed to the specific heat  
5 transfer area. The impact of the property data on the working fluid, given by the Prandtl  
6 number, is also negligible.

7 Apart from the analytical studies, there are some numerical analyses of the heat  
8 transfer and pressure drop through wire screen matrix using different numerical  
9 discretization techniques. The finite volume method (FVM) appears to be promising as  
10 numerical investigation tool **indicated** by Rühlich and Quack [5], Gedeon and Wood  
11 [10], Ibrahim et al. [7], Tew [18], Cheadle et al. [19], Tao et al. [20] and others. These  
12 numerical studies suggest that the fluid flow and thermal simulations are highly  
13 required to understand the flow of interest and hence to characterize fluid flow friction  
14 behavior for such systems of regenerator applications. The **work of Cheadle** et al. [19]  
15 outlines the development of a design tool that is capable of deriving Nusselt number and  
16 friction factor correlations based on computational fluid dynamic (CFD) analysis of a 2-  
17 D unit-cell model that considers the microscopic interactions between the fluid and  
18 solid.

19 Kolodziej et al. [13] indicate that despite the fact stacked wire screen are used for  
20 years in different applications that involves heat recuperation or regenerators, their  
21 transport and friction phenomena are still not described well enough. The number of  
22 studies dealing with the gauze flow resistance and heat transfer is rather limited.  
23 Moreover, there is a considerable lack of more general models that could be able to

1 predict transport properties of any wire gauze, which have not been experimentally  
2 described before.

3 One important issue in the progress to improvements Stirling models is the  
4 geometrical shape of the matrix in the regenerator and most regenerator models don't  
5 assume a precise geometrical shape for the elements of the regenerator [21]. Dydson et  
6 al. [21] indicate that clearly, the shape of the regenerator has an important impact on the  
7 overall Stirling system design.

8 As summarized above, the majority of experimental studies and correlations are  
9 generally conducted for stacked woven wire screen regenerator matrices as they are the  
10 most widely used ones. However, this kind of regenerator tends to be the one of the  
11 most expensive components of the Stirling engines, which nowadays limits the use of  
12 this technology for micro-cogeneration application in domestic environments. For this  
13 reason, the use of wound woven wire matrix regenerators could be a more cost effective  
14 alternative solution that would overcome such limitations [16]. Therefore, heat transfer  
15 and flow friction characteristics of these matrices are of interest for Stirling cycle  
16 applications. Even though, very few research works have been carried out for this type  
17 of regenerator, no specific heat transfer correlations are known to exist in literature.  
18 Thus, there is still a very high necessity of characterize heat transfer in this type of  
19 regenerator.

20 Consequently, the objective of this study is to numerically develop a heat transfer  
21 correlation for wound woven matrix regenerator. With this respect, numerical 3-D  
22 detailed models for a stacked woven wire matrix are initially developed to obtain heat  
23 transfer correlations for different configurations and the results are compared with well-

1 known experimentally obtained correlations in order to validate the proposed models  
2 over a specified range of Reynolds number. Later, the numerical study is extended to  
3 obtain heat transfer correlation equation for wound woven wire matrices. The good  
4 correspondence of the stacked woven wire matrix configuration with experimental data  
5 suggests that the derived correlations can be used with confidence to characterize and  
6 hence to optimize wound woven wire matrix Stirling regenerator. However, it is  
7 expected that the developed correlations will be experimentally validated for future  
8 applications and used to limit the try and error cost in Stirling design. It should be  
9 noticed that a similar study dealing with the development of numerical correlation for  
10 the flow friction factor through a wound woven matrix regenerator, has been recently  
11 published by the authors [16].

12

## 13 **2. Computational Principles**

14

### 15 *2.1. Numerical methodology*

16

17 The numerical methodology adopted in the previous work of the authors [16] for the  
18 numerical resolution of pressure drop characteristics of Stirling flow under isothermal  
19 flow condition is extended here to investigate the heat transfer phenomena by solving  
20 additional governing integral equation for the conservation of energy in de-coupled  
21 (segregated) manner.

22

23 In this study, the fluid is considered to be viscous, unsteady, incompressible and  
24 Newtonian with constant fluid flow properties, and three-dimensional (3-D) with  
25 assumption of laminar flow behavior at very low Reynolds number range and of  
turbulent flow behavior at high Reynolds number. As authors demonstrate in previous

1 work [16], when the Reynolds number exceeds a certain value depending on the  
2 configuration of the wire matrix used, the local instabilities due to emergence of  
3 turbulence leads to numerical convergence problem and the simulations are conducted  
4 in turbulent manner.

5 In this study due to the small range of temperature used in each case, all fluid  
6 properties (including density, viscosity, specific heat, and conductivity) are assumed  
7 constant. The present flow is mathematically governed by continuity, momentum and  
8 energy equation. The governing equations are discretized and solved sequentially using  
9 a finite volume method (FVM) based numerical flow solver [22] with a second order  
10 upwind scheme for the discretization of the continuity, momentum and energy  
11 equations for the laminar flow solutions. The convergence criterion for all the velocity  
12 components and for the continuity is set to  $10^{-6}$ , whereas it is set to  $10^{-8}$  for the energy  
13 for all simulations. The non-dimensional time step,  $\tau = u_{\max} t / s$  is expressed as the  
14 product of the maximum velocity component at the inflow boundary and time elapsed  
15 divided by the volume cell size. **The non-dimensional time step values are chosen as**  
16 **0.01 following an initial sensitivity analysis performed for the variation of Nusselt**  
17 **number with respect to different non-dimensional time step size ranging from 0.001 to**  
18 **0.01 for different Re number of 64 and 355. This test shows that there is no significant**  
19 **influence of choice of non-dimensional time step size between 0.01 and 0.001 on the**  
20 **results of Nusselt number obtained for the investigated Re number.**

21  
22  
23  
24

## 2.2. Computational domain and boundary conditions

Figure 1 illustrates the region of flow of interest (geometry set-up) in which the woven wire matrix and the flow through woven wire matrix geometry is extensively analyzed as a representation of a differential part of a Stirling regenerator arrangement. As Cheadle et al. [19] mention the modeling of typical regenerator geometries would require detailed 3-D models with prohibitively long solutions times. For this reason, in order to capture the heat and momentum interactions at the microscopic level, a small representative portion of the regenerator is modeled. The inlet and outlet flow areas are set to approximately  $0.5 \text{ mm}^2$  and woven wire matrix length is approximately 1.5 mm.

Figure 1

The Reynolds number based on hydraulic diameter is varied from 4 to 400. In some simulations the computational domain is further extended in the downstream direction (in the nominal direction of the outlet flow) in order to avoid reverse flow conditions at the outflow boundary.

In the geometrical model to simulate the random stacking of the different sheets, two different misaligned configurations, parallel and cross, for stacked woven wire matrix are generated and studied. In the wound woven wire matrix just the misaligned parallel configuration is generated and studied because in a winding process the cross case is more difficult to obtain. All the configurations are generated based on two woven wire mesh,  $80 \text{ }\mu\text{m}$  and  $110 \text{ }\mu\text{m}$  as described in Table 1. Furthermore, for each

1 woven wire mesh small changes in the volumetric porosity ranges,  $\Pi_v$ , are realized. The  
2 range of porosity evaluates is from 0.60 to 0.68. Figs. 2a and b show the configurations  
3 for parallel and cross local matrix for stacked woven models, respectively.

4  
5 **Figures (2a) - (b)**

6  
7 Miyabe [9] indicates that the empirical equation derived for Nusselt is expressed in  
8 a generalized form, and it is recommended that the matrix be made so that all screens  
9 are closely stacked. If each screen is not stacked perfectly, or when any gap exists  
10 between the screens, the friction coefficient and Nusselt number will deviate from the  
11 actual value to some extent.

12 **In Figure 3 are shown the matrix surface mesh for a stacked and wound woven wire**  
13 **matrix and a two-dimension section in the flow direction for fluid.**

14  
15 **Figure (3a) - (c)**

16  
17 The computational domain is constructed of non-uniformly distributed different  
18 hybrid mesh systems containing over 2.5 million tetrahedral and/or hexahedral volume  
19 cells for the final mesh system. The tetrahedral cells are used in the wire matrix and air  
20 volume inside the matrix with very fine mesh resolution in the close vicinity of the wire  
21 surfaces to resolve sharply varying velocity and pressure gradients there. The effect of  
22 the mesh resolution on the flow has been previously assessed with the authors [16] for  
23 three different mesh systems containing non-uniformly distributed hybrid grid cells in a  
24 quarter of the computational domain. It is demonstrated that there is no major difference

1 among the computed values and the mesh system of over 2.5 million hybrid volume  
2 cells, in the current study the number of cell is multiplying by four. Thus, the final mesh  
3 system could be considered to be fine enough to study the effects of Reynolds number  
4 on the heat transfer characterization.

5 For all woven wire matrix configurations, all model simulations are carried out by  
6 considering the following boundary conditions:

- 7 1. Inflow boundary: Velocity inlet boundary conditions at constant temperature are used  
8 to define the fluid uniform velocity profile.
- 9 2. Outflow boundary: Pressure outlet boundary conditions are assigned to define the  
10 static (gauge) pressure by eliminating reverse flow problem.
- 11 3. Side boundary: Free-slip symmetry flow boundary conditions at the four side  
12 boundaries of the computational domain are imposed. The normal velocity components  
13 and the normal gradients of all velocity components are assumed to have a zero value.
- 14 4. Interior wall boundaries: No-slip wall boundary conditions together with the  
15 enhanced wall functions are assigned to interior wall boundaries between wires and  
16 fluid for turbulent simulation cases. Moreover, any thermal condition is assigned to the  
17 wall between the fluid and the solid matrix, and the two sides of the wall are coupled.

18

### 19 *2.3. Heat transfer model*

20

21 The energy equation form solves in ANSYS FLUENT [22] is the following:

$$22 \quad \frac{\partial}{\partial t}(\rho E) + \nabla \cdot (\vec{v}(\rho E + p)) = \nabla \cdot (k_{eff} \nabla T - \sum_j h_j \vec{J}_j + (\bar{\tau}_{eff} \cdot \vec{v})) + S_h \quad (2)$$

1        Where  $k_{eff}$  is the effective conductivity ( $k + k_t$ ), where  $k_t$  is the turbulence  
2        thermal conductivity, defined according to the turbulence model being **used**, and  $\vec{J}_j$  is  
3        the diffusion flux of species  $j$ . The first three terms on the right-hand side of Equation  
4        (2) represent energy transfer due to conduction, species diffusion, and viscous  
5        dissipation respectively.  $S_h$  includes the heat of chemical reaction, and any other  
6        volumetric heat sources defined.

7        In Eq. (2)

$$8 \qquad \qquad \qquad E = h - \frac{p}{\rho} + \frac{v^2}{2} \qquad (3)$$

9        where sensible enthalpy  $h$  is defined for incompressible flow as

$$10 \qquad \qquad \qquad h = \sum_j Y_j h_j + \frac{p}{\rho} \qquad (4)$$

11        for ideal gas the last term of Eq. (4) is eliminated. In Eq. (4),  $Y_j$  is the mass fraction  
12        of species  $j$  and

$$13 \qquad \qquad \qquad h_j = \int_{T_{ref}}^T c_{p,j} dT \qquad (5)$$

14        In one-dimensional the gas energy Eq. (2) is written as:

$$15 \qquad \qquad \qquad \frac{\partial}{\partial t} (\rho E) + \frac{\partial}{\partial x} \cdot (u(\rho E + p) + q) - Q = 0 \qquad (6)$$

16        Solid matrix to gas heat transfer  $Q$  can be expressed in terms of a heat transfer  
17        coefficient  $h$  as follow:

$$18 \qquad \qquad \qquad Q = hA(T_r - T_g) \qquad (7)$$

1 Ignoring the kinetic energy term ( $u^2/2$ ) in Eq. (6), and expressing  $\rho E = (c_v/R)p$   
 2 and  $+p = c_p\rho T$ , the alternative form of the energy equation is:

$$3 \quad \left(c_{vg}/R\right) \frac{\partial p}{\partial t} + \frac{\partial}{\partial x} \cdot \left(c_{pg} \dot{m} T_g + q\right) - hA(T_r - T_g) = 0 \quad (8)$$

4 Eq. (8) is transformed into Eq. (9) assuming that the first term of the Eq. (8) is  
 5 negligible, the mass flow is uniform in the matrix, the matrix temperature is linear and  
 6 the apparent conductivity is not a function of  $x$ . By combining the last two assumptions  
 7 the term becomes as  $\frac{\partial q}{\partial x} = k_a \frac{\partial^2 T}{\partial x^2} \approx 0$ .

$$8 \quad \dot{m} c_{pg} \frac{\partial T_g}{\partial x} = hA(T_r - T_g) \quad (9)$$

9 Eq. (9) is easily solved to given the heat transfer coefficient based on numerical  
 10 modeling results between two planes  $\Delta x$  as follows:

$$11 \quad h = \frac{\dot{m} c_{pg} \Delta T_g}{A_{wr} \Delta T_{m_{log}}} \quad (10)$$

12 Where the  $\dot{m}$  is the mass flow of the working gas,  $c_{pg}$  is the gas specific heat at  
 13 constant pressure,  $\Delta T_g$  is the different in gas temperature between the entrance and exit  
 14 plane in the model,  $A_{wr}$  is the regenerator wetted area and  $\Delta T_{m_{log}}$  is a logarithmic  
 15 average of the temperature difference between the regenerator matrix surface and  
 16 working gas.

17 Eq. (10) shows that in regenerator matrices experimental analysis the specific heat  
 18 transfer area is necessary to calculate the heat transfer coefficient. In the majority of  
 19 experimental studies [6,10] the heat transfer area of woven wire screens is expressed as

1  $\varphi = \pi/s V_t$  where  $s$  is the pitch of the mesh and  $V_t$  is the total volume of the regenerator  
2 [17]. Miyabe [9] suggests reducing the gross heat transfer area, given by the total  
3 surface of the wires in the matrix, by the contact areas between each two wires. Thomas  
4 and Bolleber [17] prove that the reduction of the total surface area of the matrix by the  
5 contact areas between the wires is necessary in order to correlate experimental heat  
6 transfer data of Stirling engine regenerators. Moreover, the results presented by  
7 Kolodziej et al. [13] indicate that the number of wire sheet stacked in the test did not  
8 influence the heat transfer intensity because in their experiments the sheets were  
9 separated by thin gaps to avoid their contact.

10 In the present study the wetted regenerator area  $A_{wr}$  is measured in the detailed  
11 geometry (CFD or CAD program) where only the contact between solid matrix and  
12 fluid is considered. For stacked woven wire mesh the contact volumetric porosity is  
13 decreased in a similar range that Gedeon and Wood [10] as **can be compared between**  
14 **Table 1 and Table 2**. The computational domain is initially at a uniform temperature  
15 different from inflow temperature.

### 16 **3. Results and Discussion**

17

#### 18 *3.1. Numerical Validation: Heat transfer correlation for stacked woven wire matrix*

19

20 **In this section, the numerical simulations are performed using a proposed FVM**  
21 **method based numerical solution for the stacked woven wire matrix and a Nusselt**  
22 **number correlation equation is derived from the results. The derived correlation is**  
23 **validated against empirical results provided by Tanaka [6] and Gedeon and Wood [10],**

1 over a range of wire diameter, Re number and volumetric porosity summarize in Table  
2 1.

3 Tanaka [6] investigates the flow and heat transfer characteristics of regenerator  
4 materials in an oscillating flow for conventional stacked woven wire matrix, sponge  
5 metal (felt) and sintered metal. Tanaka [6] obtains the heat transfer area by multiplying  
6 the specific area of the mesh by the regenerator total volume. Tanaka [6] suggests that  
7 the heat transfer coefficient in the oscillating flow may be higher than that in  
8 unidirectional flow.

9 Gedeon and Wood [10] present correlating expressions in terms of Reynolds or  
10 Peclet number for friction factors, Nusselt numbers, enhanced axial conduction ratios  
11 and overall heat flux ratios in stacked woven wire matrices and metal felt test  
12 regenerator samples. One of the main conclusions of the Gedeon and Wood [10]  
13 investigation is that under the range of conditions tested, which were intended to be  
14 representative of most Stirling applications, they found no essential differences  
15 compared to steady flow. In other words, instantaneous local Reynolds number or  
16 Peclet number appear to characterize the flow quite adequately.

17 As can be observed there is not a clear consensus about the effect of the oscillating  
18 flow conditions in the Stirling regenerators. On one hand, Tanaka [6] suggests that it  
19 could enhance the heat transfer and in the other hand, Gedeon and Wood [10] conclude  
20 that there are not significant different with steady conditions in the Stirling regenerator  
21 working range. In the previous authors work [16] the numerical results show good  
22 agreement with the experimental results obtained under oscillating flow conditions,  
23 despite the study is conducted under not oscillating flow conditions. Therefore, those

1 experimental investigations are considered for the validation of the numerical model  
2 presented for the study of stacked woven wire matrix regenerator.

3 In both studies the maximum Reynolds number is calculated based on hydraulic  
4 diameter,  $d_h$  instead of wire diameter. The hydraulic diameter is defined by Tanaka [6]  
5 as:

$$6 \quad d_h = 4\Pi_v / \phi(1 - \Pi_v) \quad (11)$$

7 Where  $\Pi_v$  is the volumetric porosity and  $\phi$  is the shape factor defined as the ratio of  
8 the mesh surface area to the mesh volume.

9 The hydraulic diameter is defined by Gedeon and Wood [10] as:

$$10 \quad d_h = d_w \Pi_v / (1 - \Pi_v) \quad (12)$$

11 The different between these two definitions (Eqs. (11) and (12)) of diameter  
12 hydraulic is not significant. In the present study the hydraulic diameter is determined  
13 by Eq. (12).

14 The specific heat transfer area in a woven wire mesh,  $\varphi$ , is generally defined as:

$$15 \quad \varphi = 4/d_w (1 - \Pi_v) \quad (13)$$

16 Therefore, Reynolds number can be defined as:

$$17 \quad Re = \rho u_{max} d_h / \mu \quad (14)$$

1 The maximum flow velocity  $u_{max}$  is obtained by dividing the frontal maximum  
2 velocity by porosity. The Nusselt number is then defined as follows:

$$3 \quad Nu = h d_h / k_g \quad (15)$$

4 In the present numerical study the heat transfer coefficient is calculated from the  
5 numerical result using Eq. (10).

6 Although the purpose of the present study is to estimate the heat transfer in a wound  
7 woven wire matrix, since there is no experimental data available for this case, the first  
8 step is to validate the computational model for a stacked woven wire matrix in  
9 comparison with the experimentally obtained empirical correlations proposed by cited  
10 researchers above. The validation is made using two different wire diameters and two  
11 configurations of matrices in which, the first configuration is a stacked woven wire  
12 screens parallel misaligned and the second matrix configuration is oriented  $45^\circ$  with its  
13 neighbor so as to simulate a “random stacking”. Furthermore, the stacking volumetric  
14 porosity has two levels for the same woven wire mesh in order to cover any possible  
15 stacking process variation. In Table 2 below the parametric study range for stacked  
16 woven wire matrices is summarized.

17 **Table (1)**

18 Tanaka [6] proposes the following empirical relationship for Nusselt number in a  
19 range of  $10 < Re < 150$ :

$$20 \quad Nu = 0.33Re^{0.67} \quad (16)$$

1 Gedeon and Wood [10] based on combining data sets proposes the following master  
2 correlation for woven wire matrix in terms of Peclet number ( $RePr$ ):

$$3 \quad Nu = (1 + 0.99Pe^{0.66})\Pi_v^{1.79} \quad (17)$$

4 Gedeon and Wood [10] justify the constant 1 in the Nusselt number expression (Eq.  
5 (17)) because  $Nu$  tends to some constant value for  $Pe \approx 0$  as occurs in fully developed  
6 internal laminar flow. Gedeon and Wood [10] claim that a value of  $Nu_0 \approx 1$  seems  
7 reasonable in light of the published limiting value of 0.43 for flow normal to a single  
8 cylinder. Eq. (17) becomes Equation (18) for  $Pr \approx 0.73$  and  $\Pi_v \approx 0.69$  (Average  
9 volumetric porosity in the present study):

$$10 \quad Nu = 0.51 + 0.40Re^{0.66} \quad (18)$$

11 The relative accuracy of the results of Gedeon and Wood [10] for heat transfer  
12 correlations is more dependent on Reynolds number. Thus the worst relative error is  
13 about 10% at peak Reynolds number on the order of 1000 and it is about 50% for peak  
14 Reynolds numbers below about 5.

15 Table 1 summarizes the geometrical characteristics of the woven wire mesh and the  
16 samples tested for different authors. It is important highlighted that in the regenerator  
17 samples used by Gedeon and Wood [10] for obtained empirical correlations the  $\Pi_v$  is  
18 approximated 5% lower than the single mesh  $\Pi_v$ . However, in the samples used by  
19 Tanaka [6] the  $\Pi_v$  is approximated 3% higher, this could means that there is not contact  
20 between different layers. In the present study the models are similar to the Gedeon and  
21 Wood [10] as is shown in Table 2.

1 Eight different configurations of stacked woven wire matrices are numerically  
2 studied, four of them are parallel configuration (Fig. 2a) and the others are cross  
3 configurations (Fig. 2b). Based on heat transfer results the Nusselt number is calculated  
4 for a Reynolds number range from 4 to 400. By fitting these results to the three  
5 coefficient equation form (Eq. (1)), Nusselt number correlation equation is obtained.

7 **Figure (4)**

8 **Figure (5)**

9  
10 Fig. 4 shows the numerical results obtained for stacked woven wire matrices, 110  
11  $\mu\text{m}$  wire diameter, together with the Nusselt number evolution determined due to  
12 Tanaka [6] and Gedeon and Wood [10] for a volumetric porosity of 0.66. The  
13 volumetric porosity chosen corresponds to the volumetric porosity of a single 110  $\mu\text{m}$   
14 wire diameter screen. The Figure 5 on the other hand shows the results for the 80  $\mu\text{m}$   
15 wire diameter together with the distribution of the Nusselt number for a volumetric  
16 porosity of 0.72 due to Gedeon and Wood [10].

17 It is observed from Figs. 4 and 5 that no noticeable difference is reproduced for the  
18 Nusselt number obtained for parallel or cross stacked woven wire matrices  
19 configuration or even in the range of volumetric porosity studied. Nevertheless, it is  
20 necessary to emphasize here that the variation in volumetric porosity is not significant  
21 and the same behavior is also observed for the woven wire mesh geometry. Therefore,  
22 the matrix heat transfer area (**specific heat transfer area**) decreases with an increase in

1 volumetric porosity. In the majority of the samples tested by Gedeon and Wood [10] the  
2 volumetric porosity increases with the **specific heat transfer area** (Table 1).

3 Regarding the correspondence of the present numerical results with the Nusselt  
4 number derived from empirical correlations, it is obvious from Figs. 4 and 5 that the  
5 numerical results are not good correspondence with correlation proposed by Tanaka [6].  
6 However, the numerical results fit well with the correlation proposed by Gedeon and  
7 Wood [10].

8 **Eq. 19** shows the derived numerical correlation for the stacking woven wire matrix  
9 which fit the numerical results for the Nusselt number.

10 
$$Nu = 1.14 + 0.39Re^{0.66} \tag{19}$$

11 **Fig. 6 demonstrates** that Nusselt number correlation equation proposed in the  
12 present study for stacked woven wire matrices (Eq. (19)) shows a good agreement with  
13 the numerical results obtained for the Nusselt number as a function of Reynolds  
14 number. Moreover, for Nusselt number, with the exception of the Reynolds number  
15 range below 40, the agreement is within 10% with Gedeon and Wood [10] empirical  
16 correlations (Eq. (17)). However, for  $Re < 40$  the present numerical results deviate  
17 significantly from the Gedeon and Wood [10] empirical correlations. Gedeon and Wood  
18 [10] conclude that the experimental correlation proposed is not appropriate for low  
19 Reynolds number range. The agreement with Tanaka [6] proposed correlation is not  
20 good.

21 **Figure (6)**

22 **Table (3)**

1 The effect of the volumetric porosity on the Nusselt number is not observed and this  
2 is probably due to the fact that the **specific heat transfer area** in the configuration studied  
3 (Table 2) does not present a significant range of variation. Moreover, it is expected that  
4 the heat transfer behavior be improved with the increase of **specific heat transfer area**.  
5 The effect of the volumetric porosity and **specific heat transfer area** on the regenerator  
6 heat transfer will be studied in future investigation.

7  
8 **Figure (7a) - (d)**  
9

10 The qualitative results for velocity and temperature fields the stacked woven wire  
11 matrices are illustrated in Figs. 7a to d at  $Re$  number of 60 for two different wire  
12 diameters of 80  $\mu\text{m}$  and 110  $\mu\text{m}$ . No significant differences are observed at different  
13 wire diameters except slightly higher maximum local velocity distributions obtained  
14 from the higher wire diameter of **110  $\mu\text{m}$**  for the stacked woven wire matrices as  
15 illustrated in Figs. 7a and c. The velocity contours in the wire matrix domain also  
16 signifies the importance of local increase of velocity magnitudes as an indication of  
17 shear gradients leading to the higher shear stress and hence friction pressure drops for  
18 each case. The higher local temperature values obtained in the flow entry region for  
19 each wire diameter case can be considered to be main source of the heat energy to be  
20 transferred to the entire flow domain as the flow progresses.

1 3.2. Heat Transfer correlation for wound woven wire matrix

2  
3 Having been validated for the stacked woven wire matrices, the present numerical  
4 approach is extended to investigate the heat transfer characteristics and the  
5 corresponding heat transfer coefficients for wound wire matrix configurations. The  
6 configurations studied are the same studied for parallel misaligned stacked woven wire  
7 matrices.

8 Figure (8a) - (d)

9  
10 Figures 8a-d also signifies the local variation of velocity and temperature field  
11 values for the wound woven wire matrices at  $Re$  number of 60 for two different wire  
12 diameters of 80  $\mu\text{m}$  and 110  $\mu\text{m}$ . Similar space-wise evolution of the temperature and  
13 velocity contours are also observed here except slightly higher maximum velocity  
14 values obtained from the wound woven wire matrix case.

15 Figure 9 shows the relationship between Nusselt number and Reynolds number for  
16 the wound woven wire matrix simulations and the solid line presents the Nusselt  
17 number correlation line derived from the present results. It is found that the average  
18 Nusselt number coefficients obtained for wound woven wire matrix are significantly  
19 lower (20%) than those obtained from the stacked woven case for a range of  $20 < Re <$   
20 400.

21 Figure (9)

1 For wound woven wire matrix configuration the three coefficient correlation that  
2 better fits with the numerical results is shown in the Equation (20), where the Reynolds  
3 number is calculated based on the hydraulic diameter:

$$4 \quad Nu = 1.54 + 0.29Re^{0.66} \quad (20)$$

5 The above numerically derived Nusselt correlation equation could be considered to  
6 be a good general approximation to be applied to all configurations studied here for the  
7 wound woven wire mesh matrix. In addition it should be noted here that the dispersion  
8 at high Reynolds number (Maximum standard deviation of 4.4) for the wound woven  
9 wire mesh matrix is higher than that for the stacked woven wire mesh (Maximum  
10 standard deviation of 1.4). Therefore, it is suggested that the geometrical parameters  
11 should be studied carefully in this configuration.

12 Figure 9 shows the Nusselt number results for different volumetric porosities,  
13 specific heat transfer areas and hydraulic diameters in a range of Reynolds number. As  
14 expected, the higher Nusselt numbers are obtained for the matrix configuration with  
15 higher specific heat transfer area (Eq. (7)). Regarding the influence of the hydraulic  
16 diameter, the results show an inverse proportionality with the Nusselt number, in other  
17 words, the Nusselt numbers increase when the hydraulic diameter decreases. Finally, the  
18 results tendency in function of the volumetric porosity is not clear for the matrix  
19 configurations studies; therefore, no clear influence of the volumetric porosity in the  
20 Nusselt number can be concluded. Thus, no relation between increase/decrease  
21 volumetric porosity and the Nusselt number increase/decrease was observed.

1 The matrix geometrical parameters, hydraulic diameter (Eq. (12)) and specific heat  
2 transfer area (Eq.(13)), are function of wire diameter and volumetric porosity.  
3 Consequently, an decrease the volumetric porosity causes a decrease in the hydraulic  
4 diameter and an increase in the specific heat transfer area for the same wire mesh.  
5 Accordingly, the interaction between the matrix geometrical parameters, specific heat  
6 transfer area, hydraulic diameter and volumetric porosity require an in-depth study to  
7 isolate the influence of each one.

#### 8 9 **4. Conclusions**

10 In the present numerical study, a specific correlation is derived to numerically  
11 characterize heat transfer for wound woven wire regenerator matrices following by an  
12 initial numerical validation against experimentally obtained correlation for stacked  
13 woven wire.

14 The validation results show that the derived correlation can be successfully applied  
15 in the  $Re$  number working range in Stirling engine regenerators ( $4 < Re < 400$ ), for  
16 diameter range from 0,08 to 0,11 mm and a volumetric porosity range from 0,60 to  
17 0,68. The numerical study, which is extended to wound wire model case, also  
18 demonstrates an easy and effective use of the derived correlation for determining the  
19 Nusselt number for the **wound woven wire** model for a large Reynolds number range up  
20 to 400. The behavior reported in the present study for stacked and wound woven wire  
21 matrices are for “random or misaligned stacking” in contrast to “regular or aligned  
22 stacking”. It is believed that this new correlation can be also used as a generalized cost-  
23 effective tool for heat transfer characterization and further optimization in wound  
24 woven wire matrix type of regenerator.

1        In the Stirling engine calculation program are needed correlations to determine the  
2 heat transfer and flow friction behaviour of the working gas in the different components,  
3 for this reason is fundamental the characterization of the main components as heat  
4 exchangers and regenerators. The results shown here demonstrate that the present  
5 numerical tool can be used to study the influence or effect of matrix geometrical  
6 parameters (volumetric porosity, hydraulic diameter, specific heat transfer area, etc.) to  
7 improve the woven wire matrix heat transfer mechanism. Therefore, further efforts are  
8 necessary, in order to derive more experimental data which may support the new  
9 correlations.

10

## 1   **References**

- 2   [1]   Dorer V., Weber A. “Energy and CO<sup>2</sup> emissions performance assessment of  
3       residential micro-cogeneration systems with dynamic whole-building simulation  
4       programs”. *Energy Conversion and Management*, vol. 50(2009), p. 648-657.
- 5   [2]   Formosa F., “Despesse G. Analytical model for Stirling cycle machine design”.  
6       *Energy Conversion and Management*, vol. 51 (2010), p.1855-1863
- 7   [3]   Timoumi Y., Tlili I., Nasrallah B. “Performance optimization of Stirling  
8       engines”. *Renewable Energy*, vol. 33 (2008), p. 2134-2144.
- 9   [4]   Organ, A.J. *The Regenerator and the Stirling Engine*. London: Mechanical  
10       Engineering Publications; 1997.
- 11  [5]   Rühlich, I. and Quack, H. “New Regenerator Design for Cryocoolers”. Dresden,  
12       Germany: Technische Universität Dresden, 1999.
- 13  [6]   Tanaka, M., Yamashita, I. and Chisaka, F. “Flow and Heat Transfer  
14       characteristics of the Stirling Engine Regenerator in an Oscillating Flow”. *JSME*  
15       *International Journal*, vol. 33(1990), p. 283-289.
- 16  [7]   Ibrahim, M., et al. “Improving Performance of the Stirling Converter: Redesign of  
17       the Regenerator with Experiments, Computation and Modern Fabrication  
18       Techniques”. Cleveland State University, 2001.
- 19  [8]   Andersen, S.K., Carlsen, H. and Thomsen, P.G. “Numerical study on optimal  
20       stirling engine regenerator matrix designs taking into account the effects of matrix  
21       temperature oscillations”. *Energy Conversion and Management*, vol. 47 (2006), p.  
22       894-908.

- 1 [9] Miyabe, H., Takahashi, S. and Hamaguchi, K. “An approach to the design of  
2 Stirling Engine Regenerator matrix using packs of wire gauzes”. *Proc. IECEC*,  
3 vol. 17 (1982), p. 1839-1844.
- 4 [10] Gedeon, D and Wood, J.G. “Oscillating-Flow regenerator Test Rig: Hardware and  
5 Theory With derived Correlations for Screens and Felts”. NASA CR-198442,  
6 1996.
- 7 [11] Thomas, B. and Pittman, D. “Update on the Evaluation of Different Correlations  
8 for the FLOW Friction Factor and Heat Transfer of Stirling Engine Regenerators”.  
9 *American Institute of Aeronautics and Astronautics*, 2000.
- 10 [12] Tong, L.S. and London, A.L. “Heat transfer and flow friction characteristics of  
11 woven screen and crossed rod matrices”. The American Society of Mechanical  
12 Engineer. Paper No. 56-A-124 (1960).
- 13 [13] Kolodziej, A., Lojewska, J., Jaroszynski, M., Gancarczyk, A. and Jodlowski, P.  
14 “Heat transfer and flow resistance for stacked wire gauzes: Experiments and  
15 modeling”. *International Journal of Heat and Fluid Flow*, vol. 33 (2012), p. 101-  
16 108.
- 17 [14] Golneshan, Ali A and Zarinchang, Jafar. “3-D Numerical Analysis of  
18 Thermal/Fluid Characteristics of Woven mesh Structures as Heat Regenerators”.  
19 *Proc. International Stirling Engine Conference*, 13<sup>th</sup> (2007), p. 112-115.
- 20 [15] Ibrahim, Mounir B. and Tew, Roy C. *Stirling Converter Regenerators*. Florida:  
21 CRC Press City Boca Raton, 2012. ISBN 9781439830062.

- 1 [16] Costa, S.C., Barrutia, H., Esnaola, J.A. and Tutar, M. “Numerical study of the  
2 pressure drop phenomena in wound woven wire matrix of a Stirling regenerator”.  
3 *Energy Conversion and Management*, vol. 67 (2013), p. 57–65
- 4 [17] Thomas, B. and Bolleber, F. “Evaluation of 5 different correlations for the heat  
5 transfer in Stirling engine regenerators”. *Proceedings of Europaisches Stirling  
6 Forum*, vol. 35 (2000), p. 111.119.
- 7 [18] Tew, R., et al. “Stirling Convertor CFD Model Development and Regenerator  
8 R&D Efforts”. NASA TM-213404 (2004).
- 9 [19] Cheadle, M.J.; Nellis, G.F. and Klein, S.A. “Regenerator Friction Factor and  
10 Nusselt Number Information derived from CFD analysis”. *International  
11 Cryocoolers Conference*, 2011.
- 12 [20] Tao, Y.B.; Liu, Y.W.; Gao, F.; Chen, X.Y. and He, Y.L. “Numerical analysis on  
13 pressure drop and heat transfer performance of mesh regenerators used in  
14 cryocoolers”. *Cryogenics*, vol. 49 (2009), p. 497-503.
- 15 [21] Dyson, R.W.; Wilson, S.D.; Tew, R.C. and Demko, R. “On the Need for  
16 Mulidimensional Stirling Simulation”. NASA/TM-2005-213975. AIAA-2005-  
17 5557.
- 18 [22] Fluent Dynamics Software. ANSYS FLUENT. Lebanon, NT 6.1.7601, (2010).  
19

1 **Figures Captions**

2

3 Figure 1. Global computational domain for stacked woven wire matrix

4 Figure 2. 2D flow perpendicular plane layouts: a) Parallel staked misaligned and b)  
5 cross stacked misaligned configurations.

6 **Figure 3. a) 3D view of the surface mesh for a stacked woven wire matrix; b) 3D view**  
7 **of the surface mesh for a wound woven wire matrix and c) 2D plane view of**  
8 **stacked woven wire flow mesh.**

9 Figure 4. Stacked woven wire matrices for 110 $\mu\text{m}$  wire diameter: Nusselt number  
10 versus Reynolds number

11 Figure 5. Stacked woven wire matrices for 80 $\mu\text{m}$  wire diameter: Nusselt number  
12 versus Reynolds number

13 Figure 6. Nusselt number correlation comparison for Stacked woven wire matrices.

14 **Figure 7. Stacked woven wire matrices results for  $\text{Re} \approx 60$  ( $u_{\text{in}} = 1$  m/s) at 0.02s: a)**  
15 **Velocity vector through 80 $\mu\text{m}$  matrix; b) Velocity vector colored by**  
16 **temperature through 80 $\mu\text{m}$  matrix; c) Velocity vector through 110 $\mu\text{m}$  and d)**  
17 **Velocity vector colored by temperature contour through 110 $\mu\text{m}$  matrix.**

18 **Figure 8. Wound woven wire matrices results for  $\text{Re} \approx 60$  ( $u_{\text{in}} = 1$  m/s) at 0.02s: a)**  
19 **Velocity vector through 80 $\mu\text{m}$  matrix; b) Velocity vector colored by**  
20 **temperature through 80 $\mu\text{m}$  matrix; c) Velocity vector through 110 $\mu\text{m}$  and d)**  
21 **Velocity vector colored by temperature contour through 110 $\mu\text{m}$  matrix.**

22 Figure 9. Nusselt number correlation comparison for Wound woven wire matrices.

23

24

1 **Tables Captions**

2 **Table 1.** Gedeon/Wood [10] and Tanaka [6] tested regenerator matrix parameters

3 **Table 2.** Present Study modeled regenerator matrix parameters

4 **Table 3.** Tanaka [6] and Gedeon and Wood [10] experimental range for stacked woven  
5 wire matrix and experimentally obtained empirical correlations for Nusselt number,  
6 and present study numerical correlations for Nusselt number.

7

8

1 Table 1.

Study	Wire Mesh Geometry				Regenerator Matrix Geometry		
	Wire /inch	$d_w$ [ $\mu\text{m}$ ]	Opening [ $\mu\text{m}$ ]	Porosity [%]	$\Pi_v$ [%]	$\varphi$ [1/ $\mu\text{m}$ ]	$d_h$ [ $\mu\text{m}$ ]
Gedeon/Wood [10]	200	53.3	74	67.0	62.3 (-4.7)	0.028	88
Gedeon/Wood [10]	100	55.9	198	82.7	78.1 (-4.6)	0.016	199
Gedeon/Wood [10]	80	94	224	76.7	71.0 (-5.7)	0.012	230
Tanaka [6]	50	230	278	64.4	64.5 (+0.1)	0.006	418
Tanaka [6]	100	100	154	69.1	71.1 (+2.0)	0.012	246
Tanaka [6]	150	60	109	72.2	75.4 (+3.2)	0.016	184
Tanaka [6]	200	50	77	69.1	72.9 (+3.8)	0.022	135

2

3

4

1 Table 2.

Study	Wire Mesh Geometry				Regenerator Matrix Geometry		
	Wire /inch	$d_w$ [ $\mu\text{m}$ ]	Opening [ $\mu\text{m}$ ]	Porosity [%]	$\Pi_v$ [%]	$\varphi$ [1/ $\mu\text{m}$ ]	$d_h$ [ $\mu\text{m}$ ]
<i>Present Study</i>	113	80	144	72.0	66 (-6)	0.017	155
<i>Present Study</i>	113	80	144	72.0	68 (-4)	0.016	170
<i>Present Study</i>	100	110	144	66.0	60 (-6)	0.015	165
<i>Present Study</i>	100	110	144	66.0	63 (-3)	0.013	187

2

3

1 Table 3.

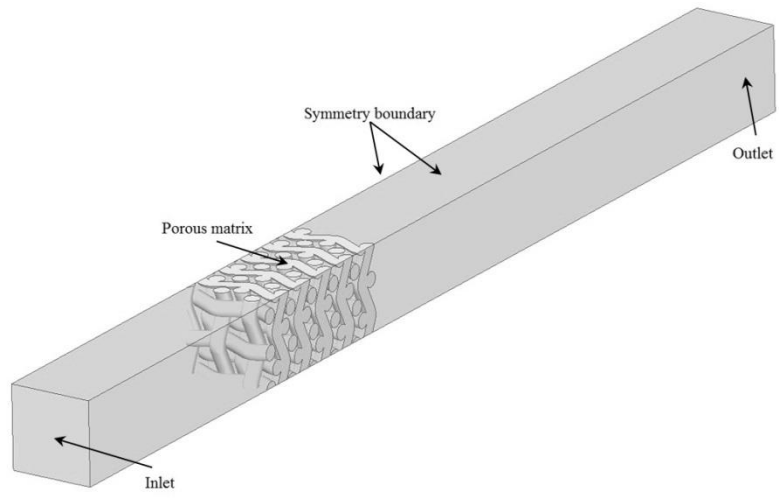
2

	Wire diameter [ $\mu\text{m}$ ]	Porosity [%]	Re range	Correlation
<b>Tanaka [6]</b>	50 to 230	64 to 73	10 to 150	$Nu = 0.33Re^{0.67}$
<b>Gedeon/Wood [10]</b>	53.3 to 94	62 to 78	1.04 to 3400	$*Nu = 0.51 + 0.40Re^{0.66}$
<b>Stacked Present Study</b>	80 to 110	60 to 68	4 to 400	$Nu = 1.14 + 0.39Re^{0.66}$
<b>Wound Present Study</b>	80 to 110	60 to 68	4 to 400	$Nu = 1.54 + 0.29Re^{0.66}$

3 \*The correlation for Nusselt number is for a  $Pr \approx 0.73$  and  $II_v \approx 0.69$

4

1 Figure 1

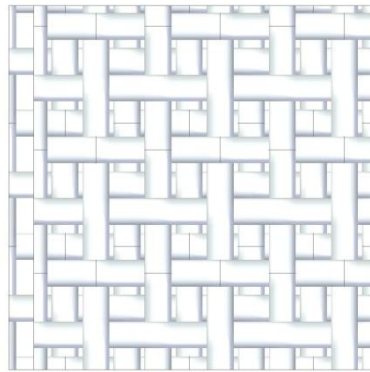


2

3

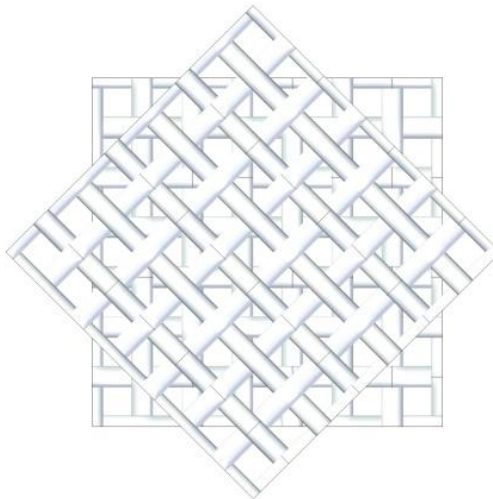
4

1 Figure 2a



2

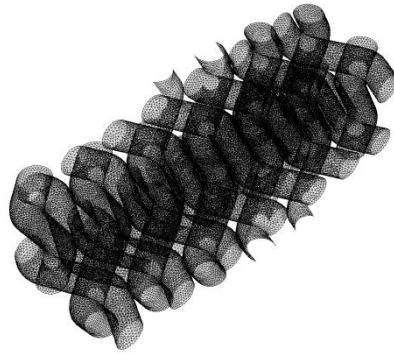
3 Figure 2b



4

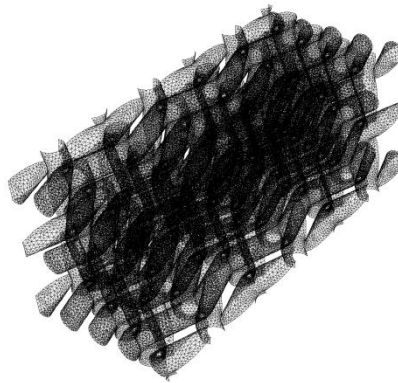
5

1 Figure 3a



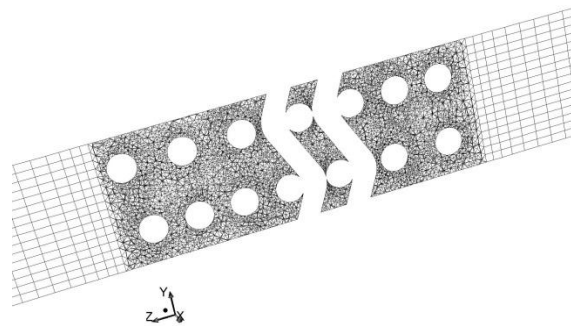
2

3 Figure 3b



4

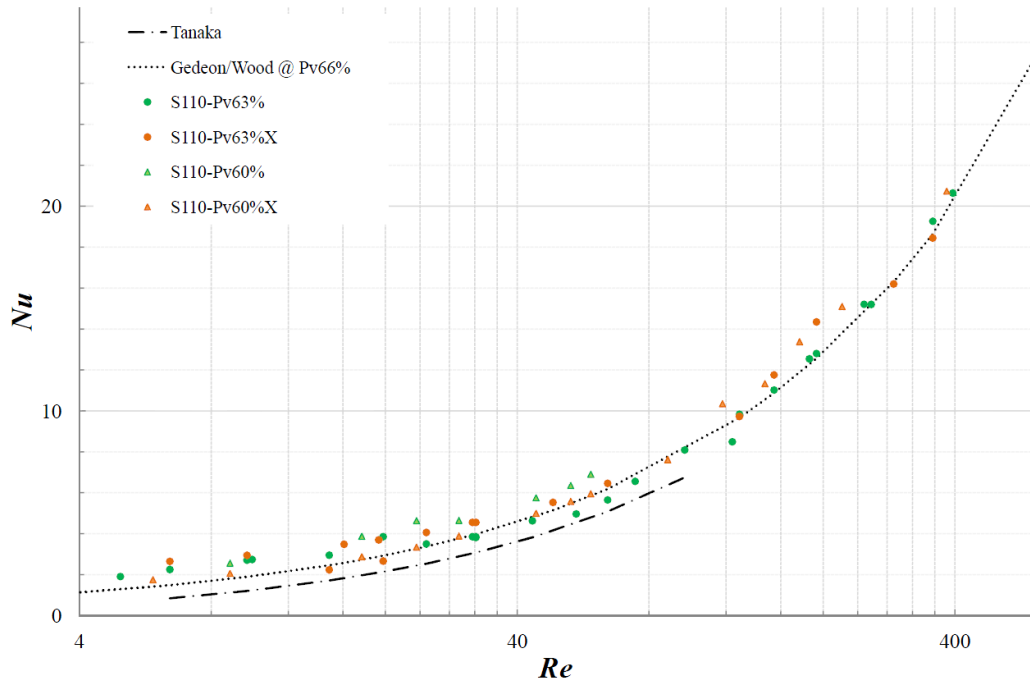
5 Figure 3c



6

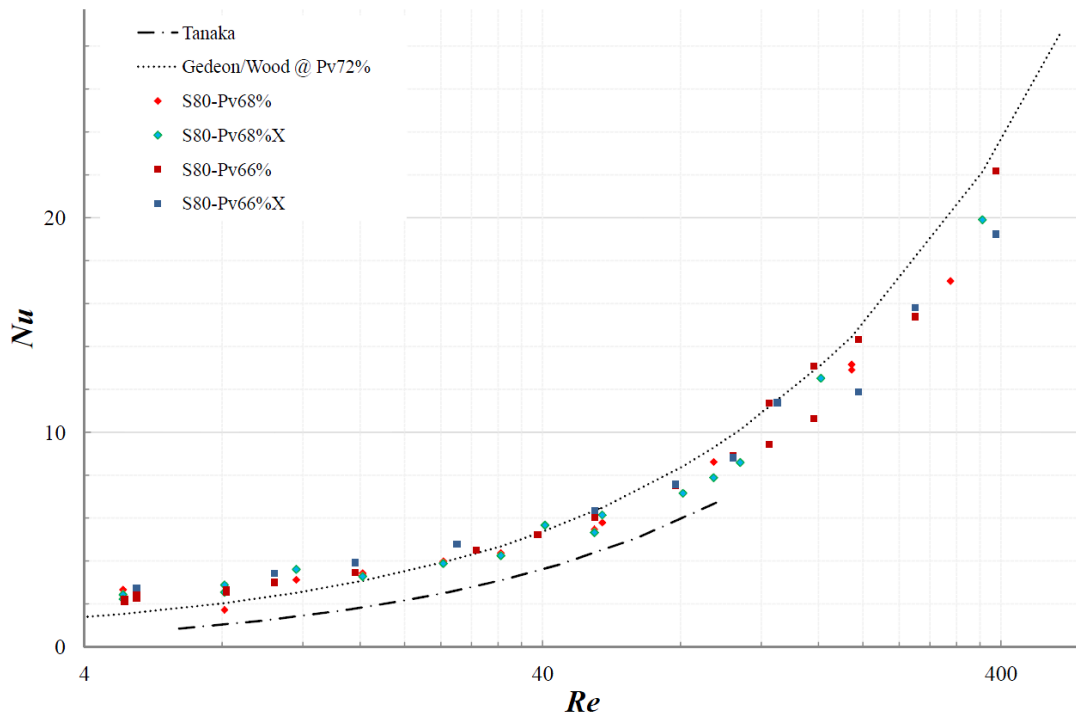
7

1 Figure 4



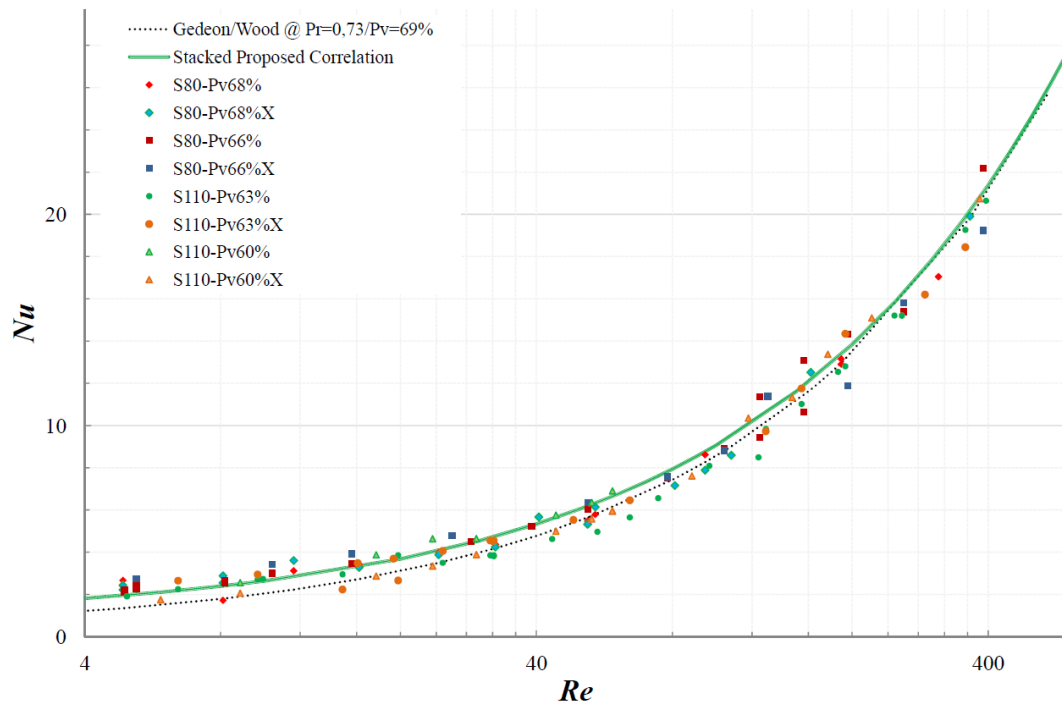
2

3 Figure 5



4

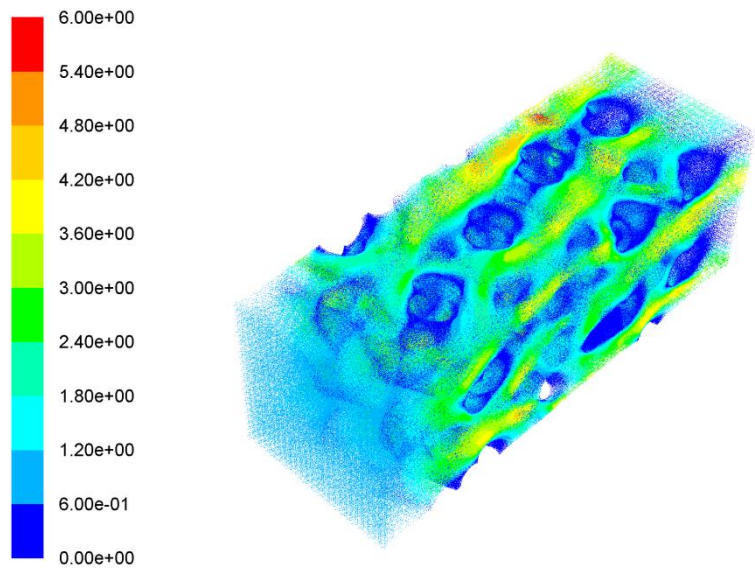
1 Figure 6



2

3

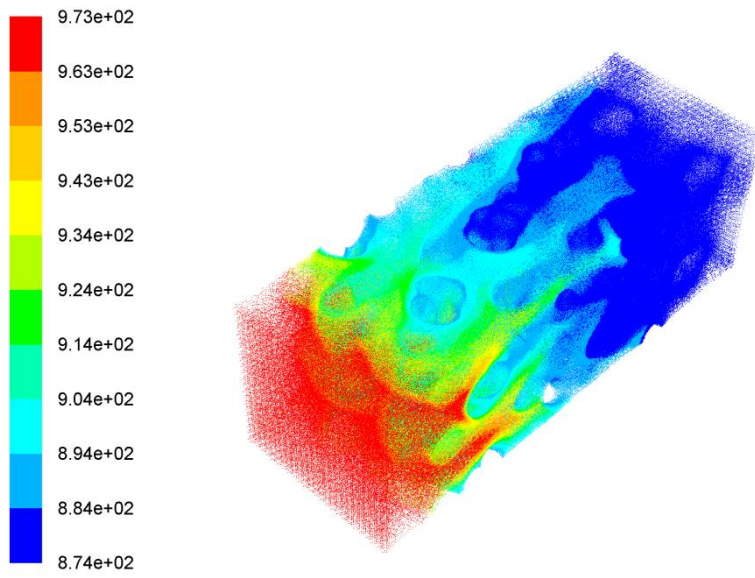
1 Figure 7a



2

3

4 Figure 7b

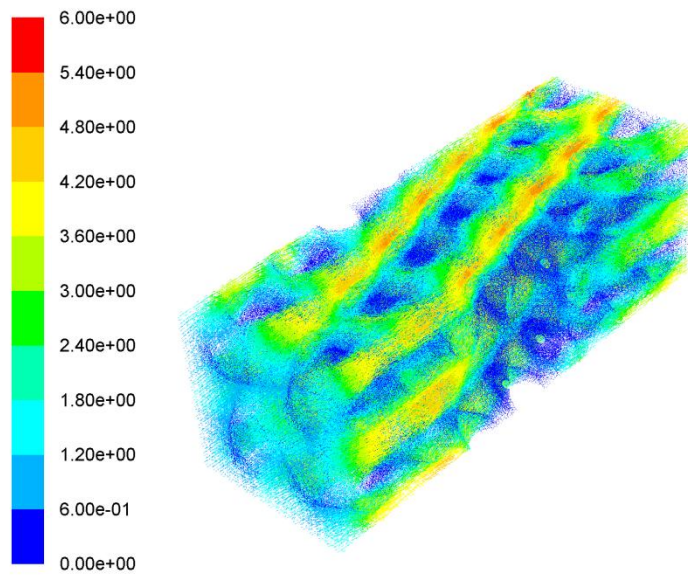


5

6

7

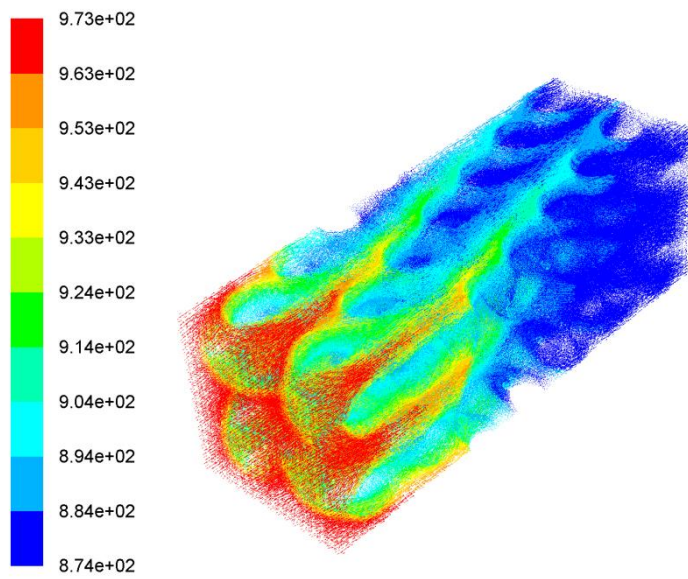
1 Figure 7c



2

3

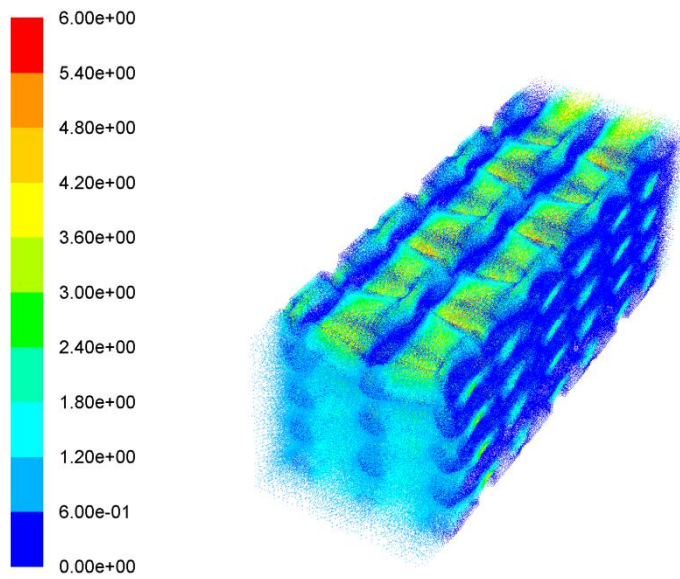
4 Figure 7d



5

6

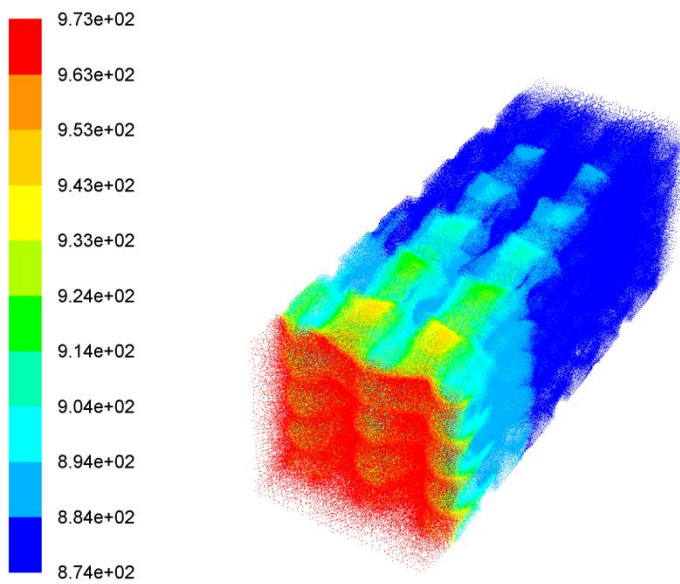
1 Figure 8a



2

3

4 Figure 8b

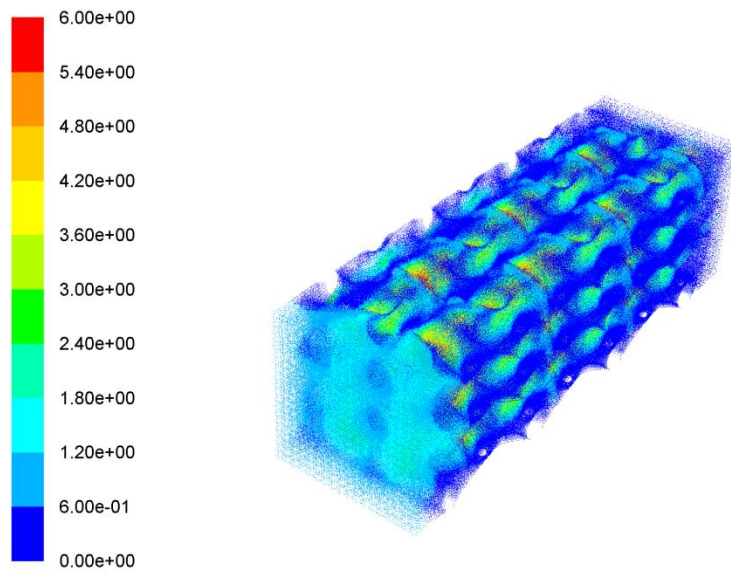


5

6

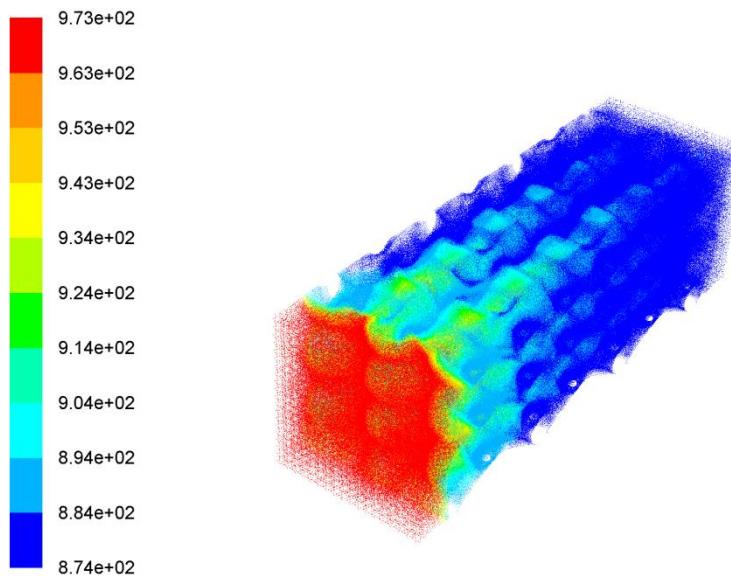
7

1 Figure 8c



2

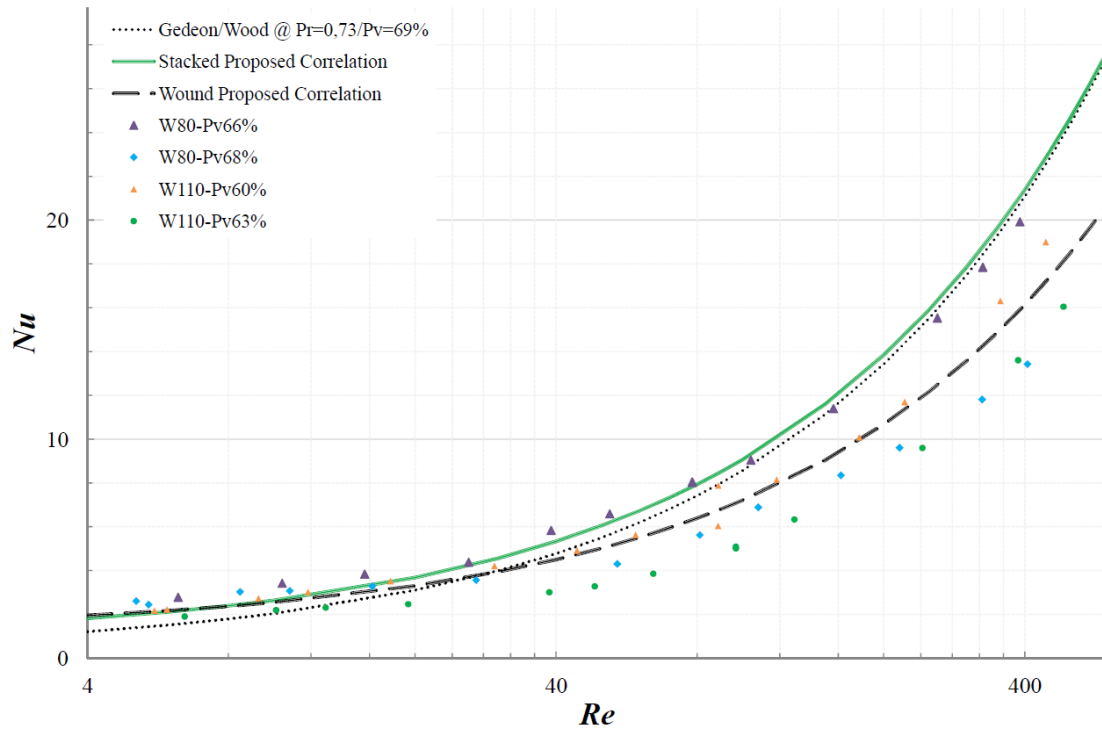
3 Figure 8d



4

5

1 Figure 9



2

## **Numerical study of the heat transfer in wound woven wire matrix of a Stirling regenerator**

S.C. Costa<sup>a\*</sup>, Harritz Barrutia<sup>b</sup>, Jon Ander Esnaola<sup>b</sup>, Mustafa Tutar<sup>b,c</sup>

<sup>a</sup> CS Centro Stirling S. Coop, Avda. Alaba 3, 20550, Aretxabaleta, Spain

<sup>b</sup> Mechanical and Manufacturing Department, Engineering Faculty of Mondragon  
University, Loramendi 4, 20500, Mondragon, Spain

<sup>c</sup> IKERBASQUE, Basque Foundation for Science, 48011, Bilbao, Spain

\*Corresponding author. Tel.: +34 943 037 948 ; Fax: +34 943 792 393

E-mail address: [ccosta@centrostirling.com](mailto:ccosta@centrostirling.com) (S.C.Costa)

## **Abstract**

Nusselt number correlation equations are numerically derived by characterizing the heat transfer phenomena through porous medium of both stacked and wound woven wire matrices of a Stirling engine regenerator over a specified range of Reynolds number, diameter and porosity. A finite volume method (FVM) based numerical approach is proposed and validated against well known experimentally obtained empirical correlations for a random stacking woven wire matrix, the most widely used due to fabrication issues, for Reynolds number up to 400. The results show that the numerically derived correlation equation corresponds well with the experimentally obtained correlations with less than 6 percent deviation with the exception of low Reynolds numbers. Once the numerical approach is validated, the study is further extended to characterize the heat transfer in a wound woven wire matrix model for a diameter range from 0,08 to 0,11 mm and a porosity range from 0,60 to 0,68 within the same Reynolds number range. Thus, the new correlation equations are numerically derived for different flow configurations of the Stirling engine Regenerator. It is believed that the developed correlations can be applied with confidence as a cost effective solution to characterize and hence to optimize stacked and wound woven wire Stirling regenerator in the above specified ranges.

*Keyword: Stirling engine; heat transfer; Nusselt number; porosity; CFD.*

## Nomenclature

$A$ :	Heat transfer area	[m <sup>2</sup> ]
$A_{wr}$ :	Regenerator matrix wetted area	[m <sup>2</sup> ]
$c_1, c_2, c_3$ :	Nusselt correlation constants	[-]
$c_p$ :	Heat capacity at constant pressure	[J/kg K]
$c_v$ :	Heat capacity at constant volume	[J/kg K]
$d_h$ :	Regenerator matrix hydraulic diameter	[m]
$d_w$ :	Wire diameter	[m]
$E$ :	Total energy	[J]
$h$ :	Heat transfer coefficient	[W/m <sup>2</sup> K]
$h$ :	Sensible enthalpy	[J/kg]
$\vec{J}_j$ :	Diffusion flux of species	[kg/m <sup>2</sup> s]
$k$ :	Thermal conductivity	[W/m K]
$k_{eff}$ :	Effective conductivity	[W/m K]
$k_g$ :	Working gas thermal conductivity	[W/m K]
$k_t$ :	Turbulent thermal conductivity	[W/m K]
$\dot{m}$ :	Mass flow rate	[kg/s]
$Nu$ :	Nusselt number	[-]
$p$ :	Pressure	[Pa]
$Pe$ :	Peclet number	[-]
$Q$ :	Heat transfer	[W]
$q$ :	Heat flux	[W/m <sup>2</sup> ]
$R$ :	Gas-law constant	[J/kg K]
$Re$ :	Reynolds number	[-]
$S_h$ :	Volumetric rate of heat generation	[W/m <sup>3</sup> ]
$s$ :	Cell size	[m]
$s$ :	Pitch of the mesh	[-]
$T$ :	Temperature	[K]
$T_g$ :	Working gas temperature	[K]
$T_r$ :	Regenerator matrix temperature	[K]

$t$ :	Time	[s]
$u$ :	Velocity magnitude in x direction	[m/s]
$u_{max}$ :	Matrix velocity	[m/s]
$V_t$ :	Total volume of regenerator matrix	[m <sup>3</sup> ]
$\vec{v}$ :	Overall velocity vector	[m/s]
$Y_j$ :	Mass fraction of species	[-]
$\mu$ :	Fluid dynamic viscosity	[kg/m s]
$\rho$ :	Fluid density	[kg/m <sup>3</sup> ]
$\Pi_v$ :	Regenerator matrix volumetric porosity	[-]
$\varphi$ :	Regenerator matrix specific heat transfer area	[1/m]
$\phi$ :	Regenerator matrix shape factor	[1/m]
$\tau$ :	Non-dimensional time	[-]
$\bar{\tau}$ :	Stress tensor	[Pa]

## 1. Introduction

Stirling engine technology has been identified as an excellent candidate for energy cogeneration applications due to its elevated total efficiency (higher than 90%), the possibility to operate with any kind of temperature heat source (solar, combustible material, field waste, biomass, nuclear, etc.) and low noise and contamination levels [1-3]. The regenerator is considered by many researchers as the key component to improve the efficiency of the next generation of Stirling engine systems [4-8]. In the Stirling-engine regenerators, the heat transfer and the pressure drop are the main phenomena associated to energy efficiency and have been studied by many researchers [6, 9-14, 16]. For this reason, the characterization of these two phenomena through experimental, theoretical and numerical studies is crucial to maximize the thermal efficiency and incoming outsource energy in Stirling engine.

Research efforts [4-5, 8-10, 15] have shown that high fluid-to-matrix heat transfer together with low pressure drop can be obtained by using a matrix with the characteristics of: smooth heat transfer surface, controlled flow acceleration rates, minimized flow separation and uniform passages flow distribution.

Currently, regenerators are usually made of stacked woven wire screen or random fibers. Thus, most of the research studies conducted for the thermal and fluid characterization in the Stirling regenerator have mainly focused on empirical characterization of these. The heat transfer between the matrix of the regenerator and the working gas has been studied from various points of view, many of them based on Hausen's (1929) reference work. Moreover, several experimental studies have been conducted in order to evaluate the heat transfer in different regenerator's matrices determining empirical correlation for Nusselt number  $Nu$ .

Tong and London [12] study the heat transfer and flow friction characteristics of woven wire screen and crossed rod in steady flow in a wide range of Reynolds number,  $Re$ . In the experiments each “screen element” is oriented  $45^\circ$  with its neighbor so as to simulate a “random stacking” in contrast to a “regular or aligned stacking” where all the wire elements, for instances, would be either parallel or right angles with each other.

Miyabe [9] in addition to his theoretical work derives generalized experimental equations of flow friction factor and heat transfer coefficient for packed wire screens with variety of geometries. Tanaka [6] investigates the flow and heat transfer characteristics of the regenerator materials in an oscillating flow for wire net and sponge metal. Gedeon and Wood [10] derive generic correlations for friction factor, Nusselt number, enhanced axial conduction ratio and overall heat flux ratio based on the test samples of a number of wire mesh (random stacking) and metal felt, with a range of porosities.

Thomas and Bolleber [17] compare different and often used correlations for heat transfer of Stirling engine regenerators. Each author formulates a different definition for Reynolds and Nusselt numbers as well as heat transfer area. All those authors use samples of wire screen or random fiber matrices for their investigations.

Generally, the Nusselt number is a function of Reynolds and Prandtl number (Peclet number) [10]. However, when dealing with the heat transfer in the regenerator of a Stirling machine, the Prandtl number is insignificant, since it can always be approximated as 0.7 for the gases used as working fluids in Stirling machines. The impact of  $Re$  is given by the following general correlation [17]:

$$Nu = c_1 + c_2 Re^{c_3} \quad (1)$$

In Eq. (1) the coefficient are constants determined by the experimental data. Thomas and Bolleber [17] observe that the Nusselt number is not only a function of Reynolds number. The majority of experimental data reveal the additional impact of the porosity on Nusselt number. Thus the effect of the porosity must be attributed to the specific heat transfer area. The impact of the property data on the working fluid, given by the Prandtl number, is also negligible.

Apart from the analytical studies, there are some numerical analyses of the heat transfer and pressure drop through wire screen matrix using different numerical discretization techniques. The finite volume method (FVM) appears to be promising as numerical investigation tool indicated by Rühlich and Quack [5], Gedeon and Wood [10], Ibrahim et al. [7], Tew [18], Cheadle et al. [19], Tao et al. [20] and others. These numerical studies suggest that the fluid flow and thermal simulations are highly required to understand the flow of interest and hence to characterize fluid flow friction behavior for such systems of regenerator applications. The work of Cheadle et al. [19] outlines the development of a design tool that is capable of deriving Nusselt number and friction factor correlations based on computational fluid dynamic (CFD) analysis of a 2-D unit-cell model that considers the microscopic interactions between the fluid and solid.

Kolodziej et al. [13] indicate that despite the fact stacked wire screen are used for years in different applications that involves heat recuperation or regenerators, their transport and friction phenomena are still not described well enough. The number of studies dealing with the gauze flow resistance and heat transfer is rather limited. Moreover, there is a considerable lack of more general models that could be able to

predict transport properties of any wire gauze, which have not been experimentally described before.

One important issue in the progress to improvements Stirling models is the geometrical shape of the matrix in the regenerator and most regenerator models don't assume a precise geometrical shape for the elements of the regenerator [21]. Dydson et al. [21] indicate that clearly, the shape of the regenerator has an important impact on the overall Stirling system design.

As summarized above, the majority of experimental studies and correlations are generally conducted for stacked woven wire screen regenerator matrices as they are the most widely used ones. However, this kind of regenerator tends to be the one of the most expensive components of the Stirling engines, which nowadays limits the use of this technology for micro-cogeneration application in domestic environments. For this reason, the use of wound woven wire matrix regenerators could be a more cost effective alternative solution that would overcome such limitations [16]. Therefore, heat transfer and flow friction characteristics of these matrices are of interest for Stirling cycle applications. Even though, very few research works have been carried out for this type of regenerator, no specific heat transfer correlations are known to exist in literature. Thus, there is still a very high necessity of characterize heat transfer in this type of regenerator.

Consequently, the objective of this study is to numerically develop a heat transfer correlation for wound woven matrix regenerator. With this respect, numerical 3-D detailed models for a stacked woven wire matrix are initially developed to obtain heat transfer correlations for different configurations and the results are compared with well-

known experimentally obtained correlations in order to validate the proposed models over a specified range of Reynolds number. Later, the numerical study is extended to obtain heat transfer correlation equation for wound woven wire matrices. The good correspondence of the stacked woven wire matrix configuration with experimental data suggests that the derived correlations can be used with confidence to characterize and hence to optimize wound woven wire matrix Stirling regenerator. However, it is expected that the developed correlations will be experimentally validated for future applications and used to limit the try and error cost in Stirling design. It should be noticed that a similar study dealing with the development of numerical correlation for the flow friction factor through a wound woven matrix regenerator, has been recently published by the authors [16].

## **2. Computational Principles**

### *2.1. Numerical methodology*

The numerical methodology adopted in the previous work of the authors [16] for the numerical resolution of pressure drop characteristics of Stirling flow under isothermal flow condition is extended here to investigate the heat transfer phenomena by solving additional governing integral equation for the conservation of energy in de-coupled (segregated) manner.

In this study, the fluid is considered to be viscous, unsteady, incompressible and Newtonian with constant fluid flow properties, and three-dimensional (3-D) with assumption of laminar flow behavior at very low Reynolds number range and of turbulent flow behavior at high Reynolds number. As authors demonstrate in previous

work [16], when the Reynolds number exceeds a certain value depending on the configuration of the wire matrix used, the local instabilities due to emergence of turbulence leads to numerical convergence problem and the simulations are conducted in turbulent manner.

In this study due to the small range of temperature used in each case, all fluid properties (including density, viscosity, specific heat, and conductivity) are assumed constant. The present flow is mathematically governed by continuity, momentum and energy equation. The governing equations are discretized and solved sequentially using a finite volume method (FVM) based numerical flow solver [22] with a second order upwind scheme for the discretization of the continuity, momentum and energy equations for the laminar flow solutions. The convergence criterion for all the velocity components and for the continuity is set to  $10^{-6}$ , whereas it is set to  $10^{-8}$  for the energy for all simulations. The non-dimensional time step,  $\tau = u_{\max} t / s$  is expressed as the product of the maximum velocity component at the inflow boundary and time elapsed divided by the volume cell size. The non-dimensional time step values are chosen as 0.01 following an initial sensitivity analysis performed for the variation of Nusselt number with respect to different non-dimensional time step size ranging from 0.001 to 0.01 for different Re number of 64 and 355. This test shows that there is no significant influence of choice of non-dimensional time step size between 0.01 and 0.001 on the results of Nusselt number obtained for the investigated Re number.

## 2.2. Computational domain and boundary conditions

Figure 1 illustrates the region of flow of interest (geometry set-up) in which the woven wire matrix and the flow through woven wire matrix geometry is extensively analyzed as a representation of a differential part of a Stirling regenerator arrangement. As Cheadle et al. [19] mention the modeling of typical regenerator geometries would require detailed 3-D models with prohibitively long solutions times. For this reason, in order to capture the heat and momentum interactions at the microscopic level, a small representative portion of the regenerator is modeled. The inlet and outlet flow areas are set to approximately  $0.5 \text{ mm}^2$  and woven wire matrix length is approximately 1.5 mm.

Figure 1

The Reynolds number based on hydraulic diameter is varied from 4 to 400. In some simulations the computational domain is further extended in the downstream direction (in the nominal direction of the outlet flow) in order to avoid reverse flow conditions at the outflow boundary.

In the geometrical model to simulate the random stacking of the different sheets, two different misaligned configurations, parallel and cross, for stacked woven wire matrix are generated and studied. In the wound woven wire matrix just the misaligned parallel configuration is generated and studied because in a winding process the cross case is more difficult to obtain. All the configurations are generated based on two woven wire mesh,  $80 \text{ }\mu\text{m}$  and  $110 \text{ }\mu\text{m}$  as described in Table 1. Furthermore, for each

woven wire mesh small changes in the volumetric porosity ranges,  $\Pi_v$ , are realized. The range of porosity evaluates is from 0.60 to 0.68. Figs. 2a and b show the configurations for parallel and cross local matrix for stacked woven models, respectively.

### Figures (2a) - (b)

Miyabe [9] indicates that the empirical equation derived for Nusselt is expressed in a generalized form, and it is recommended that the matrix be made so that all screens are closely stacked. If each screen is not stacked perfectly, or when any gap exists between the screens, the friction coefficient and Nusselt number will deviate from the actual value to some extent.

In Figure 3 are shown the matrix surface mesh for a stacked and wound woven wire matrix and a two-dimension section in the flow direction for fluid.

### Figure (3a) - (c)

The computational domain is constructed of non-uniformly distributed different hybrid mesh systems containing over 2.5 million tetrahedral and/or hexahedral volume cells for the final mesh system. The tetrahedral cells are used in the wire matrix and air volume inside the matrix with very fine mesh resolution in the close vicinity of the wire surfaces to resolve sharply varying velocity and pressure gradients there. The effect of the mesh resolution on the flow has been previously assessed with the authors [16] for three different mesh systems containing non-uniformly distributed hybrid grid cells in a quarter of the computational domain. It is demonstrated that there is no major difference

among the computed values and the mesh system of over 2.5 million hybrid volume cells, in the current study the number of cell is multiplying by four. Thus, the final mesh system could be considered to be fine enough to study the effects of Reynolds number on the heat transfer characterization.

For all woven wire matrix configurations, all model simulations are carried out by considering the following boundary conditions:

1. Inflow boundary: Velocity inlet boundary conditions at constant temperature are used to define the fluid uniform velocity profile.
2. Outflow boundary: Pressure outlet boundary conditions are assigned to define the static (gauge) pressure by eliminating reverse flow problem.
3. Side boundary: Free-slip symmetry flow boundary conditions at the four side boundaries of the computational domain are imposed. The normal velocity components and the normal gradients of all velocity components are assumed to have a zero value.
4. Interior wall boundaries: No-slip wall boundary conditions together with the enhanced wall functions are assigned to interior wall boundaries between wires and fluid for turbulent simulation cases. Moreover, any thermal condition is assigned to the wall between the fluid and the solid matrix, and the two sides of the wall are coupled.

### 2.3. Heat transfer model

The energy equation form solves in ANSYS FLUENT [22] is the following:

$$\frac{\partial}{\partial t}(\rho E) + \nabla \cdot (\vec{v}(\rho E + p)) = \nabla \cdot (k_{eff} \nabla T - \sum_j h_j \vec{J}_j + (\bar{\tau}_{eff} \cdot \vec{v})) + S_h \quad (2)$$

Where  $k_{eff}$  is the effective conductivity ( $k + k_t$ ), where  $k_t$  is the turbulence thermal conductivity, defined according to the turbulence model being used, and  $\vec{J}_j$  is the diffusion flux of species  $j$ . The first three terms on the right-hand side of Equation (2) represent energy transfer due to conduction, species diffusion, and viscous dissipation respectively.  $S_h$  includes the heat of chemical reaction, and any other volumetric heat sources defined.

In Eq. (2)

$$E = h - \frac{p}{\rho} + \frac{v^2}{2} \quad (3)$$

where sensible enthalpy  $h$  is defined for incompressible flow as

$$h = \sum_j Y_j h_j + \frac{p}{\rho} \quad (4)$$

for ideal gas the last term of Eq. (4) is eliminated. In Eq. (4),  $Y_j$  is the mass fraction of species  $j$  and

$$h_j = \int_{T_{ref}}^T c_{p,j} dT \quad (5)$$

In one-dimensional the gas energy Eq. (2) is written as:

$$\frac{\partial}{\partial t} (\rho E) + \frac{\partial}{\partial x} \cdot (u(\rho E + p) + q) - Q = 0 \quad (6)$$

Solid matrix to gas heat transfer  $Q$  can be expressed in terms of a heat transfer coefficient  $h$  as follow:

$$Q = hA(T_r - T_g) \quad (7)$$

Ignoring the kinetic energy term ( $u^2/2$ ) in Eq. (6), and expressing  $\rho E = (c_v/R)p$  and  $+p = c_p\rho T$ , the alternative form of the energy equation is:

$$\left(c_{vg}/R\right)\frac{\partial p}{\partial t} + \frac{\partial}{\partial x} \cdot \left(c_{pg}\dot{m}T_g + q\right) - hA(T_r - T_g) = 0 \quad (8)$$

Eq. (8) is transformed into Eq. (9) assuming that the first term of the Eq. (8) is negligible, the mass flow is uniform in the matrix, the matrix temperature is linear and the apparent conductivity is not a function of  $x$ . By combining the last two assumptions the term becomes as  $\frac{\partial q}{\partial x} = k_a \frac{\partial^2 T}{\partial x^2} \approx 0$ .

$$\dot{m}c_{pg} \frac{\partial T_g}{\partial x} = hA(T_r - T_g) \quad (9)$$

Eq. (9) is easily solved to given the heat transfer coefficient based on numerical modeling results between two planes  $\Delta x$  as follows:

$$h = \frac{\dot{m}c_{pg}\Delta T_g}{A_{wr}\Delta T_{m_{log}}} \quad (10)$$

Where the  $\dot{m}$  is the mass flow of the working gas,  $c_{pg}$  is the gas specific heat at constant pressure,  $\Delta T_g$  is the different in gas temperature between the entrance and exit plane in the model,  $A_{wr}$  is the regenerator wetted area and  $\Delta T_{m_{log}}$  is a logarithmic average of the temperature difference between the regenerator matrix surface and working gas.

Eq. (10) shows that in regenerator matrices experimental analysis the specific heat transfer area is necessary to calculate the heat transfer coefficient. In the majority of experimental studies [6,10] the heat transfer area of woven wire screens is expressed as

$\varphi = \pi/s V_t$  where  $s$  is the pitch of the mesh and  $V_t$  is the total volume of the regenerator [17]. Miyabe [9] suggests reducing the gross heat transfer area, given by the total surface of the wires in the matrix, by the contact areas between each two wires. Thomas and Bolleber [17] prove that the reduction of the total surface area of the matrix by the contact areas between the wires is necessary in order to correlate experimental heat transfer data of Stirling engine regenerators. Moreover, the results presented by Kolodziej et al. [13] indicate that the number of wire sheet stacked in the test did not influence the heat transfer intensity because in their experiments the sheets were separated by thin gaps to avoid their contact.

In the present study the wetted regenerator area  $A_{wr}$  is measured in the detailed geometry (CFD or CAD program) where only the contact between solid matrix and fluid is considered. For stacked woven wire mesh the contact volumetric porosity is decreased in a similar range that Gedeon and Wood [10] as can be compared between Table 1 and Table 2. The computational domain is initially at a uniform temperature different from inflow temperature.

### **3. Results and Discussion**

#### *3.1. Numerical Validation: Heat transfer correlation for stacked woven wire matrix*

In this section, the numerical simulations are performed using a proposed FVM method based numerical solution for the stacked woven wire matrix and a Nusselt number correlation equation is derived from the results. The derived correlation is validated against empirical results provided by Tanaka [6] and Gedeon and Wood [10],

over a range of wire diameter, Re number and volumetric porosity summarize in Table 1.

Tanaka [6] investigates the flow and heat transfer characteristics of regenerator materials in an oscillating flow for conventional stacked woven wire matrix, sponge metal (felt) and sintered metal. Tanaka [6] obtains the heat transfer area by multiplying the specific area of the mesh by the regenerator total volume. Tanaka [6] suggests that the heat transfer coefficient in the oscillating flow may be higher than that in unidirectional flow.

Gedeon and Wood [10] present correlating expressions in terms of Reynolds or Peclet number for friction factors, Nusselt numbers, enhanced axial conduction ratios and overall heat flux ratios in stacked woven wire matrices and metal felt test regenerator samples. One of the main conclusions of the Gedeon and Wood [10] investigation is that under the range of conditions tested, which were intended to be representative of most Stirling applications, they found no essential differences compared to steady flow. In other words, instantaneous local Reynolds number or Peclet number appear to characterize the flow quite adequately.

As can be observed there is not a clear consensus about the effect of the oscillating flow conditions in the Stirling regenerators. On one hand, Tanaka [6] suggests that it could enhance the heat transfer and in the other hand, Gedeon and Wood [10] conclude that there are not significant different with steady conditions in the Stirling regenerator working range. In the previous authors work [16] the numerical results show good agreement with the experimental results obtained under oscillating flow conditions, despite the study is conducted under not oscillating flow conditions. Therefore, those

experimental investigations are considered for the validation of the numerical model presented for the study of stacked woven wire matrix regenerator.

In both studies the maximum Reynolds number is calculated based on hydraulic diameter,  $d_h$  instead of wire diameter. The hydraulic diameter is defined by Tanaka [6] as:

$$d_h = 4\Pi_v / \phi(1 - \Pi_v) \quad (11)$$

Where  $\Pi_v$  is the volumetric porosity and  $\phi$  is the shape factor defined as the ratio of the mesh surface area to the mesh volume.

The hydraulic diameter is defined by Gedeon and Wood [10] as:

$$d_h = d_w \Pi_v / (1 - \Pi_v) \quad (12)$$

The different between these two definitions (Eqs. (11) and (12)) of diameter hydraulic is not significant. In the present study the hydraulic diameter is determined by Eq. (12).

The specific heat transfer area in a woven wire mesh,  $\varphi$ , is generally defined as:

$$\varphi = 4/d_w (1 - \Pi_v) \quad (13)$$

Therefore, Reynolds number can be defined as:

$$Re = \rho u_{max} d_h / \mu \quad (14)$$

The maximum flow velocity  $u_{max}$  is obtained by dividing the frontal maximum velocity by porosity. The Nusselt number is then defined as follows:

$$Nu = h d_h / k_g \quad (15)$$

In the present numerical study the heat transfer coefficient is calculated from the numerical result using Eq. (10).

Although the purpose of the present study is to estimate the heat transfer in a wound woven wire matrix, since there is no experimental data available for this case, the first step is to validate the computational model for a stacked woven wire matrix in comparison with the experimentally obtained empirical correlations proposed by cited researchers above. The validation is made using two different wire diameters and two configurations of matrices in which, the first configuration is a stacked woven wire screens parallel misaligned and the second matrix configuration is oriented 45° with its neighbor so as to simulate a “random stacking”. Furthermore, the stacking volumetric porosity has two levels for the same woven wire mesh in order to cover any possible stacking process variation. In Table 2 below the parametric study range for stacked woven wire matrices is summarized.

### Table (1)

Tanaka [6] proposes the following empirical relationship for Nusselt number in a range of  $10 < Re < 150$ :

$$Nu = 0.33Re^{0.67} \quad (16)$$

Gedeon and Wood [10] based on combining data sets proposes the following master correlation for woven wire matrix in terms of Peclet number ( $RePr$ ):

$$Nu = (1 + 0.99Pe^{0.66})\Pi_v^{1.79} \quad (17)$$

Gedeon and Wood [10] justify the constant 1 in the Nusselt number expression (Eq. (17)) because  $Nu$  tends to some constant value for  $Pe \approx 0$  as occurs in fully developed internal laminar flow. Gedeon and Wood [10] claim that a value of  $Nu_0 \approx 1$  seems reasonable in light of the published limiting value of 0.43 for flow normal to a single cylinder. Eq. (17) becomes Equation (18) for  $Pr \approx 0.73$  and  $\Pi_v \approx 0.69$  (Average volumetric porosity in the present study):

$$Nu = 0.51 + 0.40Re^{0.66} \quad (18)$$

The relative accuracy of the results of Gedeon and Wood [10] for heat transfer correlations is more dependent on Reynolds number. Thus the worst relative error is about 10% at peak Reynolds number on the order of 1000 and it is about 50% for peak Reynolds numbers below about 5.

Table 1 summarizes the geometrical characteristics of the woven wire mesh and the samples tested for different authors. It is important highlighted that in the regenerator samples used by Gedeon and Wood [10] for obtained empirical correlations the  $\Pi_v$  is approximated 5% lower than the single mesh  $\Pi_v$ . However, in the samples used by Tanaka [6] the  $\Pi_v$  is approximated 3% higher, this could means that there is not contact between different layers. In the present study the models are similar to the Gedeon and Wood [10] as is shown in Table 2.

Eight different configurations of stacked woven wire matrices are numerically studied, four of them are parallel configuration (Fig. 2a) and the others are cross configurations (Fig. 2b). Based on heat transfer results the Nusselt number is calculated for a Reynolds number range from 4 to 400. By fitting these results to the three coefficient equation form (Eq. (1)), Nusselt number correlation equation is obtained.

Figure (4)

Figure (5)

Fig. 4 shows the numerical results obtained for stacked woven wire matrices, 110  $\mu\text{m}$  wire diameter, together with the Nusselt number evolution determined due to Tanaka [6] and Gedeon and Wood [10] for a volumetric porosity of 0.66. The volumetric porosity chosen corresponds to the volumetric porosity of a single 110  $\mu\text{m}$  wire diameter screen. The Figure 5 on the other hand shows the results for the 80  $\mu\text{m}$  wire diameter together with the distribution of the Nusselt number for a volumetric porosity of 0.72 due to Gedeon and Wood [10].

It is observed from Figs. 4 and 5 that no noticeable difference is reproduced for the Nusselt number obtained for parallel or cross stacked woven wire matrices configuration or even in the range of volumetric porosity studied. Nevertheless, it is necessary to emphasize here that the variation in volumetric porosity is not significant and the same behavior is also observed for the woven wire mesh geometry. Therefore, the matrix heat transfer area (specific heat transfer area) decreases with an increase in

volumetric porosity. In the majority of the samples tested by Gedeon and Wood [10] the volumetric porosity increases with the specific heat transfer area (Table 1).

Regarding the correspondence of the present numerical results with the Nusselt number derived from empirical correlations, it is obvious from Figs. 4 and 5 that the numerical results are not good correspondence with correlation proposed by Tanaka [6]. However, the numerical results fit well with the correlation proposed by Gedeon and Wood [10].

Eq. 19 shows the derived numerical correlation for the stacking woven wire matrix which fit the numerical results for the Nusselt number.

$$Nu = 1.14 + 0.39Re^{0.66} \quad (19)$$

Fig. 6 demonstrates that Nusselt number correlation equation proposed in the present study for stacked woven wire matrices (Eq. (19)) shows a good agreement with the numerical results obtained for the Nusselt number as a function of Reynolds number. Moreover, for Nusselt number, with the exception of the Reynolds number range below 40, the agreement is within 10% with Gedeon and Wood [10] empirical correlations (Eq. (17)). However, for  $Re < 40$  the present numerical results deviate significantly from the Gedeon and Wood [10] empirical correlations. Gedeon and Wood [10] conclude that the experimental correlation proposed is not appropriate for low Reynolds number range. The agreement with Tanaka [6] proposed correlation is not good.

Figure (6)

Table (3)

The effect of the volumetric porosity on the Nusselt number is not observed and this is probably due to the fact that the specific heat transfer area in the configuration studied (Table 2) does not present a significant range of variation. Moreover, it is expected that the heat transfer behavior be improved with the increase of specific heat transfer area. The effect of the volumetric porosity and specific heat transfer area on the regenerator heat transfer will be studied in future investigation.

### Figure (7a) - (d)

The qualitative results for velocity and temperature fields the stacked woven wire matrices are illustrated in Figs. 7a to d at  $Re$  number of 60 for two different wire diameters of 80  $\mu\text{m}$  and 110  $\mu\text{m}$ . No significant differences are observed at different wire diameters except slightly higher maximum local velocity distributions obtained from the higher wire diameter of 110  $\mu\text{m}$  for the stacked woven wire matrices as illustrated in Figs. 7a and c. The velocity contours in the wire matrix domain also signifies the importance of local increase of velocity magnitudes as an indication of shear gradients leading to the higher shear stress and hence friction pressure drops for each case. The higher local temperature values obtained in the flow entry region for each wire diameter case can be considered to be main source of the heat energy to be transferred to the entire flow domain as the flow progresses.

### 3.2. Heat Transfer correlation for wound woven wire matrix

Having been validated for the stacked woven wire matrices, the present numerical approach is extended to investigate the heat transfer characteristics and the corresponding heat transfer coefficients for wound wire matrix configurations. The configurations studied are the same studied for parallel misaligned stacked woven wire matrices.

#### Figure (8a) - (d)

Figures 8a-d also signifies the local variation of velocity and temperature field values for the wound woven wire matrices at  $Re$  number of 60 for two different wire diameters of 80  $\mu\text{m}$  and 110  $\mu\text{m}$ . Similar space-wise evolution of the temperature and velocity contours are also observed here except slightly higher maximum velocity values obtained from the wound woven wire matrix case.

Figure 9 shows the relationship between Nusselt number and Reynolds number for the wound woven wire matrix simulations and the solid line presents the Nusselt number correlation line derived from the present results. It is found that the average Nusselt number coefficients obtained for wound woven wire matrix are significantly lower (20%) than those obtained from the stacked woven case for a range of  $20 < Re < 400$ .

#### Figure (9)

For wound woven wire matrix configuration the three coefficient correlation that better fits with the numerical results is shown in the Equation (20), where the Reynolds number is calculated based on the hydraulic diameter:

$$Nu = 1.54 + 0.29Re^{0.66} \quad (20)$$

The above numerically derived Nusselt correlation equation could be considered to be a good general approximation to be applied to all configurations studied here for the wound woven wire mesh matrix. In addition it should be noted here that the dispersion at high Reynolds number (Maximum standard deviation of 4.4) for the wound woven wire mesh matrix is higher than that for the stacked woven wire mesh (Maximum standard deviation of 1.4). Therefore, it is suggested that the geometrical parameters should be studied carefully in this configuration.

Figure 9 shows the Nusselt number results for different volumetric porosities, specific heat transfer areas and hydraulic diameters in a range of Reynolds number. As expected, the higher Nusselt numbers are obtained for the matrix configuration with higher specific heat transfer area (Eq. (7)). Regarding the influence of the hydraulic diameter, the results show an inverse proportionality with the Nusselt number, in other words, the Nusselt numbers increase when the hydraulic diameter decreases. Finally, the results tendency in function of the volumetric porosity is not clear for the matrix configurations studies; therefore, no clear influence of the volumetric porosity in the Nusselt number can be concluded. Thus, no relation between increase/decrease volumetric porosity and the Nusselt number increase/decrease was observed.

The matrix geometrical parameters, hydraulic diameter (Eq. (12)) and specific heat transfer area (Eq.(13)), are function of wire diameter and volumetric porosity.

Consequently, an decrease the volumetric porosity causes a decrease in the hydraulic diameter and an increase in the specific heat transfer area for the same wire mesh.

Accordingly, the interaction between the matrix geometrical parameters, specific heat transfer area, hydraulic diameter and volumetric porosity require an in-depth study to isolate the influence of each one.

#### **4. Conclusions**

In the present numerical study, a specific correlation is derived to numerically characterize heat transfer for wound woven wire regenerator matrices following by an initial numerical validation against experimentally obtained correlation for stacked woven wire.

The validation results show that the derived correlation can be successfully applied in the  $Re$  number working range in Stirling engine regenerators ( $4 < Re < 400$ ), for diameter range from 0,08 to 0,11 mm and a volumetric porosity range from 0,60 to 0,68. The numerical study, which is extended to wound wire model case, also demonstrates an easy and effective use of the derived correlation for determining the Nusselt number for the wound woven wire model for a large Reynolds number range up to 400. The behavior reported in the present study for stacked and wound woven wire matrices are for “random or misaligned stacking” in contrast to “regular or aligned stacking”. It is believed that this new correlation can be also used as a generalized cost-effective tool for heat transfer characterization and further optimization in wound woven wire matrix type of regenerator.

In the Stirling engine calculation program are needed correlations to determine the heat transfer and flow friction behaviour of the working gas in the different components, for this reason is fundamental the characterization of the main components as heat exchangers and regenerators. The results shown here demonstrate that the present numerical tool can be used to study the influence or effect of matrix geometrical parameters (volumetric porosity, hydraulic diameter, specific heat transfer area, etc.) to improve the woven wire matrix heat transfer mechanism. Therefore, further efforts are necessary, in order to derive more experimental data which may support the new correlations.

## References

- [1] Dorer V., Weber A. “Energy and CO<sup>2</sup> emissions performance assessment of residential micro-cogeneration systems with dynamic whole-building simulation programs”. *Energy Conversion and Management*, vol. 50(2009), p. 648-657.
- [2] Formosa F., “Despesse G. Analytical model for Stirling cycle machine design”. *Energy Conversion and Management*, vol. 51 (2010), p.1855-1863
- [3] Timoumi Y., Tlili I., Nasrallah B. “Performance optimization of Stirling engines”. *Renewable Energy*, vol. 33 (2008), p. 2134-2144.
- [4] Organ, A.J. *The Regenerator and the Stirling Engine*. London: Mechanical Engineering Publications; 1997.
- [5] Rühlich, I. and Quack, H. “New Regenerator Design for Cryocoolers”. Dresden, Germany: Technische Universität Dresden, 1999.
- [6] Tanaka, M., Yamashita, I. and Chisaka, F. “Flow and Heat Transfer characteristics of the Stirling Engine Regenerator in an Oscillating Flow”. *JSME International Journal*, vol. 33(1990), p. 283-289.
- [7] Ibrahim, M., et al. “Improving Performance of the Stirling Converter: Redesign of the Regenerator with Experiments, Computation and Modern Fabrication Techniques”. Cleveland State University, 2001.
- [8] Andersen, S.K., Carlsen, H. and Thomsen, P.G. “Numerical study on optimal stirling engine regenerator matrix designs taking into account the effects of matrix temperature oscillations”. *Energy Conversion and Management*, vol. 47 (2006), p. 894-908.

- [9] Miyabe, H., Takahashi, S. and Hamaguchi, K. "An approach to the design of Stirling Engine Regenerator matrix using packs of wire gauzes". *Proc. IECEC*, vol. 17 (1982), p. 1839-1844.
- [10] Gedeon, D and Wood, J.G. "Oscillating-Flow regenerator Test Rig: Hardware and Theory With derived Correlations for Screens and Felts". NASA CR-198442, 1996.
- [11] Thomas, B. and Pittman, D. "Update on the Evaluation of Different Correlations for the Flow Friction Factor and Heat Transfer of Stirling Engine Regenerators". *American Institute of Aeronautics and Astronautics*, 2000.
- [12] Tong, L.S. and London, A.L. "Heat transfer and flow friction characteristics of woven screen and crossed rod matrices". The American Society of Mechanical Engineer. Paper No. 56-A-124 (1960).
- [13] Kolodziej, A., Lojewska, J., Jaroszynski, M., Gancarczyk, A. and Jodlowski, P. "Heat transfer and flow resistance for stacked wire gauzes: Experiments and modeling". *International Journal of Heat and Fluid Flow*, vol. 33 (2012), p. 101-108.
- [14] Golneshan, Ali A and Zarinchang, Jafar. "3-D Numerical Analysis of Thermal/Fluid Characteristics of Woven mesh Structures as Heat Regenerators". *Proc. International Stirling Engine Conference*, 13<sup>th</sup> (2007), p. 112-115.
- [15] Ibrahim, Mounir B. and Tew, Roy C. *Stirling Converter Regenerators*. Florida: CRC Press City Boca Raton, 2012. ISBN 9781439830062.

- [16] Costa, S.C., Barrutia, H., Esnaola, J.A. and Tutar, M. “Numerical study of the pressure drop phenomena in wound woven wire matrix of a Stirling regenerator”. *Energy Conversion and Management*, vol. 67 (2013), p. 57–65
- [17] Thomas, B. and Bolleber, F. “Evaluation of 5 different correlations for the heat transfer in Stirling engine regenerators”. *Proceedings of Europaisches Stirling Forum*, vol. 35 (2000), p. 111.119.
- [18] Tew, R., et al. “Stirling Convertor CFD Model Development and Regenerator R&D Efforts”. NASA TM-213404 (2004).
- [19] Cheadle, M.J.; Nellis, G.F. and Klein, S.A. “Regenerator Friction Factor and Nusselt Number Information derived from CFD analysis”. *International Cryocoolers Conference*, 2011.
- [20] Tao, Y.B.; Liu, Y.W.; Gao, F.; Chen, X.Y. and He, Y.L. “Numerical analysis on pressure drop and heat transfer performance of mesh regenerators used in cryocoolers”. *Cryogenics*, vol. 49 (2009), p. 497-503.
- [21] Dyson, R.W.; Wilson, S.D.; Tew, R.C. and Demko, R. “On the Need for Mulidimensional Stirling Simulation”. NASA/TM-2005-213975. AIAA-2005-5557.
- [22] Fluent Dynamics Software. ANSYS FLUENT. Lebanon, NT 6.1.7601, (2010).

## Figures Captions

- Figure 1. Global computational domain for stacked woven wire matrix
- Figure 2. 2D flow perpendicular plane layouts: a) Parallel staked misaligned and b) cross stacked misaligned configurations.
- Figure 3. a) 3D view of the surface mesh for a stacked woven wire matrix; b) 3D view of the surface mesh for a wound woven wire matrix and c) 2D plane view of stacked woven wire flow mesh.
- Figure 4. Stacked woven wire matrices for 110 $\mu\text{m}$  wire diameter: Nusselt number versus Reynolds number
- Figure 5. Stacked woven wire matrices for 80 $\mu\text{m}$  wire diameter: Nusselt number versus Reynolds number
- Figure 6. Nusselt number correlation comparison for Stacked woven wire matrices.
- Figure 7. Stacked woven wire matrices results for  $\text{Re} \approx 60$  ( $u_{\text{in}} = 1$  m/s) at 0.02s: a) Velocity vector through 80 $\mu\text{m}$  matrix; b) Velocity vector colored by temperature through 80 $\mu\text{m}$  matrix; c) Velocity vector through 110 $\mu\text{m}$  and d) Velocity vector colored by temperature contour through 110 $\mu\text{m}$  matrix.
- Figure 8. Wound woven wire matrices results for  $\text{Re} \approx 60$  ( $u_{\text{in}} = 1$  m/s) at 0.02s: a) Velocity vector through 80 $\mu\text{m}$  matrix; b) Velocity vector colored by temperature through 80 $\mu\text{m}$  matrix; c) Velocity vector through 110 $\mu\text{m}$  and d) Velocity vector colored by temperature contour through 110 $\mu\text{m}$  matrix.
- Figure 9. Nusselt number correlation comparison for Wound woven wire matrices.

## Tables Captions

- Table 1. Gedeon/Wood [10] and Tanaka [6] tested regenerator matrix parameters
- Table 2. Present Study modeled regenerator matrix parameters
- Table 3. Tanaka [6] and Gedeon and Wood [10] experimental range for stacked woven wire matrix and experimentally obtained empirical correlations for Nusselt number, and present study numerical correlations for Nusselt number.

Table 1.

Study	Wire Mesh Geometry				Regenerator Matrix Geometry		
	Wire /inch	$d_w$ [ $\mu\text{m}$ ]	Opening [ $\mu\text{m}$ ]	Porosity [%]	$\Pi_v$ [%]	$\varphi$ [1/ $\mu\text{m}$ ]	$d_h$ [ $\mu\text{m}$ ]
Gedeon/Wood [10]	200	53.3	74	67.0	62.3 (-4.7)	0.028	88
Gedeon/Wood [10]	100	55.9	198	82.7	78.1 (-4.6)	0.016	199
Gedeon/Wood [10]	80	94	224	76.7	71.0 (-5.7)	0.012	230
Tanaka [6]	50	230	278	64.4	64.5 (+0.1)	0.006	418
Tanaka [6]	100	100	154	69.1	71.1 (+2.0)	0.012	246
Tanaka [6]	150	60	109	72.2	75.4 (+3.2)	0.016	184
Tanaka [6]	200	50	77	69.1	72.9 (+3.8)	0.022	135

Table 2.

Study	Wire Mesh Geometry				Regenerator Matrix Geometry		
	Wire /inch	$d_w$ [ $\mu\text{m}$ ]	Opening [ $\mu\text{m}$ ]	Porosity [%]	$\Pi_v$ [%]	$\varphi$ [1/ $\mu\text{m}$ ]	$d_h$ [ $\mu\text{m}$ ]
<i>Present Study</i>	113	80	144	72.0	66 (-6)	0.017	155
<i>Present Study</i>	113	80	144	72.0	68 (-4)	0.016	170
<i>Present Study</i>	100	110	144	66.0	60 (-6)	0.015	165
<i>Present Study</i>	100	110	144	66.0	63 (-3)	0.013	187

Table 3.

	Wire diameter [ $\mu\text{m}$ ]	Porosity [%]	Re range	Correlation
<b>Tanaka [6]</b>	50 to 230	64 to 73	10 to 150	$Nu = 0.33Re^{0.67}$
<b>Gedeon/Wood [10]</b>	53.3 to 94	62 to 78	1.04 to 3400	$*Nu = 0.51 + 0.40Re^{0.66}$
<b>Stacked Present Study</b>	80 to 110	60 to 68	4 to 400	$Nu = 1.14 + 0.39Re^{0.66}$
<b>Wound Present Study</b>	80 to 110	60 to 68	4 to 400	$Nu = 1.54 + 0.29Re^{0.66}$

\*The correlation for Nusselt number is for a  $Pr \approx 0.73$  and  $II_v \approx 0.69$

Figure 1

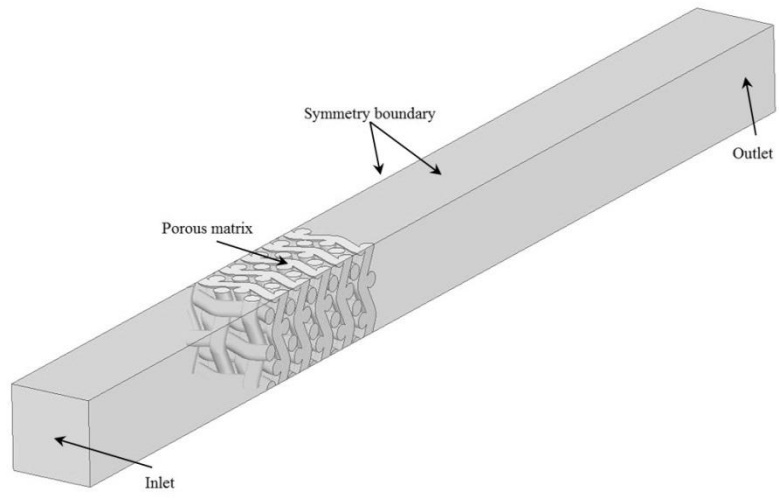


Figure 2a

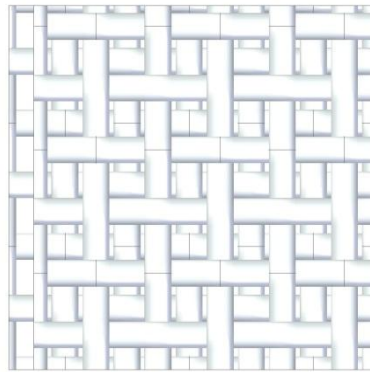


Figure 2b

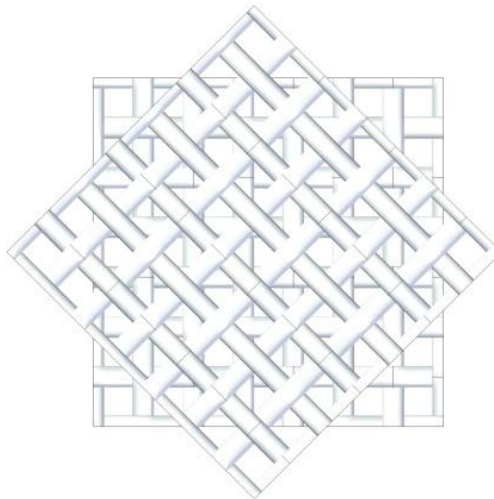


Figure 3a

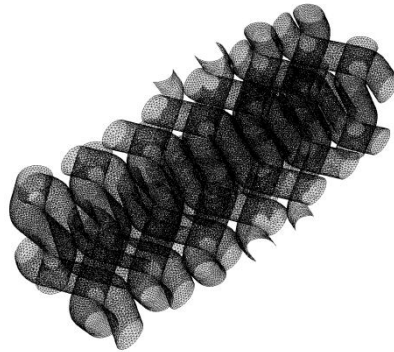


Figure 3b

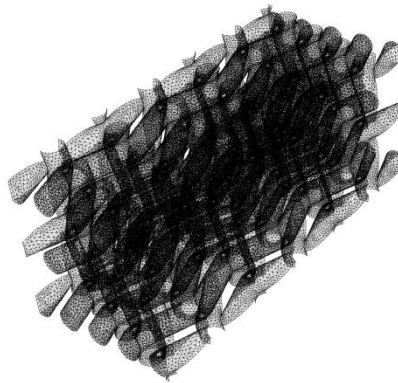


Figure 3c

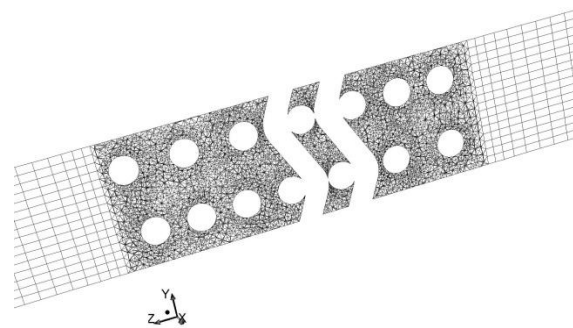


Figure 4

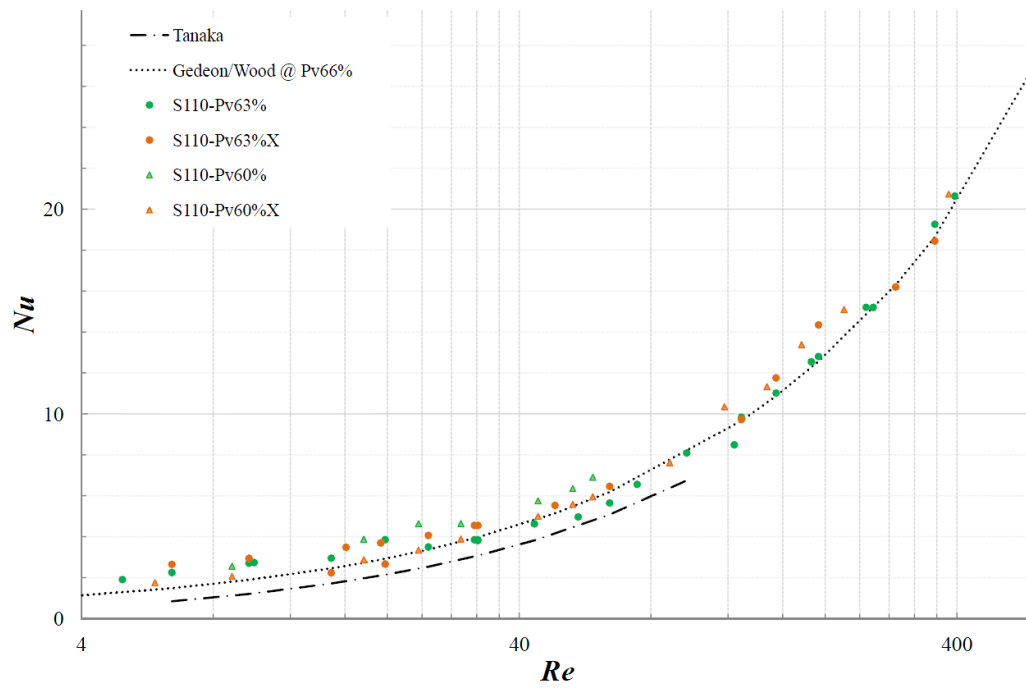


Figure 5

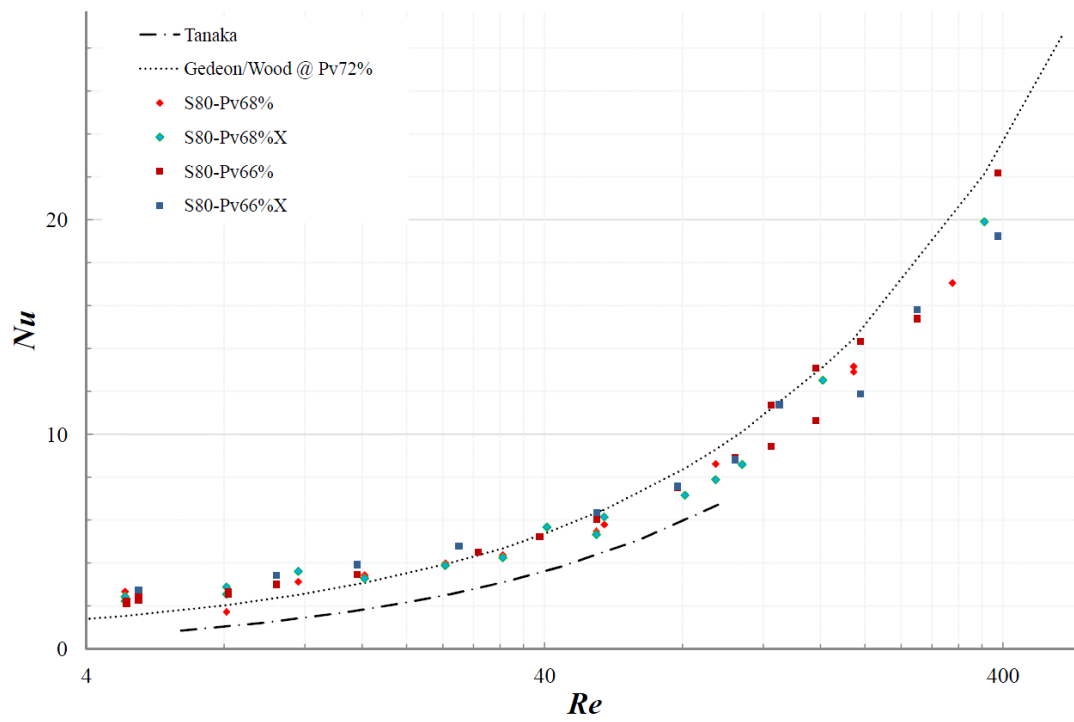


Figure 6

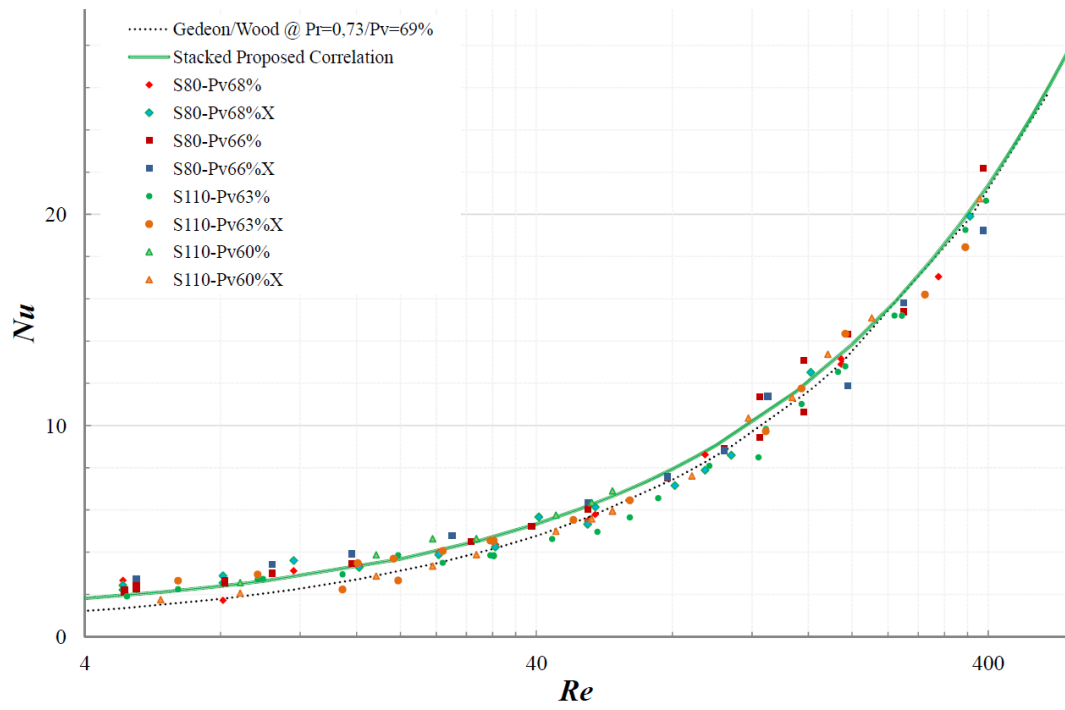


Figure 7a

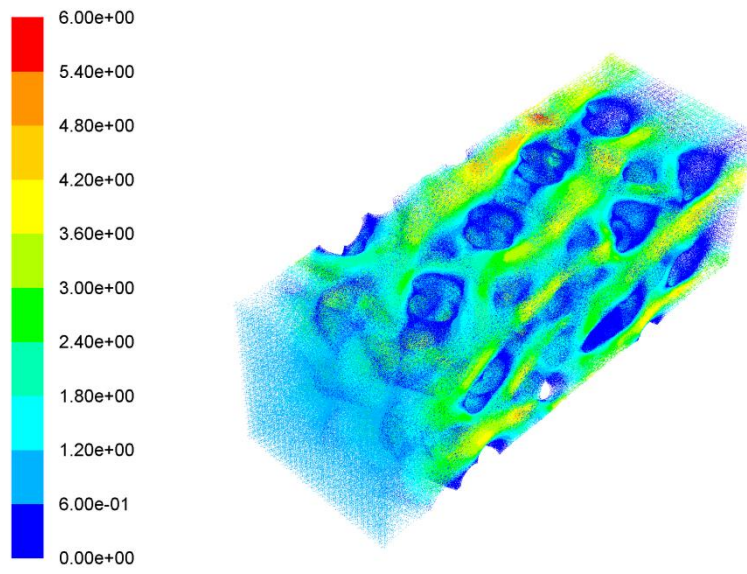


Figure 7b

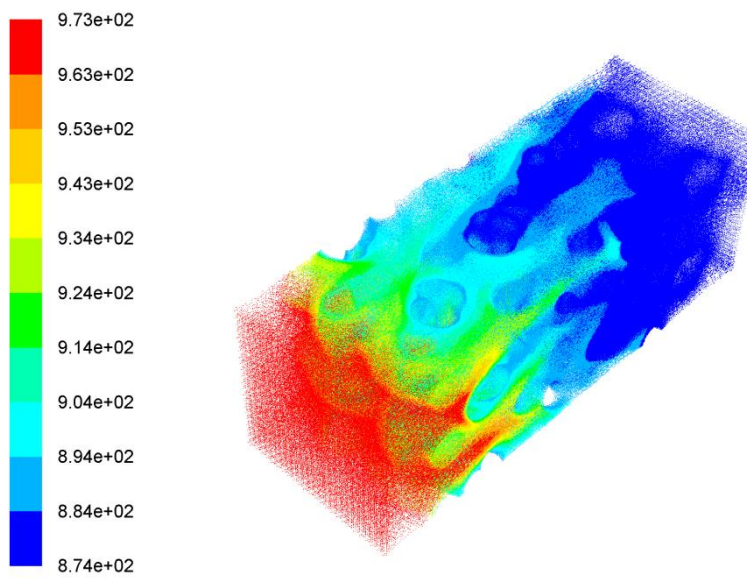


Figure 7c

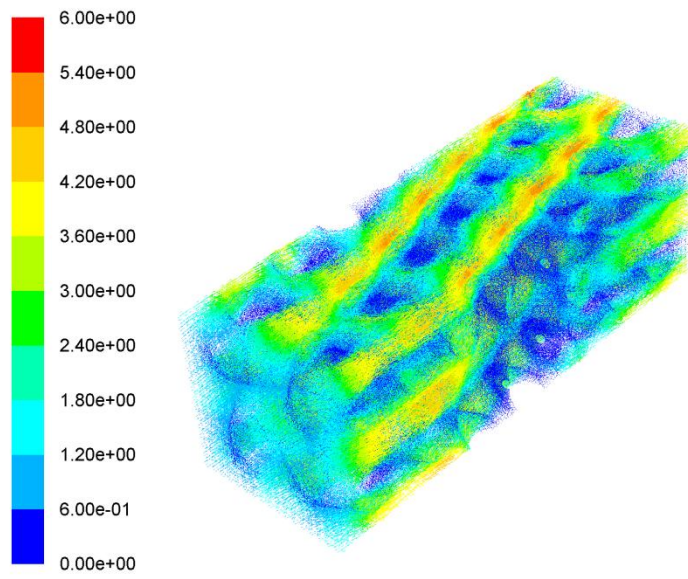


Figure 7d

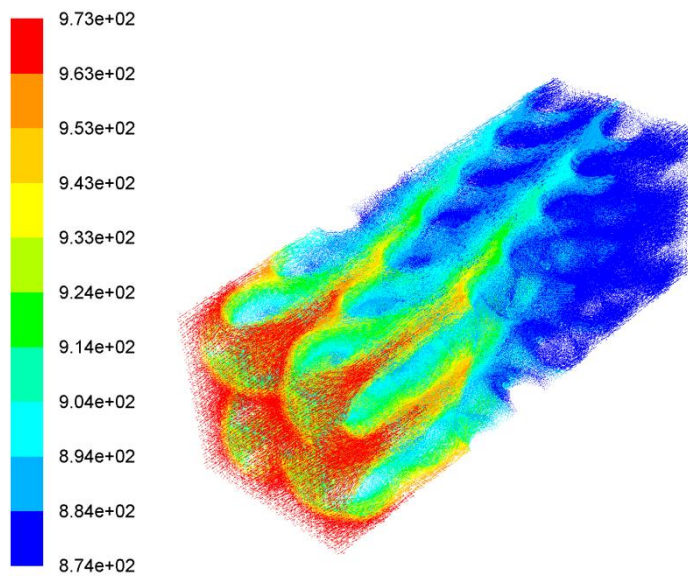


Figure 8a

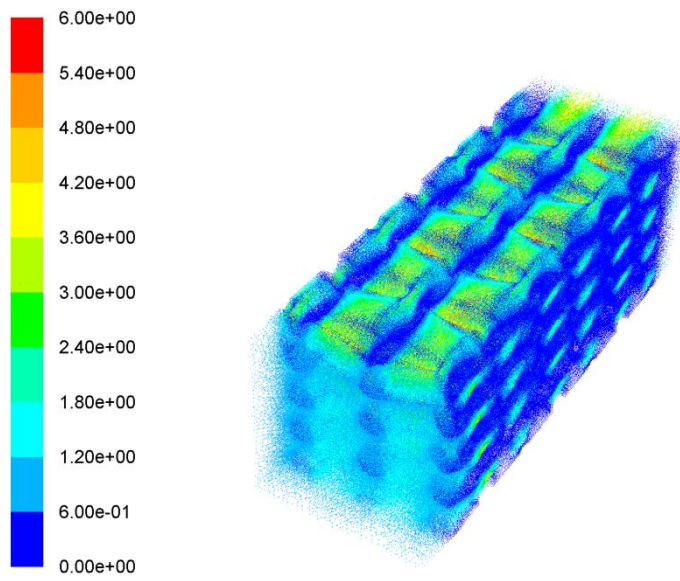


Figure 8b

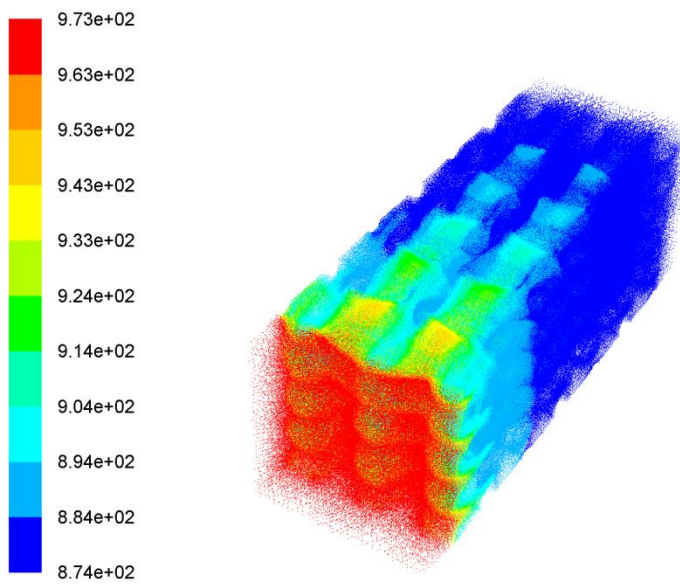


Figure 8c

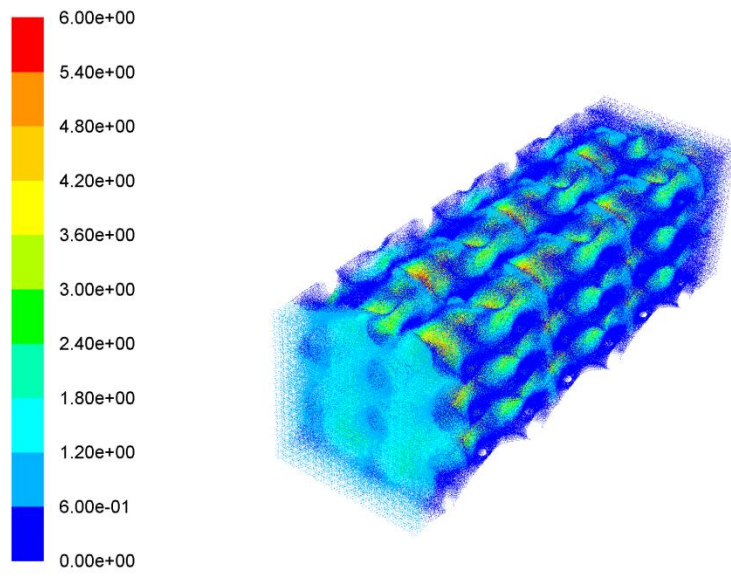


Figure 8d

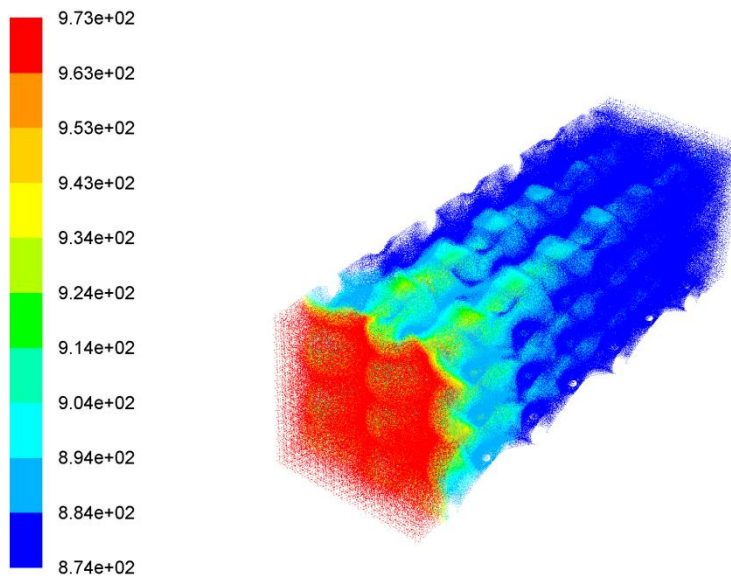


Figure 9

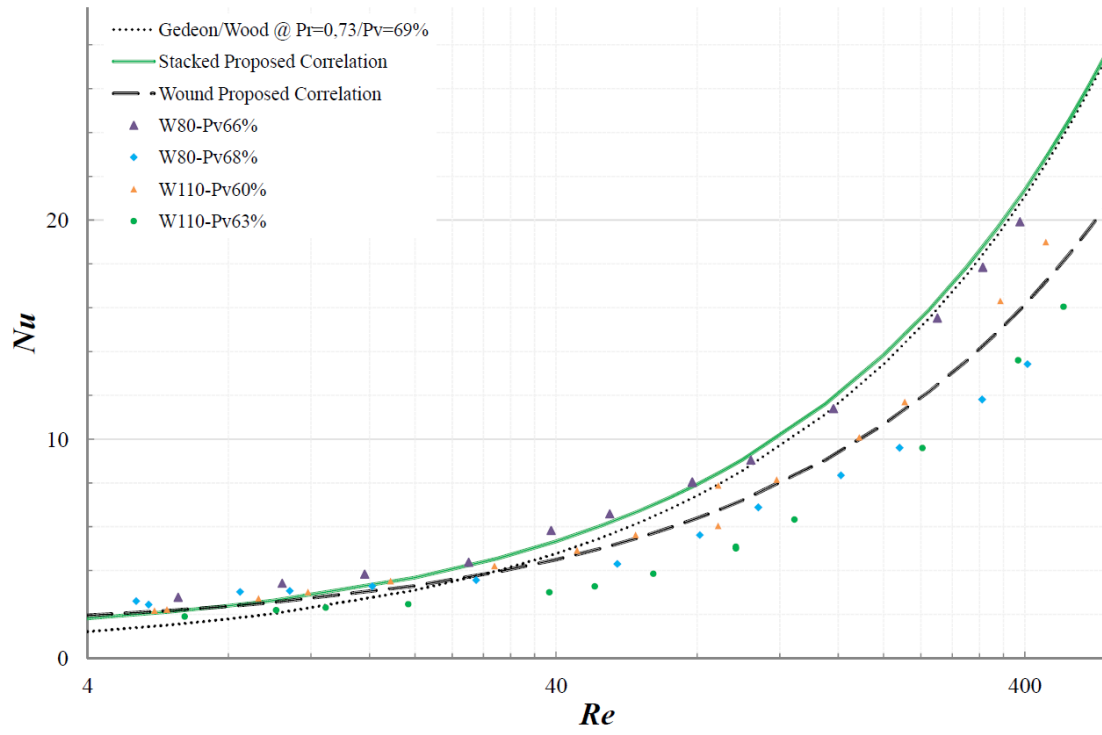


Figure1

[Click here to download high resolution image](#)

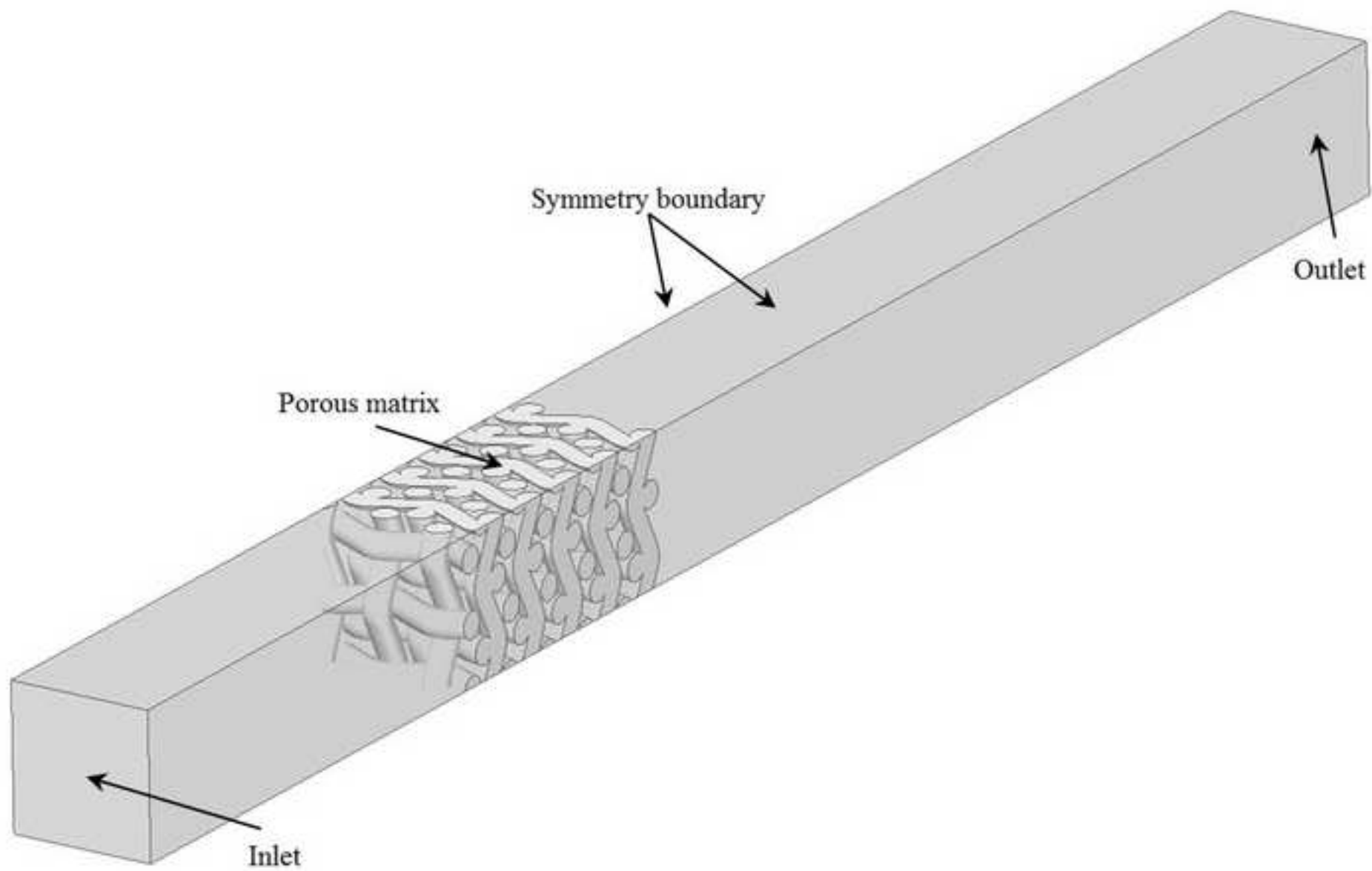


Figure2a

[Click here to download high resolution image](#)

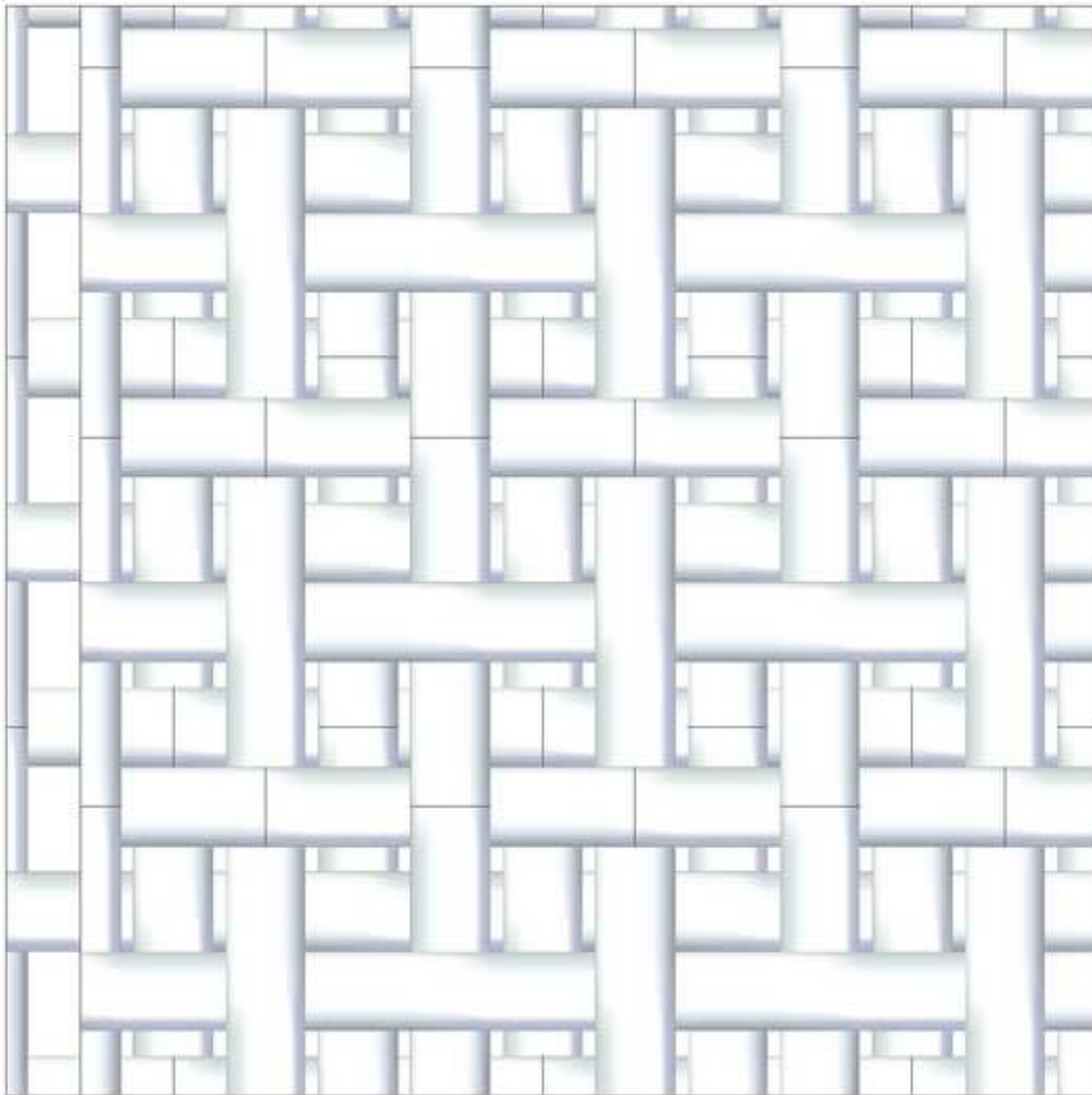


Figure2b  
[Click here to download high resolution image](#)

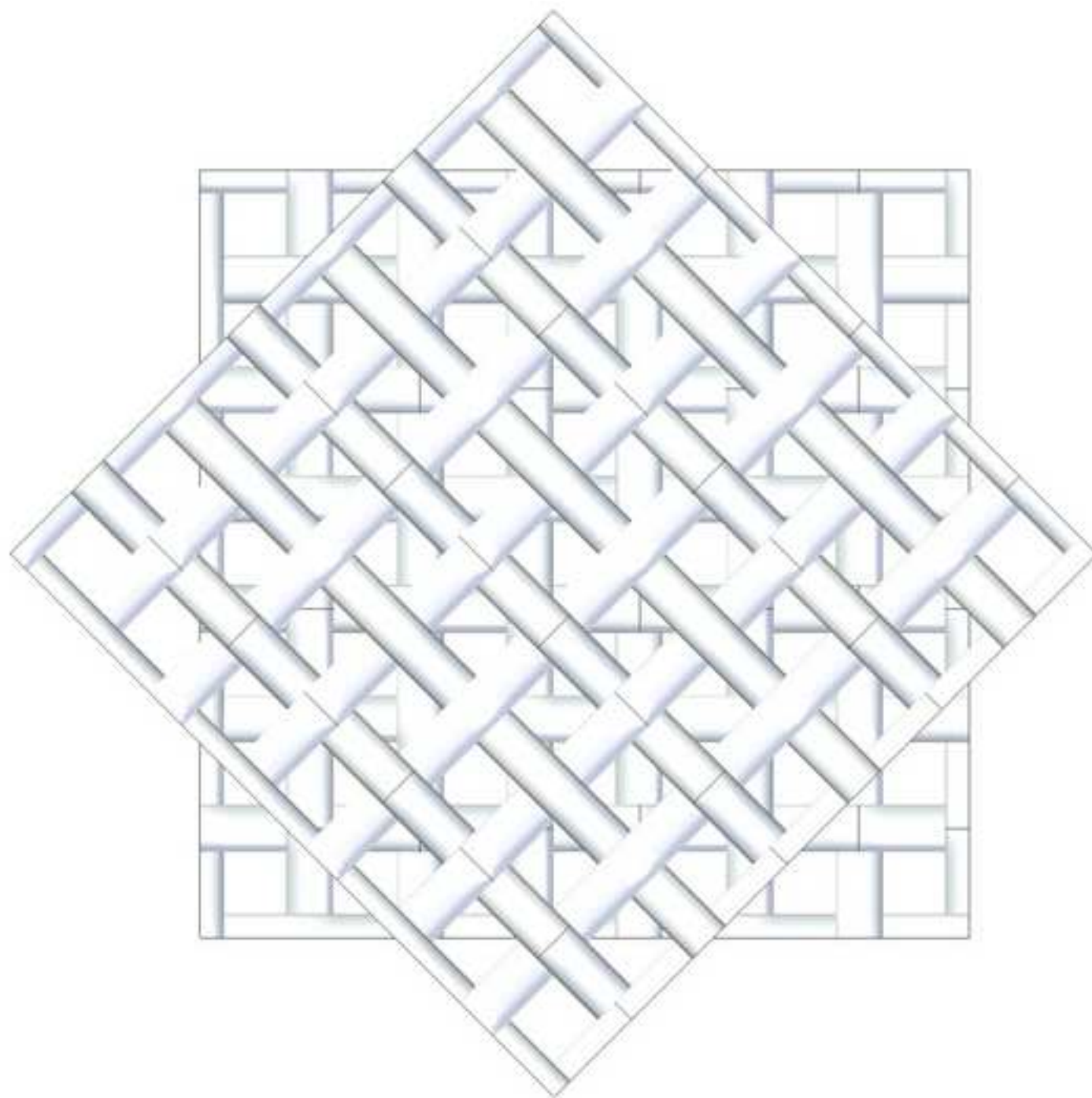


Figure3a

[Click here to download high resolution image](#)

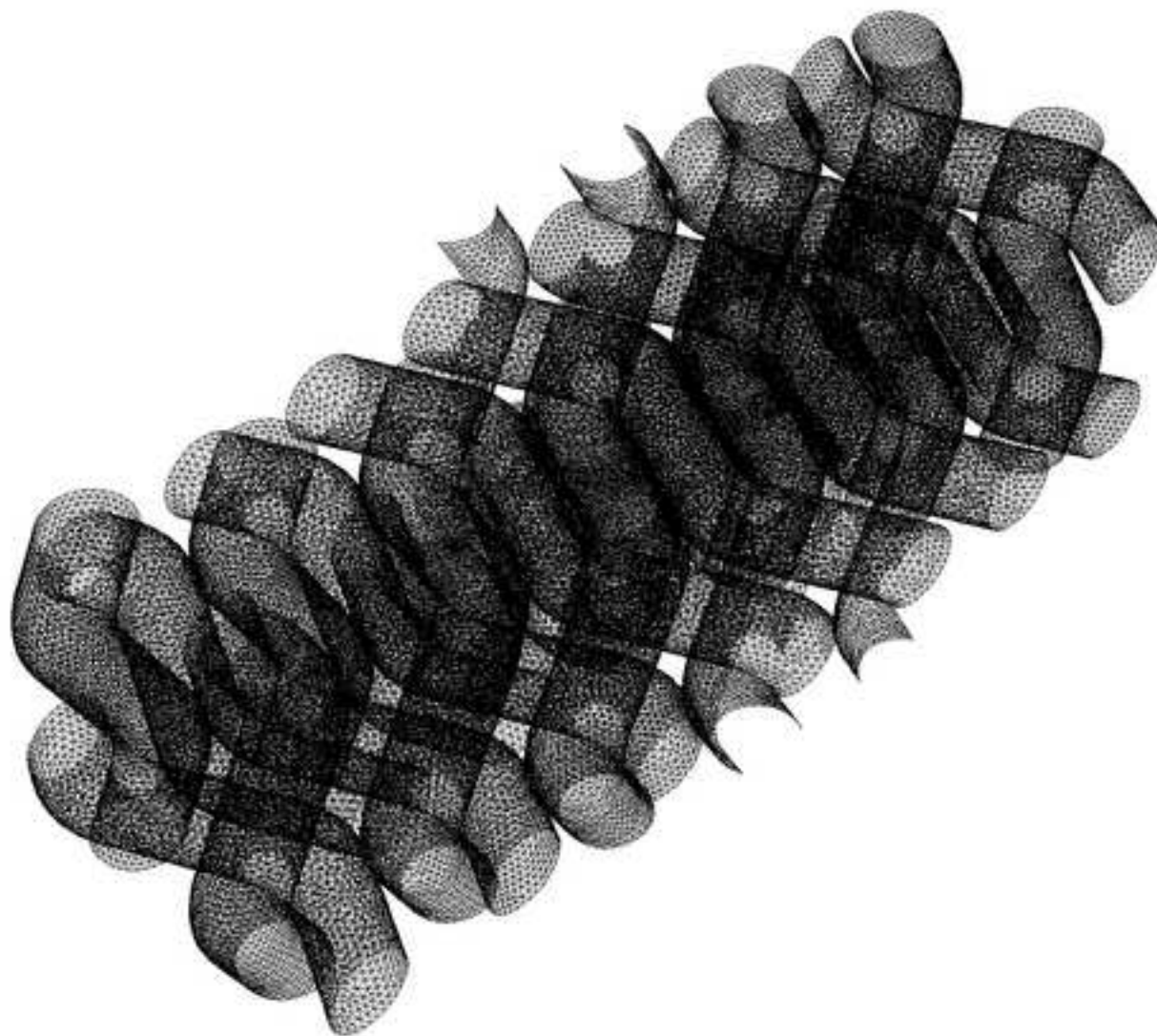


Figure3b  
[Click here to download high resolution image](#)

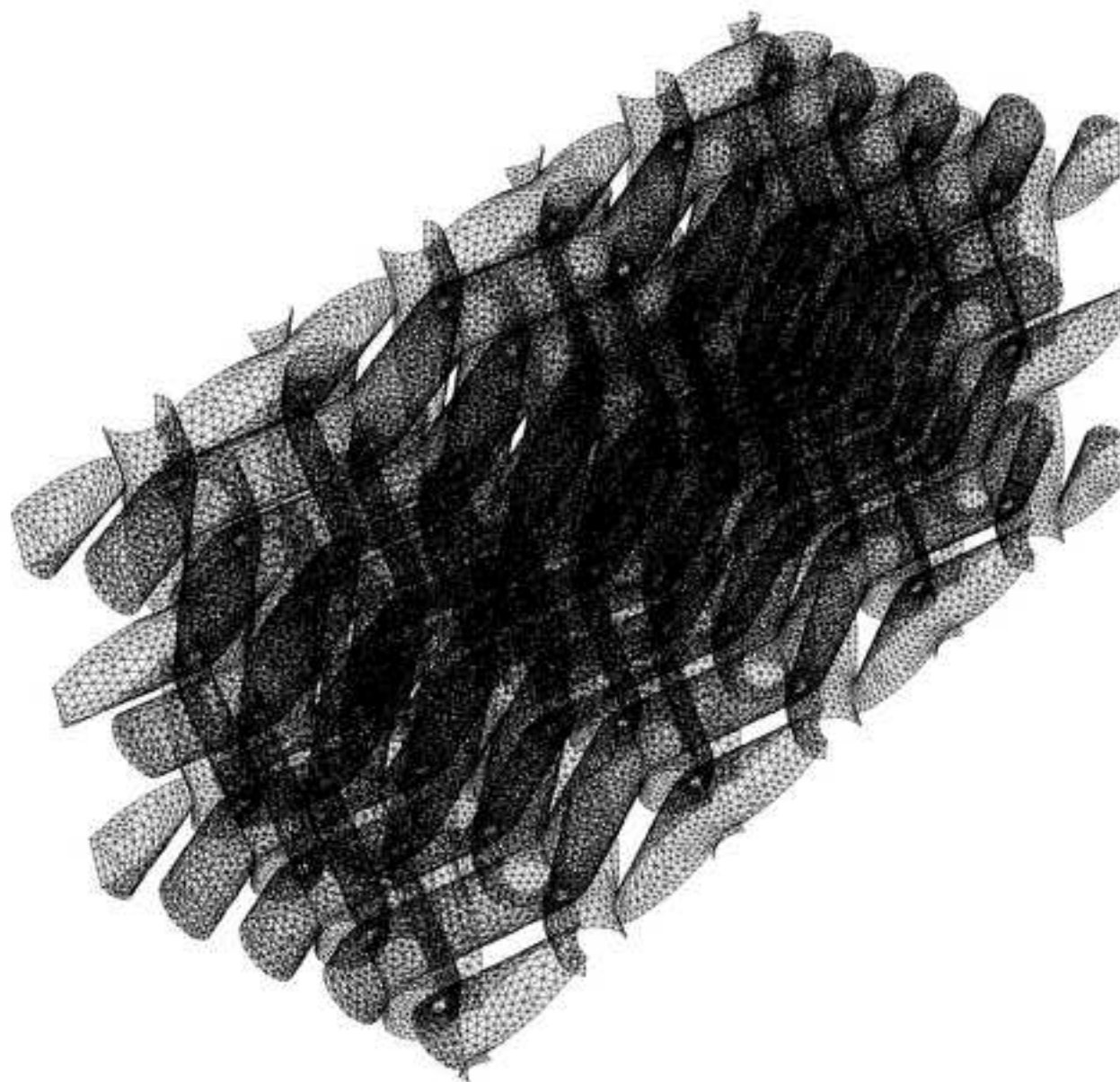


Figure3c  
[Click here to download high resolution image](#)

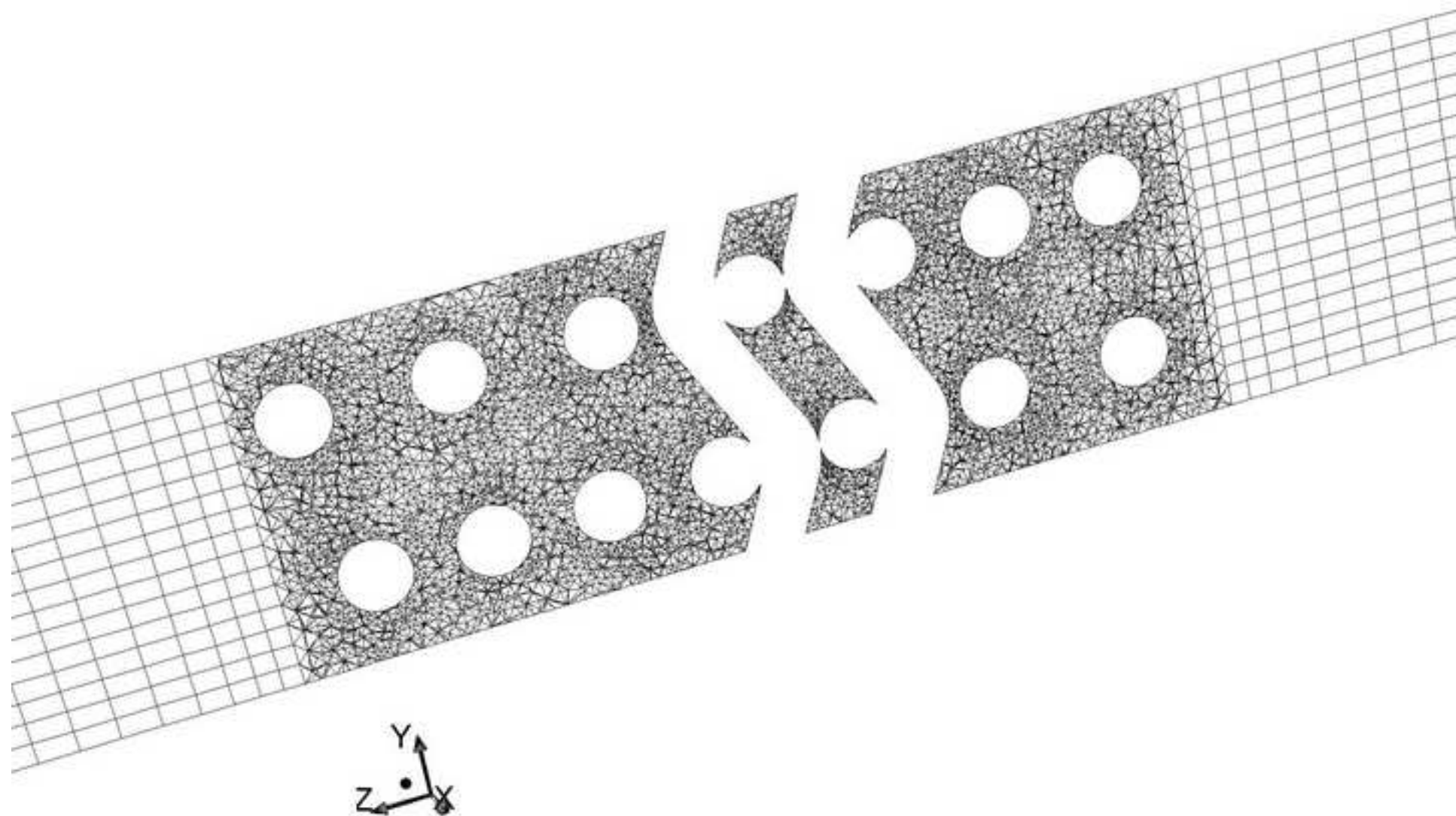


Figure4

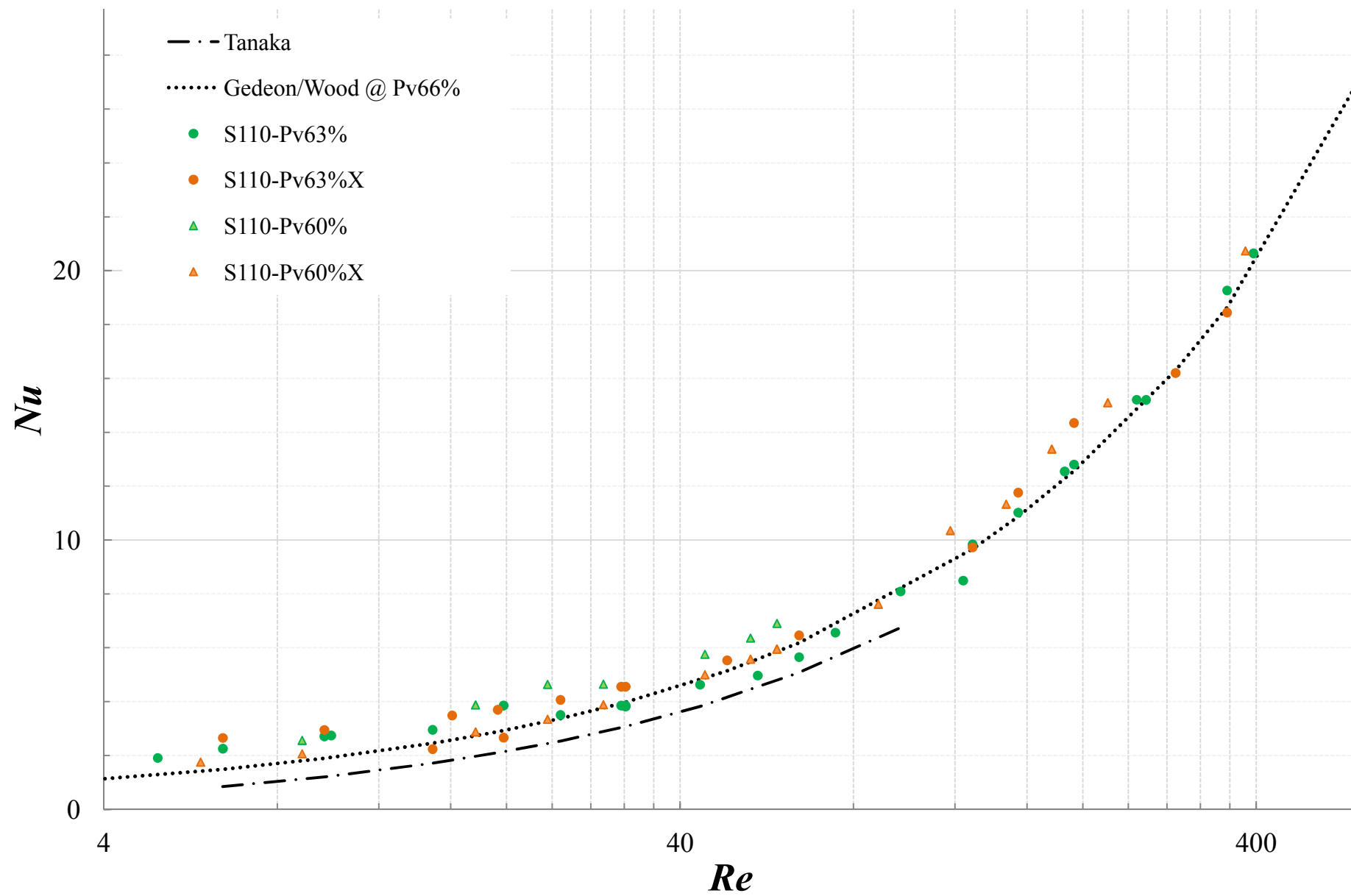


Figure5

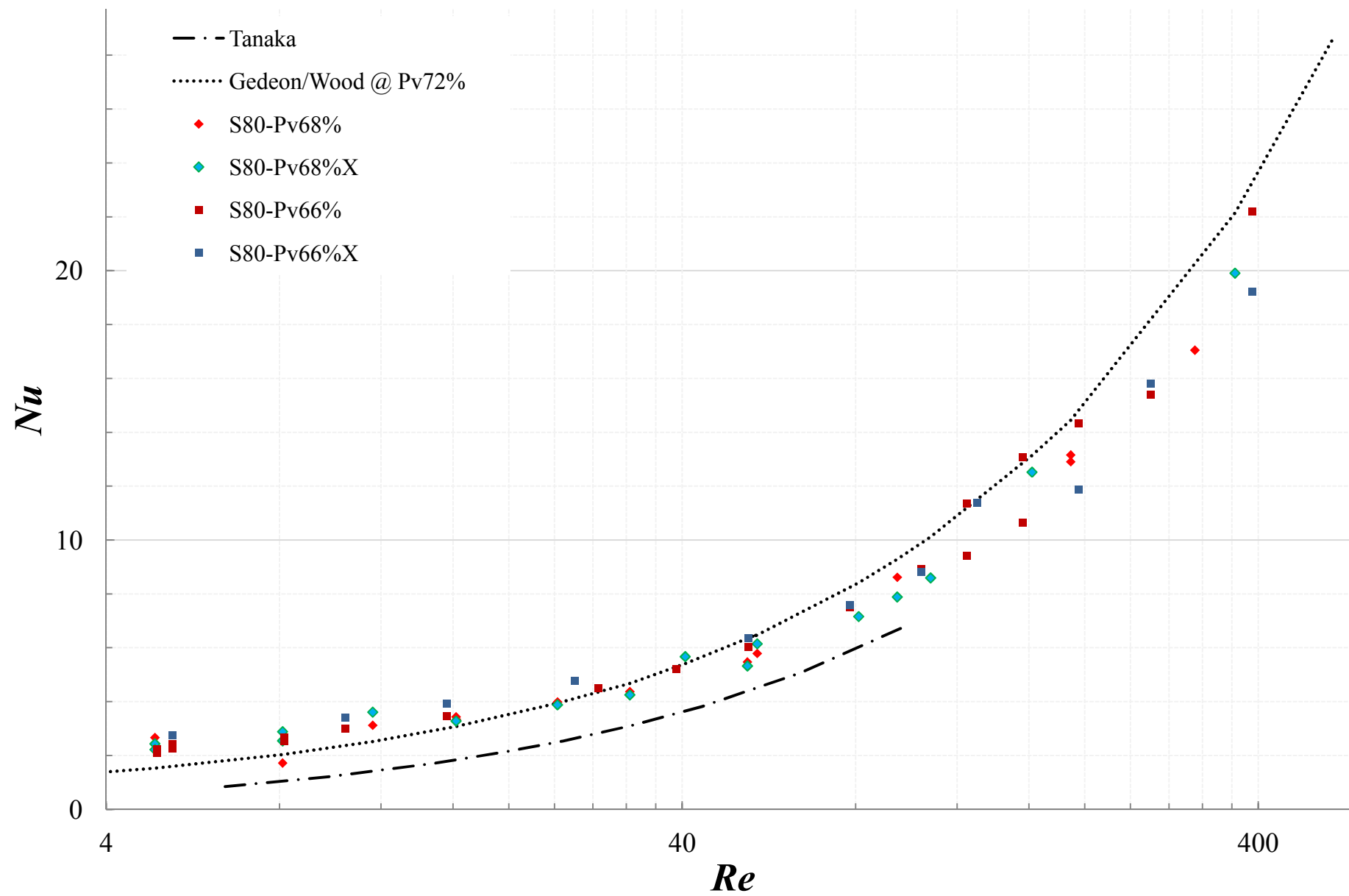


Figure6

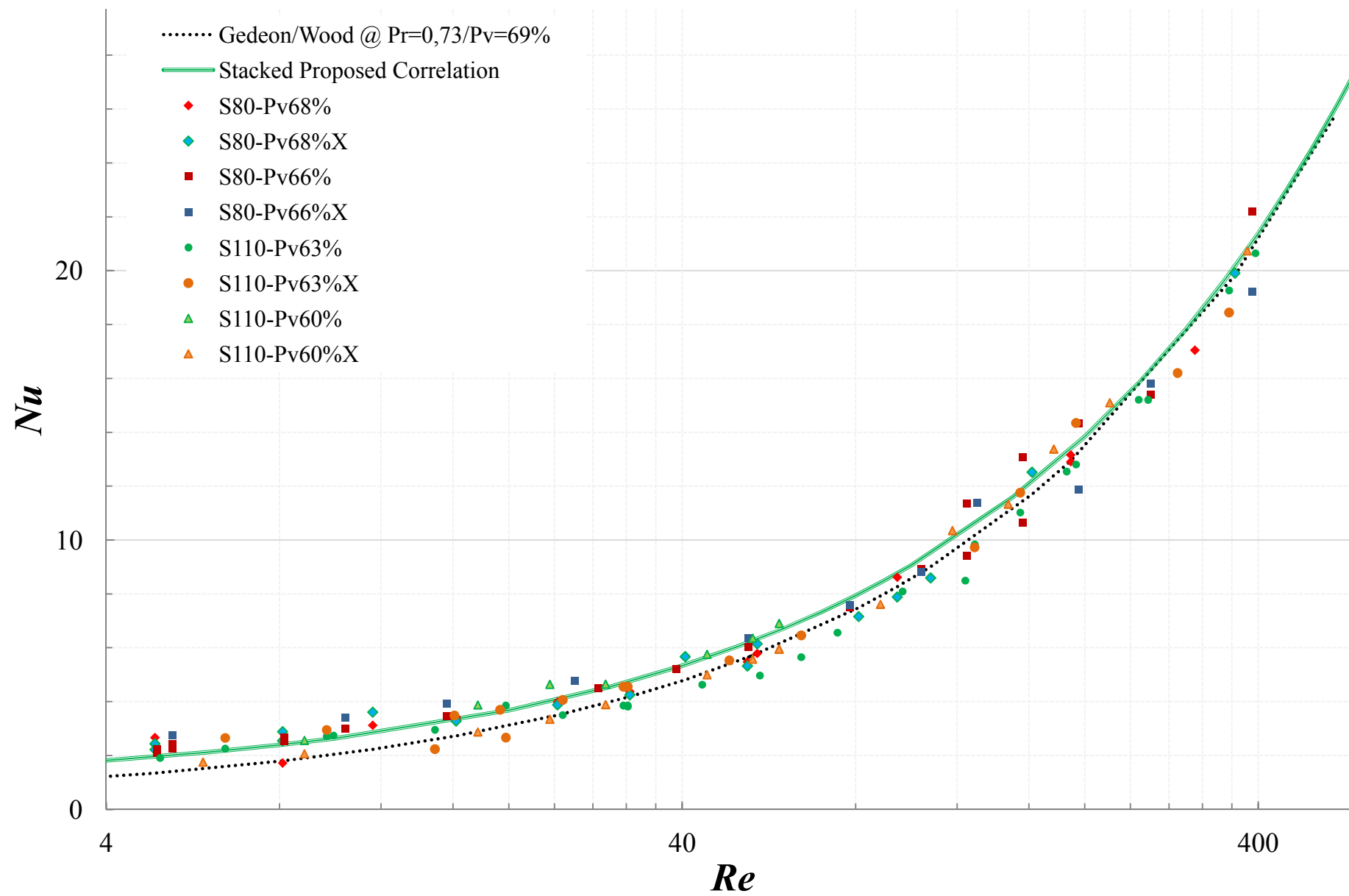


Figure7a  
[Click here to download high resolution image](#)

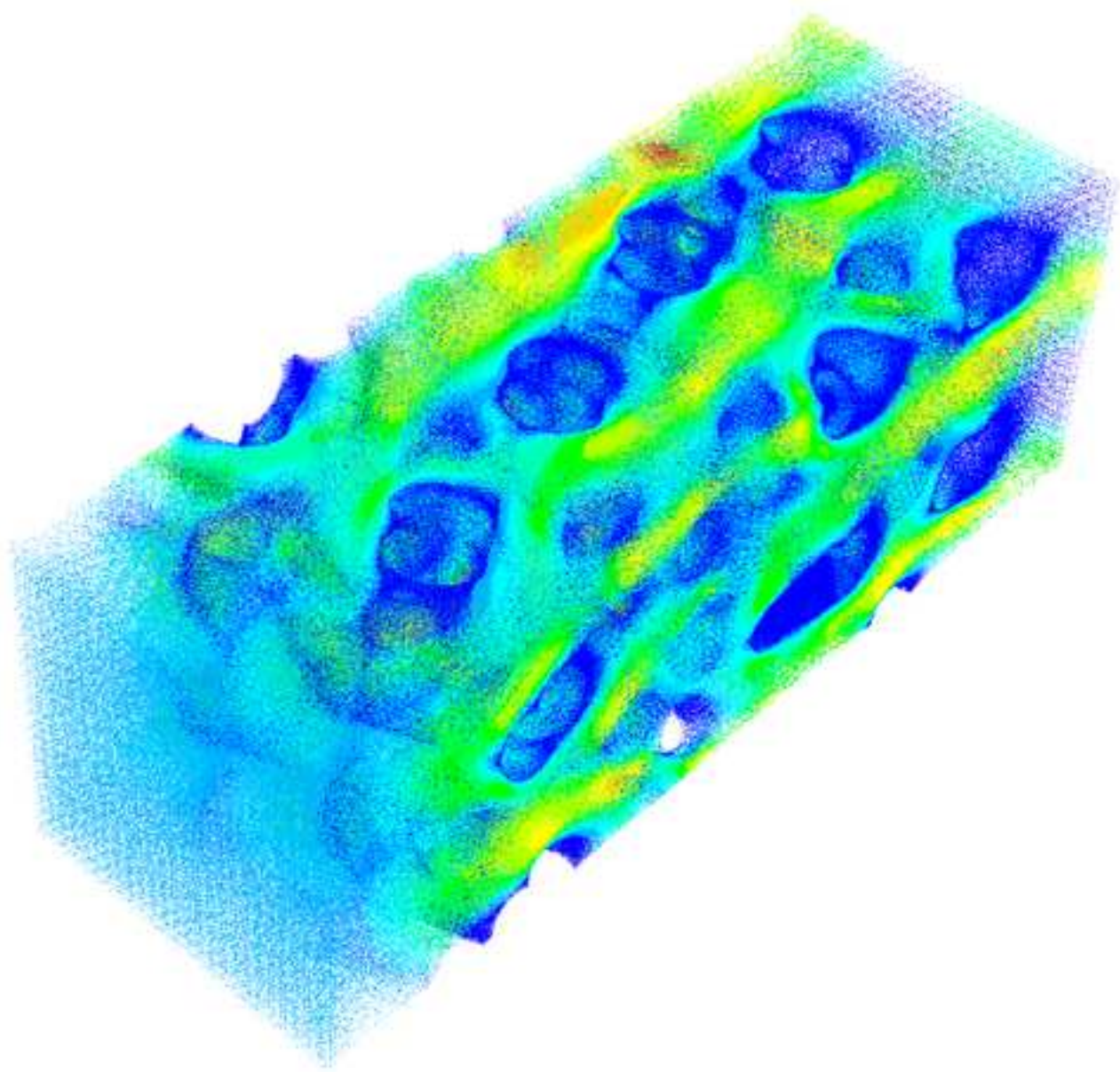
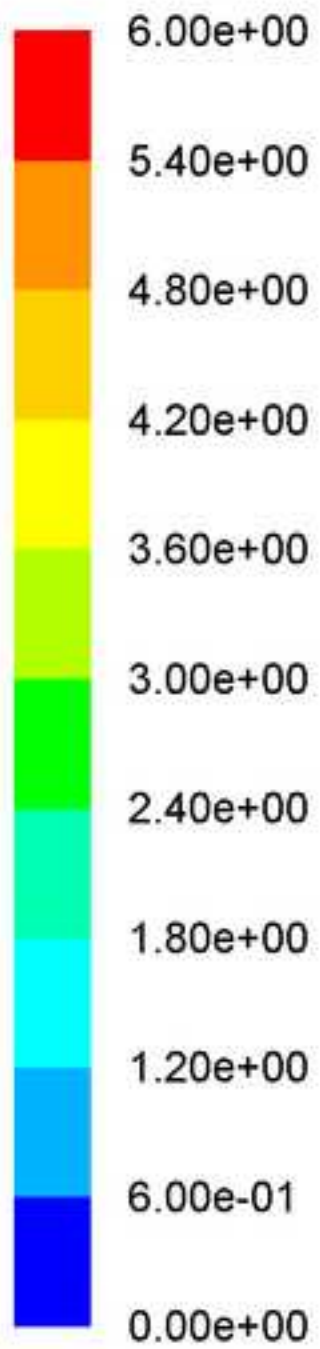


Figure7b  
[Click here to download high resolution image](#)

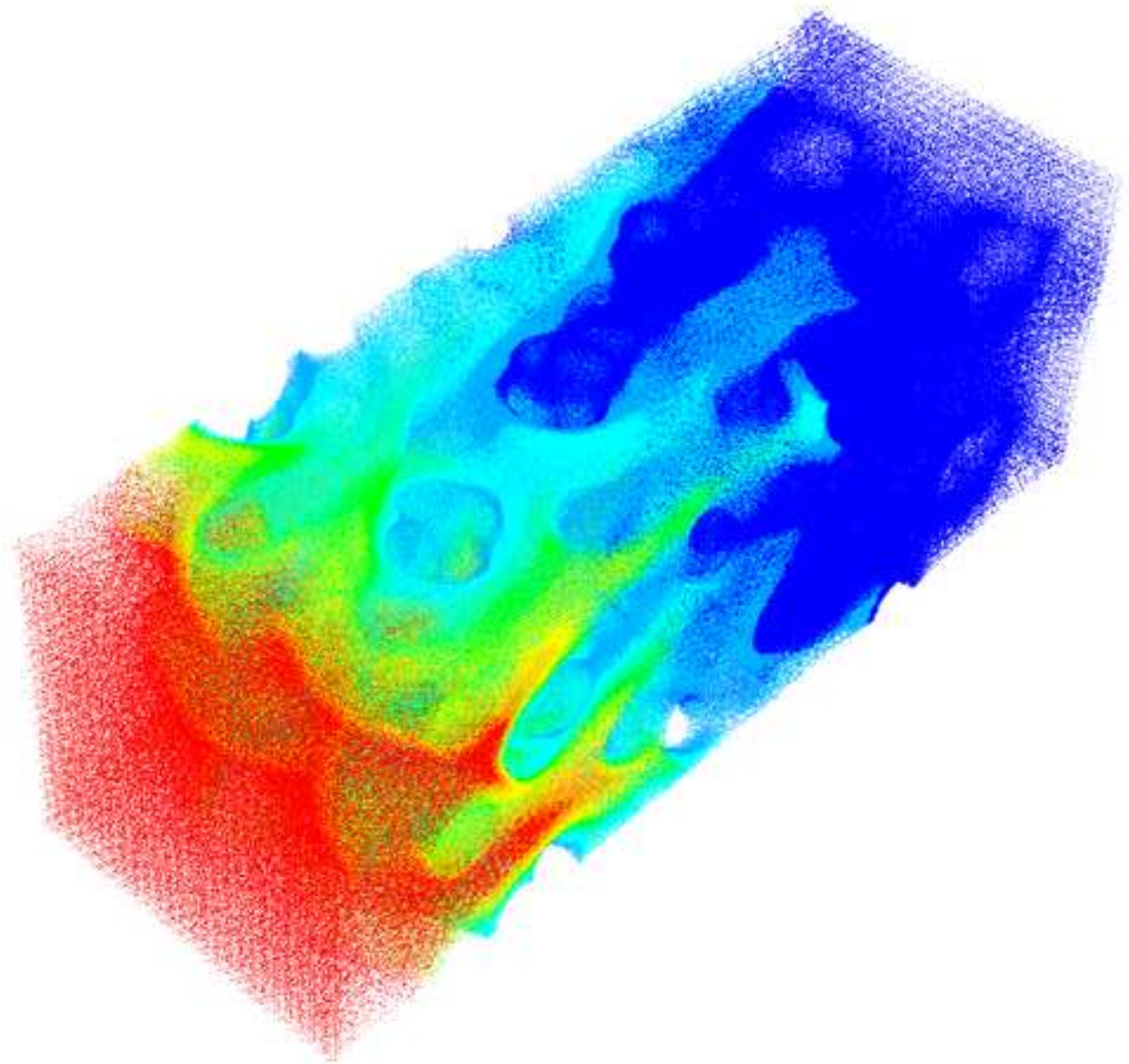
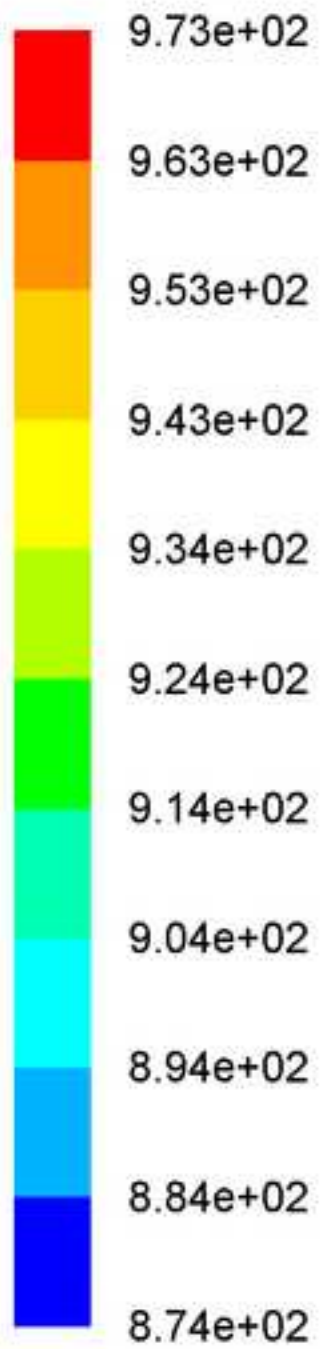


Figure7c  
[Click here to download high resolution image](#)

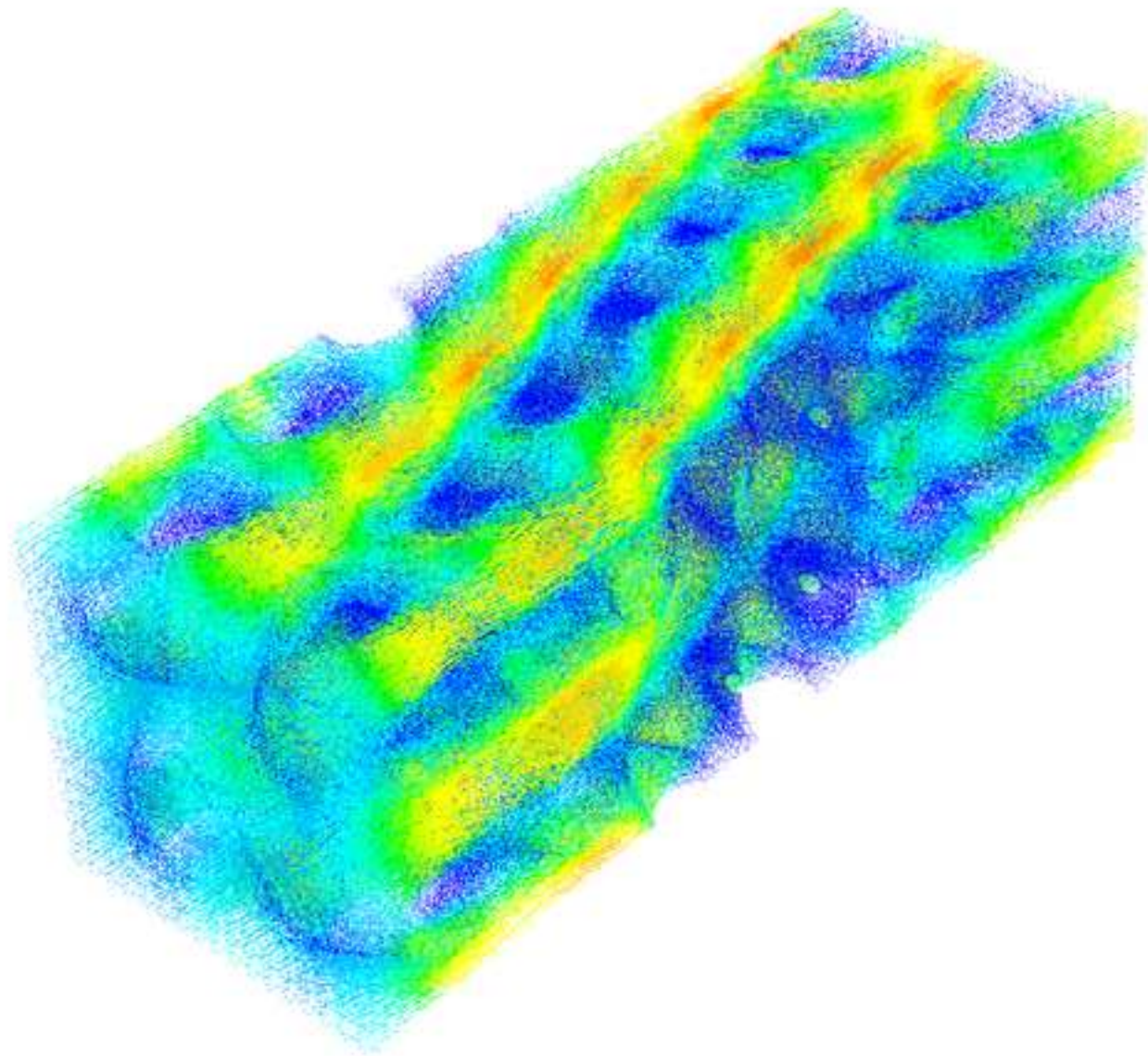
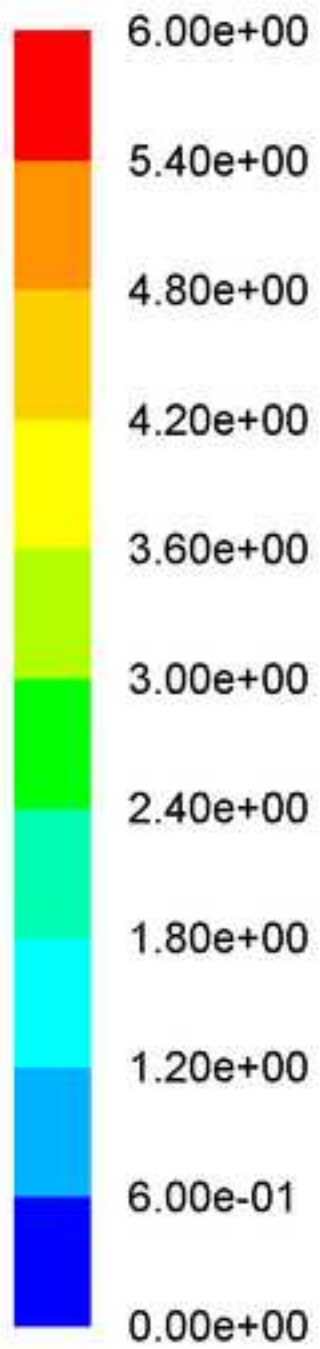


Figure7d  
[Click here to download high resolution image](#)

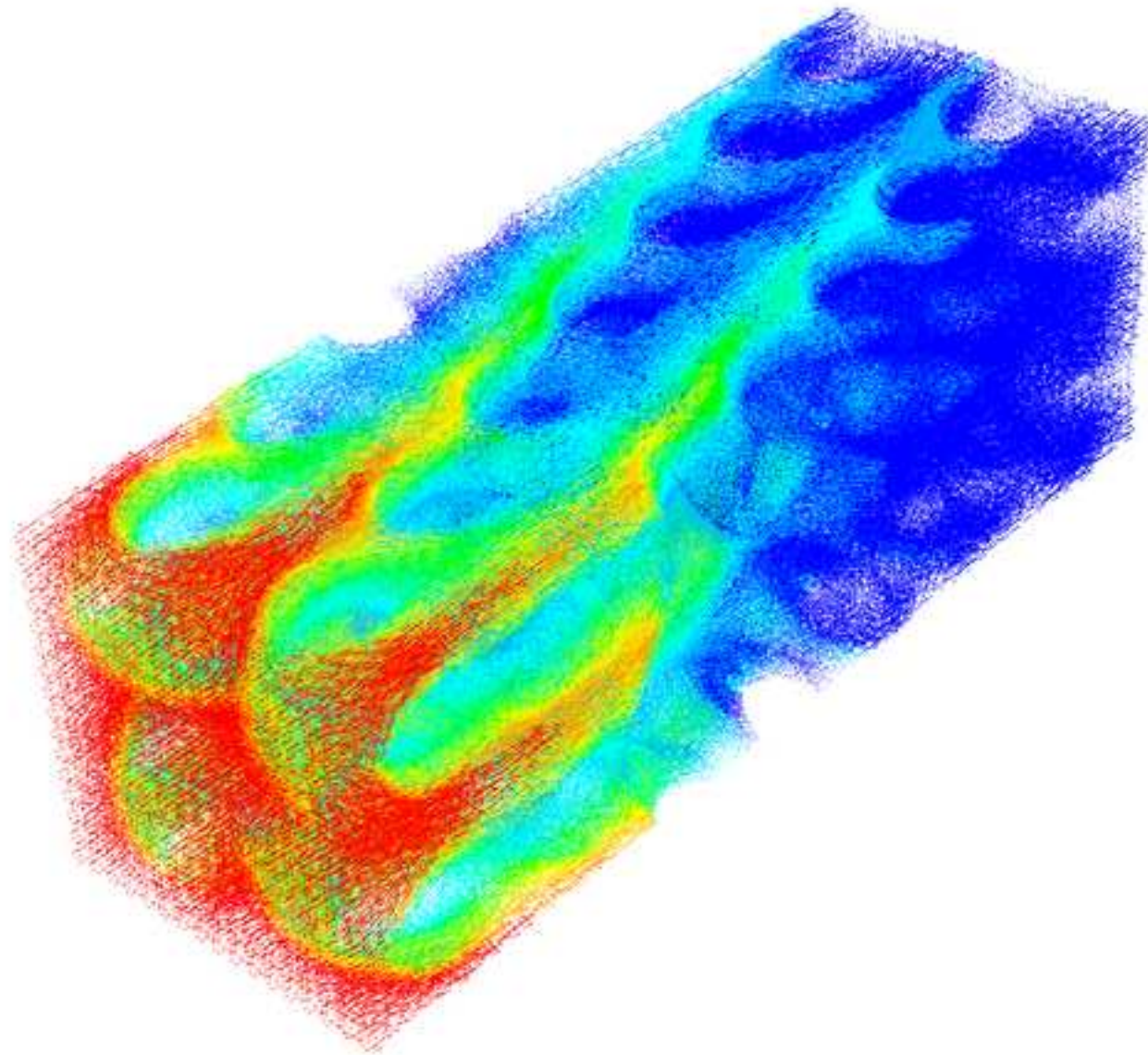
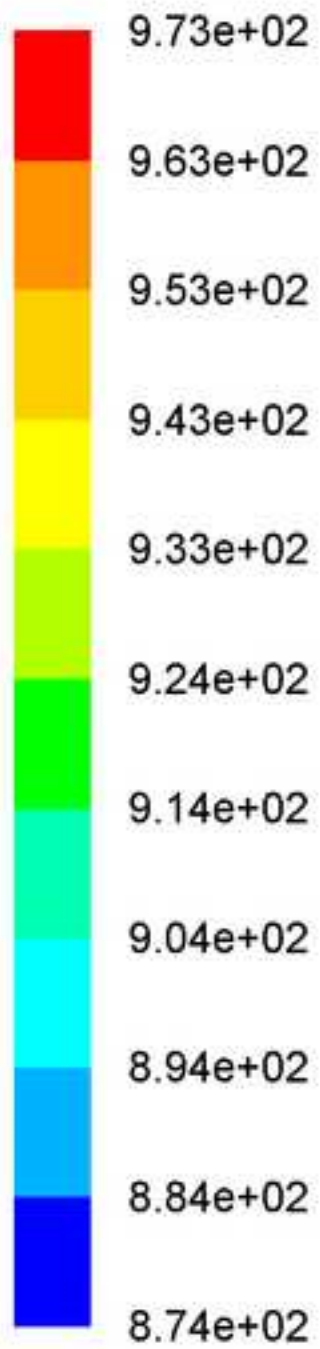


Figure8a  
[Click here to download high resolution image](#)

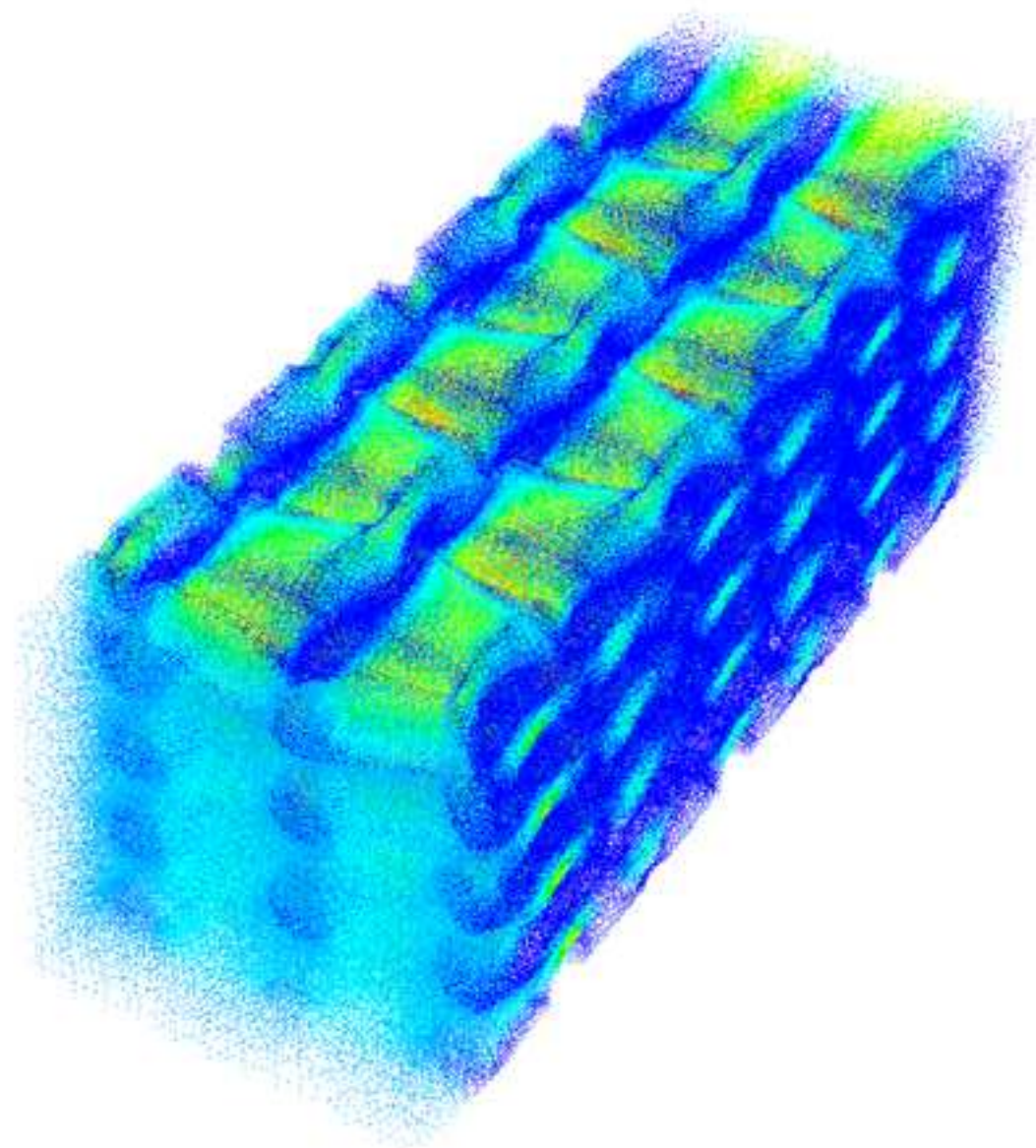
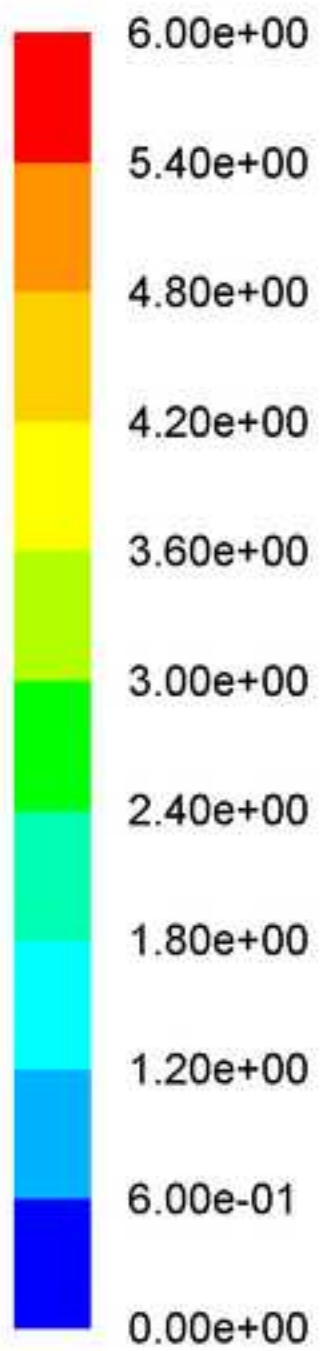


Figure8b  
[Click here to download high resolution image](#)

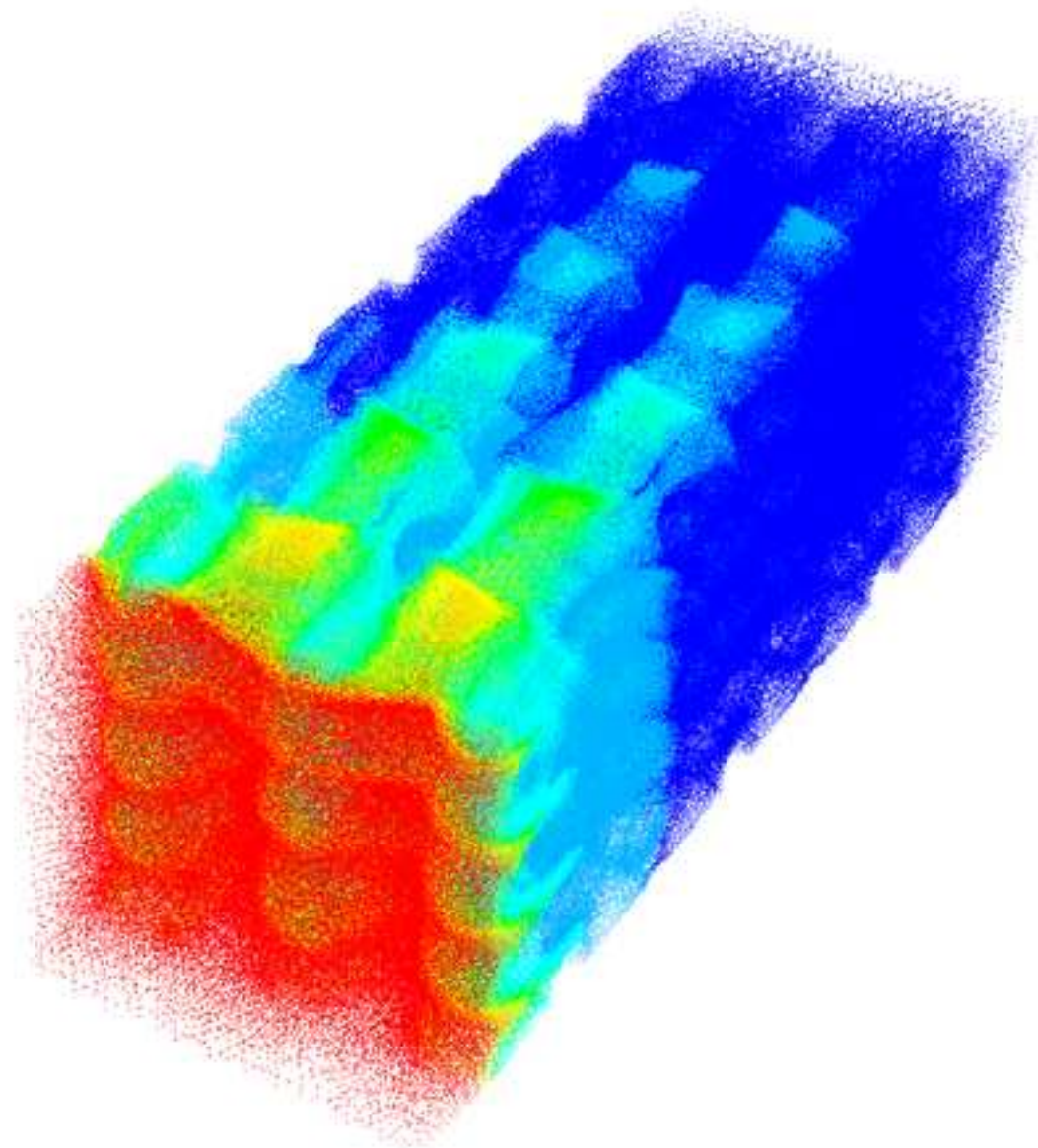
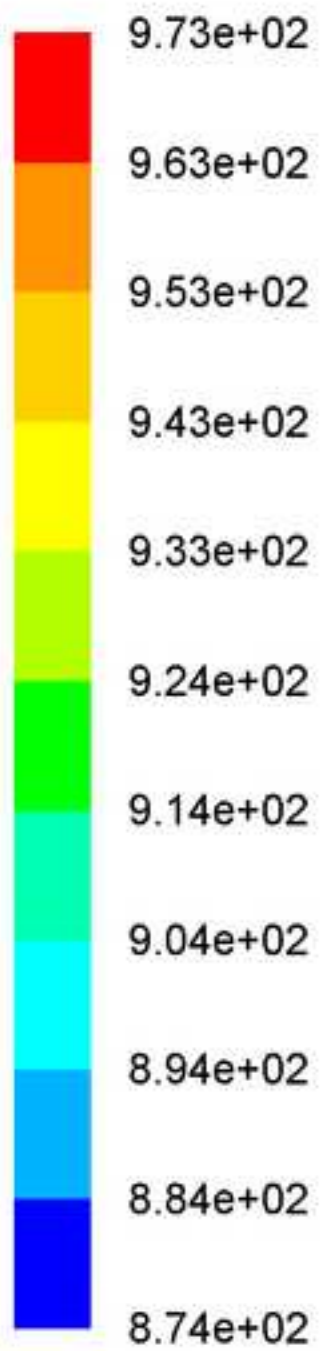


Figure8c  
[Click here to download high resolution image](#)

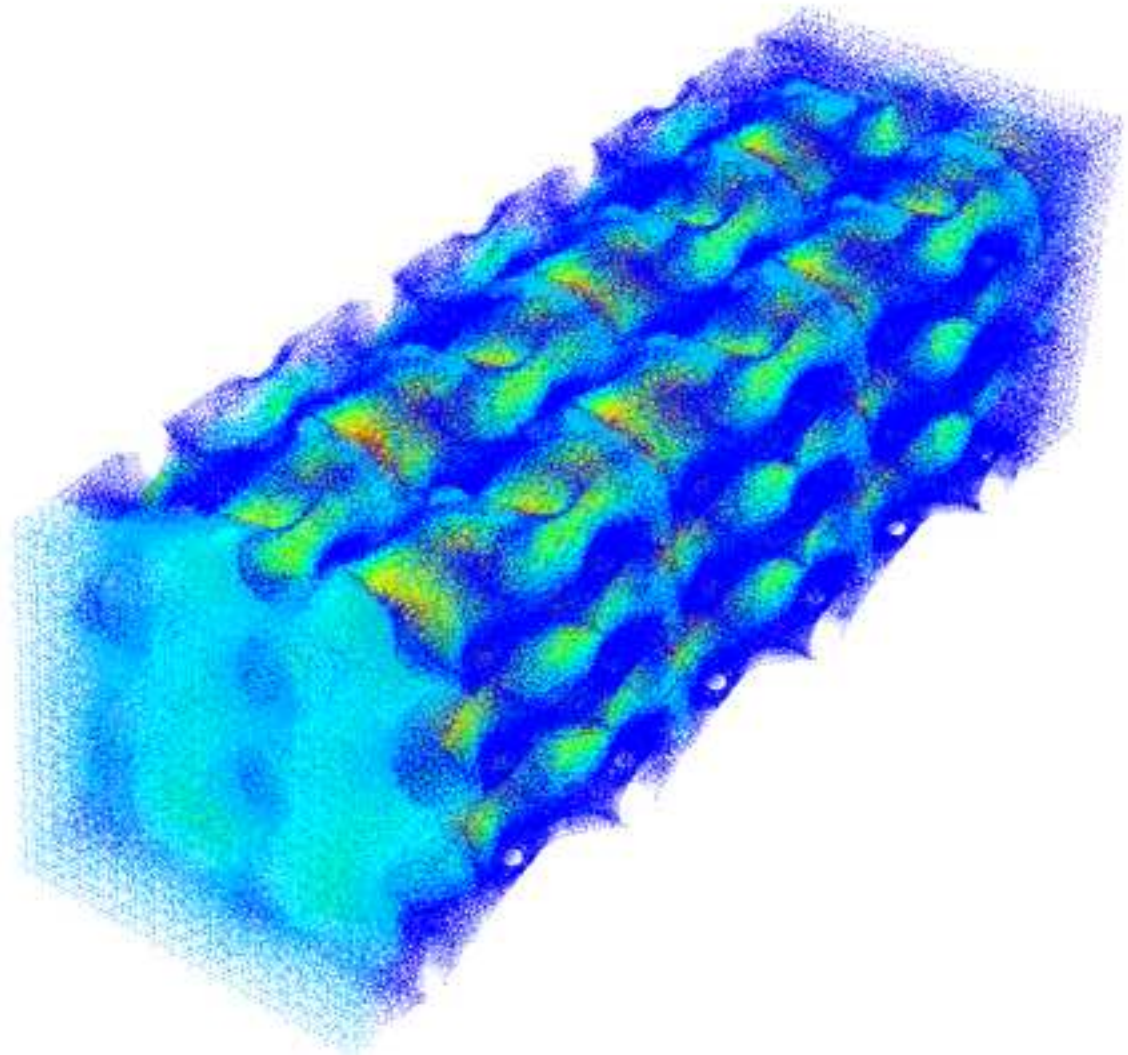
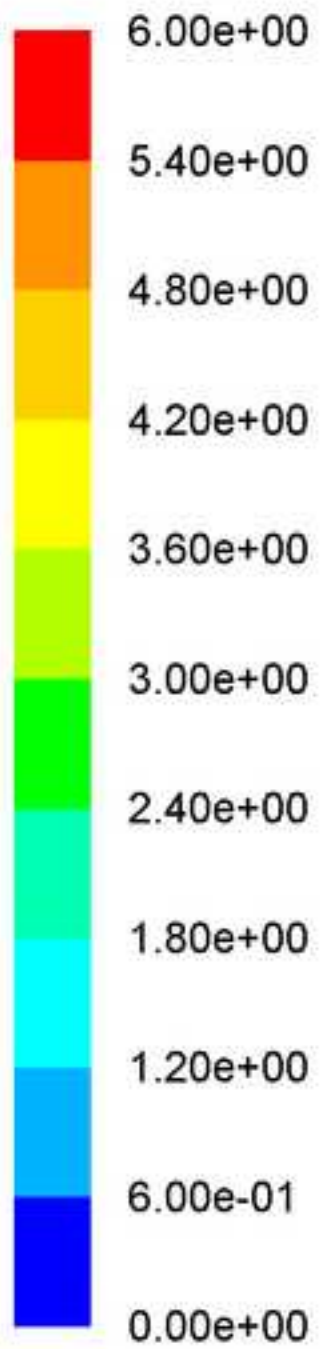


Figure8d  
[Click here to download high resolution image](#)

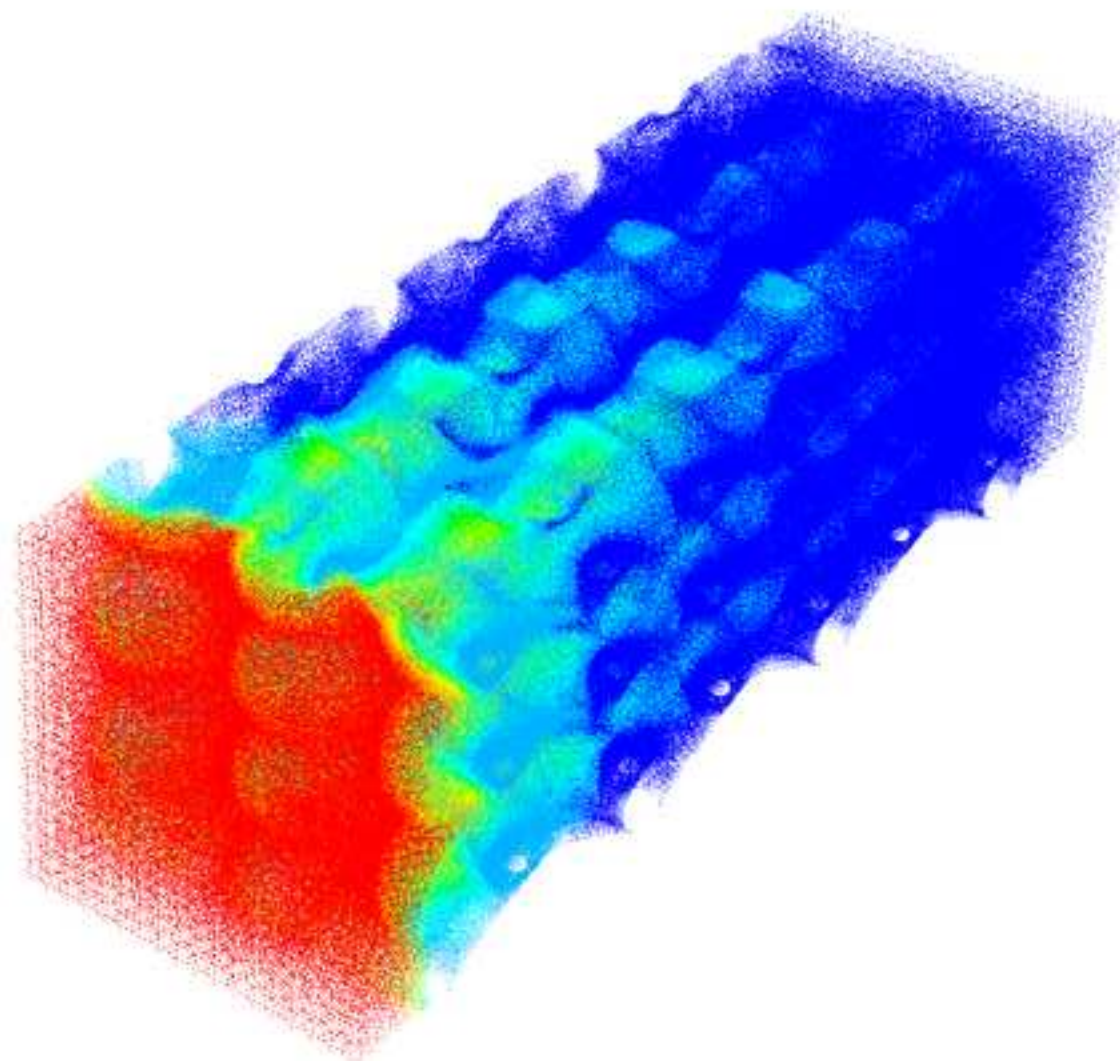
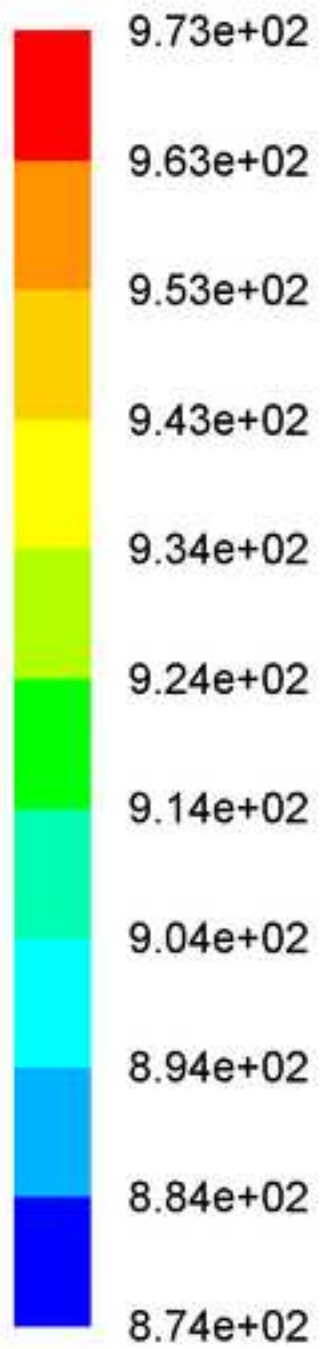
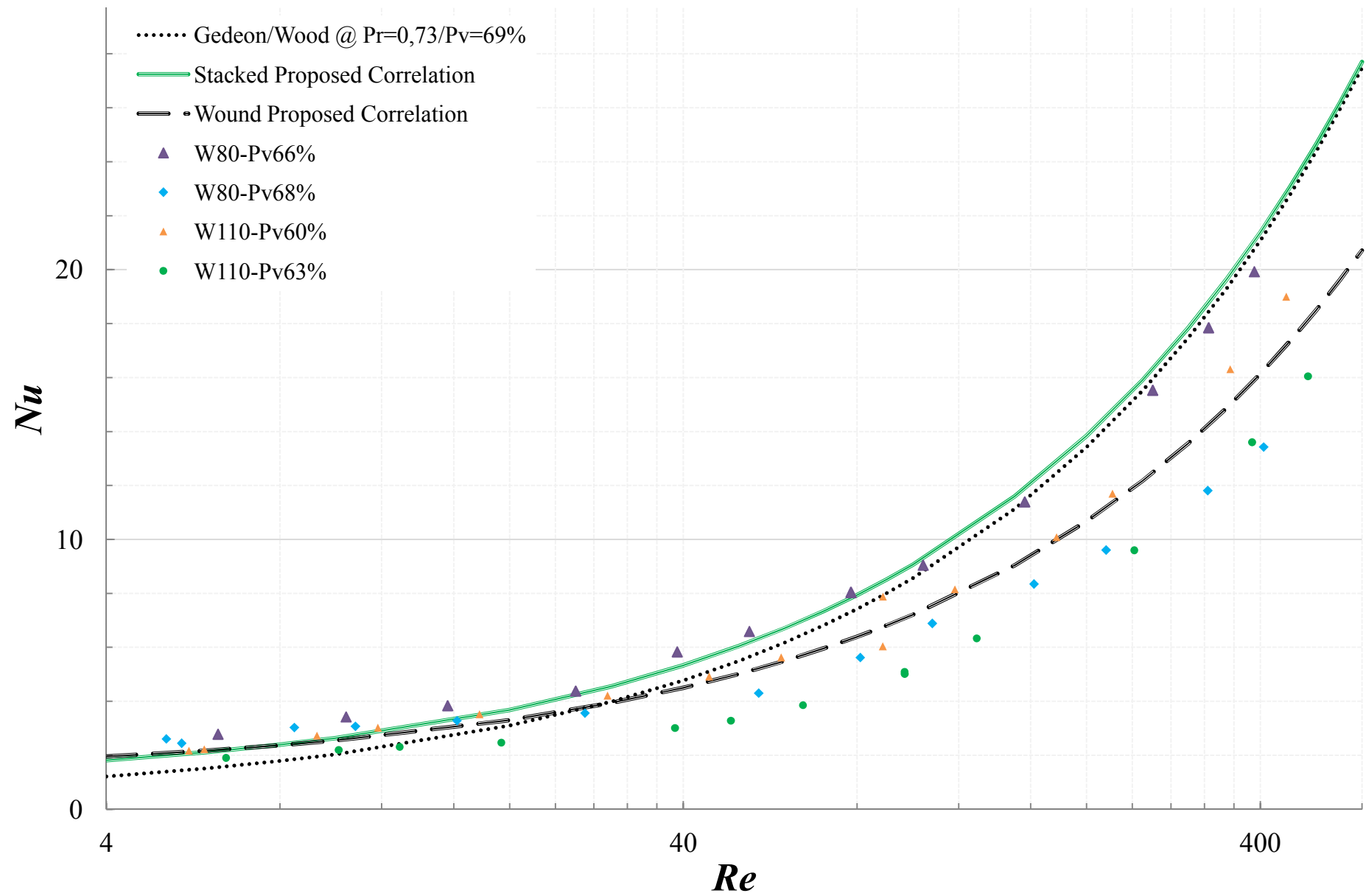


Figure9



## Authors' response

Dear Editor Professor Moh'd A. Al-Nimr

The authors would like to thank the reviewers and the editor very much for their time and efforts for making this manuscript a higher quality paper. A point by point reply to the reviewers' comments is given below. The required changes and corrections to the questions/comments/suggestions have been also included in the revised manuscript by using red colored text and highlighted in yellow.

The following is the detailed response to the questions/comments/suggestions:

### Reviewer #2:

Please find a list of corrections done following the Editorial comments and other corrections:

Page / line	Author's response/correction
3 & 4	The nomenclature section is included.
5/3	The word "global" is replaced with "total".
5/9	The word "for" is replaced with "by".
7/10	The word "indicate" is replaced with "indicated".
7/14	The word "by" is erased.
10/15	The last part of second paragraph is rewritten.
12/7	The word "of" is replaced with "for".
12/12	The second paragraph is rewritten and a Figure 3 is changed.
14/2	The character ")" is erased.
16/13	The phrase "as seen in Table 1 and 2" is replaced with "as can be compared between Table 1 and Table 2"
16/20	The first paragraph after point 3.1 is rewritten.
17/12	A new sentence is included: "One of the main conclusions..." and a new paragraph is included.
18/12	The equation 12 is modified and a sentence is deleted.
18/14	A new sentence and equation are included: "In the present..." and Eq. (13)
20/21	The word "show" is replaced with "shown".
21/22 & 22/2	The word "area density" is replaced with "specific heat transfer area".
22/11	The word "is" is erased.
23/2,4,5	The word "area density" is replaced with "specific heat transfer area".
23/14	The word "80 $\mu\text{m}$ " is replaced with "110 $\mu\text{m}$ ".
25/5	The word "friction correlation" is replaced with "Nusselt correlation".
25/various	The discussion section is modified.
26/19	The word "wound wire woven" is replaced with "wound woven wire".
27/ various	The paragraph "In the Stirling engine ..." is rewritten.
28-30	The bibliography section is modified.
31/various	The figures captions for Figures 3,7 and 8 are modified.
32/2, 3	The tables captions for table 1 & 2 are changed.
33 (Table 1)	The Table 1 is modified. The Tanaka reference is included "[6]".
34 (Table 2)	The Table 2 is modified.
All	Equations from number 12 are renumbered.

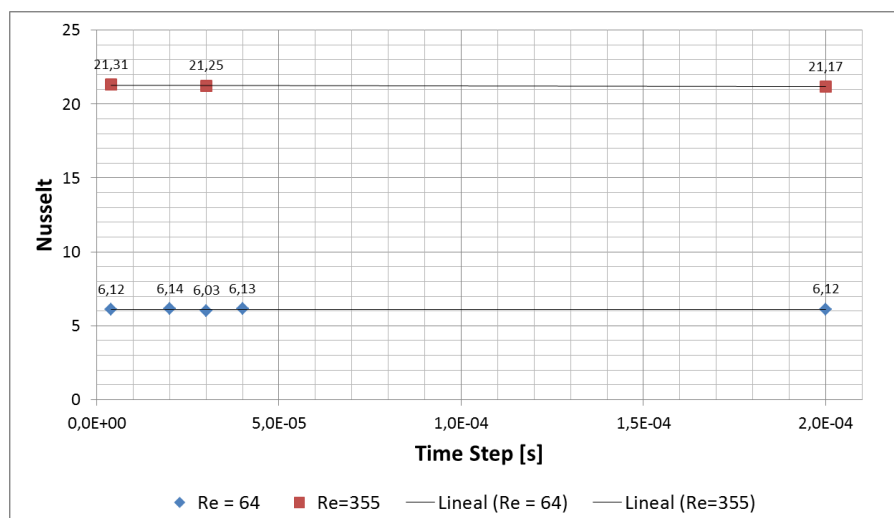
\* A nomenclature would be appropriated, since there are several different symbols and Indices used throughout the paper

A.R. > Nomenclature section is added into the manuscript (pages 3-4).

\* page 8: A non-dimensional time step value of 0.01 is used. It would be interesting to know about the effect of this parameter. What is the gain or the reduction in accuracy, if this parameter is set to i.e. 0.001 or 0.1 ?

A.R. > It is known fact that the time step size,  $\Delta t$  and time stepping scheme are both influential on the convergence rate and the simulation results unless the mesh independency of the results have been satisfied. The step size effect is also more crucial for the accuracy of the numerical simulation at very high Reynolds number which signifies the onset of turbulence. In generally, the order or magnitude of an appropriate time step size is estimated as  $\Delta t \approx \Delta x / v$ , where  $\Delta x$  is the typical cell size and  $v$  is the characteristic flow velocity. In the present study, the time step size chosen on a basis of the time step size selection criteria,  $\Delta t \approx \tau \Delta x / v$ , where  $\tau$  is the non-dimensional time step value chosen of 0.01. The initial numerical tests show that the convergence has been attained in 5-10 iteration at each time instant for the selected final mesh configuration with fairly accurate representation of physical flow in terms of chosen non-dimensional time parameter.

In the below figure is shown a time step sensibility analysis for a matrix configuration model at two Reynolds numbers, the non-dimensional time step range is from 0.1 to 0.001. The Figure demonstrates that the Nusselt number is not affected by the non-dimensional step size chosen in the range of 0.001 to 0.01. In the manuscript (page 10) the following sentence is included "The non-dimensional time step values are chosen as 0.01 following an initial sensitivity analysis performed for the variation of Nusselt number with respect to different non-dimensional time step size ranging from 0.001 to 0.01 for different Re number of 64 and 355. This test shows that there is no significant influence of choice of non-dimensional time step size between 0.01 and 0.001 on the results of Nusselt number obtained for the investigated Re number."



\* page 10/11: Regarding boundary conditions: What about the fluid velocity at the inflow boundary? Is it constant in time or do you assume oscillating flow? If it is constant in time (steady flow), you should comment on the expected deviations or errors compared to the oscillating flow conditions in practical Stirling engines.

A.R. > “Uniform velocity inlet” boundary conditions are imposed at the inflow. Because, in the present study the emphasis is on characterizing heat transfer phenomena through the Stirling domain in term of instantaneous local Reynolds number through a detailed small control volume of the regenerator matrix. As stated earlier by the study of Gedeon and Wood [10] on the oscillatory inflow boundary, there are no discernible differences between the results of non-oscillatory and oscillatory inflow boundary condition for the investigated working range of Stirling regenerators as instantaneous local Reynolds number appears to characterize the flow quite adequately. Early studies conducted on oscillating flow inside a duct signify that both Reynolds number and Valensi number have significant effects on the flow. However, compared to heat exchanger ducts, Valensi numbers are typically quite low in regenerator matrices, owing to their small hydraulic diameters. Gedeon and Wood [10] suggest that the exception to this might be for Valensi numbers above around 20 and it is not a range for typical Stirling regenerator applications. Gedeon and Wood [10] also provide clear evidence that correlating pressure-drop or heat-transfer expressions solely in terms of Reynolds is sufficient for Stirling cycle purposes.

Finally, it is noteworthy here that the present study is the second part of the numerical study previously conducted by the authors on the Stirling regenerators. In the first part of the study [16] the emphasis is on characterization of the pressure drop under isothermal conditions while the second part also includes heat transfer phenomena in a small control volume of the Stirling regenerator. The next step of the actual research is to implement both correlations in an equivalent porous media model where, simplifying the high complexity of the regenerator mesh geometry, the whole regenerator will be modelled in an oscillatory flow condition and correlations will provide friction coefficient and Nusselt number to each cell in the regenerator domain according to each volume flow condition for each calculation time step along the oscillatory cycle.

\* page 14: The numerical results are compared to the correlations derived by Tanaka and Gedeon and Wood. Tanaka and Gedeon and Wood applied oscillating flow conditions during their experiments. Hence, it should be noted, if the numerical simulation was performed under oscillating flow conditions as well. If yes, it would be interesting to know, which range of frequency was applied. If not, there must be a comment about the expected deviations compared to numerical results based on steady flow. In other words: To what extent are the deviations between the numerical results and the curves given by Tanaka and Gedeon and Wood in Figures 4 and 5 attributed to the fact that the simulation was performed for steady flow conditions while the experiments by Tanaka and Gedeon and Wood were performed under oscillating flow conditions. If the numerical simulation was performed for steady flow conditions, it might be more appropriate to compare with the results derived by Miyabe and Tong and London who as well found their results under steady flow conditions.

A.R. > The present simulations are performed under steady inflow boundary conditions. The explanation for this procedure is given in the previous section where one of the conclusions about Regenerators of Gedeon and Wood [10] is highlighted *“correlating pressure-drop or heat-transfer expressions solely in terms of Reynolds is sufficient for Stirling cycle purposes”*.

In the published previous work [16], the results obtained for pressure drop correlation are compared against the results of Tanaka [6] and Gedeon and Wood [10] and are found to be in good agreement. However, the same results do not good correspondence with those of Miyabe/Tong & London/ Blass [16]. One of the possible reasons for the poor agreement with these experimental data may be due to the mesh configuration range tested for those researches. Because, in the study of Tong & London/Blas [16] the smaller wire diameter is 200 microns while the diameter range tested in the study of Miyabe [16] is larger, from 40 to 500 microns for only one correlation case.

\* In eqs. 11 and 12 two different definitions for hydraulic diameter are given, and it is stated that the difference is not significant. However, it must be noted, which definition was used in the analysis (i.e. in eq. 13).

A.R. > The following sentence is included in the manuscript (page 18) to clarify the definition used. *“In the present study the hydraulic diameter is determined by Eq. (12)”*. The definition of the specific heat transfer area is also included as Eq. (13) and the equations are renumbered.

\* On pages 16 and 17 Table 1 and 2 are referenced, and the labelling seems a little confusing. Hence, it should be checked, if the labelling Table 1 and Table 2 is correct in any case where it is used.

A.R. > In the manuscript (page 16) the following sentence *“as seen in Table 1 and 2”* is rephrased in order to avoid confusion into *“as can be compared between Table 1 and Table 2”*. Moreover, tables are modified in order to clarify the different, Table 1 is for the studies of other authors and Table 2 is for the present study.

\* On page 20 (2nd paragraph), line 5 it is said: *.the higher wire diameter of 80  $\mu$ m for the stacked*. Should this section read: *.the higher wire diameter of 110  $\mu$ m for the stacked*. ?

A.R. > Yes. This error is corrected in the revised manuscript (page23).

\* The 1st line on page 20 refers to equation 19. Hence, it should read *.derived Nusselt number correlation*. instead of *.derived friction correlation*.

A.R. > Yes. This error is corrected in the revised manuscript (page25).

\* On page 22, last paragraph, the effect of volumetric porosity is discussed based on Figure 9. Here, it should be kept in mind that the 4 samples analyzed are of different porosity

and different wire diameter. For that reason the effect of wire diameter must be recognized and explained.

A.R. > In the manuscript (page 25 and 26) the discussion section about the effect of volumetric porosity and hydraulic diameter is modified and extended.

\* Moreover, in Figure 9 the results for Nusselt number vary between roughly  $Nu = 14$  and  $Nu = 20$  at a Reynolds number of 400. Hence, there is a variation range of approx. 35% in Nusselt number (based on a mean  $Nu$ -number of 17). With respect to this variation range the first sentence of this paragraph (.the effect of the volumetric porosity on the heat transfer is not significant.) should be rewritten, since there is a pretty reasonable deviation of Nusselt number results caused by the variation of porosity and wire diameter.

A.R. > In the manuscript (page 25 and 26) the discussion section about the effect of volumetric porosity and hydraulic diameter is modified and extended.

In general the last section of the paper could be a little more elaborated. While the previous paragraphs are well discussed and explained, the discussion of the results at the end of paragraphs 3.1 and 3.2 seems a little shorthanded, which could be improved by a more thorough discussion of the results.

A.R. > In the manuscript (page 16 to 26) the discussion section is modified and extended.

\* Finally the bibliography at the end of the paper is not consistent in structure especially with regard to page numbers. (i.e. ref [17])

A.R. > The paper bibliography (page 28-30) is checked and is modified in order to keep a consistent structure.

### **Reviewer #3:**

\* Stirling engine attracts interests of many researchers. Stirling regenerator can enhance efficiency of the engine. In this article, the authors proposed a correlation equation to characterize regenerator heat transfer, which is helpful for the engine design. The authors also validate the simulation method by comparing the simulation results with other experiment results. This article gives some useful results. However, in my opinion, some figures (Fig. 7 and Fig. 8) in the article are treated badly and need to be revised.

A.R. > In the manuscript the quality of the Figures 7 and 8 is improved.

In the revision process we would like to request you return three files:

(1) Please submit a list or table of changes (or your rebuttal) against each point raised when you upload your revised article and upload this as your 'Response to Reviewers' file/doc - note our system will not allow you to complete the resubmission process without this file.

A.R. > File uploaded

(2) Also please highlight any revised text using coloured highlighting in a separate word document. This will enable the Editor /Reviewers to identify the amendments and subsequently make faster decisions on the revisions.

A.R. > File uploaded

(3) In addition we request one final file, a 'clean' word document of the revised manuscript without any annotations, highlighting or comments, in font 10 or 12 pt with double line spacing.

A.R. > File uploaded

If the modification is done carefully and completely, upon re-submission and evaluation, I think it possible that the paper will be accepted for publication in Energy Conversion and Management. Thank you again for sending this paper to Energy Conversion and Management for consideration.

A.R. > Thank you for the opportunity to modify this paper following your comments and suggestions.

Best regards,  
**Authors**